HYPERHOMOCYSTEINEMIA ACCELERATES STROKE-INDUCED BRAIN INJURY VIA PROMOTING ENDOTHELIAL ACTIVATION AND INFLAMMATORY CELL INFILTRATION: THE ROLE OF ICAM1-MEDIATED NEUTROPHIL AND MONOCYTE INFILTRATION

A Dissertation
Submitted to the
Temple University Graduate Board

In Partial Fulfillment of the
Requirement for the
Degree of Doctor of Philosophy

By
Lixiao Zhang
May, 2017

Dissertation Examining Committee Members:

Dr. Hong Wang, Department of Pharmacology (Dissertation Advisor)
Dr. Xiao-Feng Yang, Department of Pharmacology (Dissertation Co-advisor)
Dr. Barrie Ashby, Department of Pharmacology (Dissertation Examining Committee Chair)
Dr. Persidsky Yuri, Department of Pathology
Dr. Satoru Eguchi, Department of Physiology
Dr. Jun Yu, Department of Physiology
Dr. Bin Zhou, Department of genetics and medicine, Albert Einstein College of Medicine (External Examiner)

ABSTRACT

HYPERHOMOCYSTEINEMIA ACCELERATES STROKE-INDUCED BRAIN INJURY VIA PROMOTING ENDOTHELIAL ACTIVATION AND INFLAMMATORY CELL INFILTRATION: THE ROLE OF ICAM1-MEDIATED NEUTROPHIL AND MONOCYTE INFILTRATION

Lixiao Zhang

Doctor of Philosophy

Temple University, 2017

Doctoral Advisory Committee Chair: Hong Wang, MD, PhD

Background: Epidemiology, clinical trials and meta-analysis studies have established that Hyperhomocysteinemia (HHcy) is an independent risk factor for stroke. However, the exact molecular mechanism underlying the HHcy-induced risk of stroke is unclear. Our study aims to investigate the role of HHcy in stroke.

Methods and results: We established a mice mode of focal ischemic stroke, termed transient Middle Cerebral Artery Occlusion (tMCAO) and conducted surgery on a mice model of HHcy (plasma homocysteine level ~150μM), in which a Zn^{2+} inducible human cystathionine β-synthase (CBS) transgene was introduced to circumvent the neonatal lethality of the CBS gene deficiency (Tg-hCBS *Cbs*$^{-/-}$ mice). Fourteen-week-old male mice were used in the experiment. A student's t-test was used for the evaluation of the statistical

significance between the two groups. For the comparison across multiple groups, one-way ANOVA was used. We found that HHcy 1) increased the infarction volume from 42.3 ± 4.9 mm^3 in CT mice to 53.5 ± 10.5 mm3 in Tg-hCBS *Cbs*$^{-/-}$ mice (p=0.055) at 24h post-tMCAO, as examined by TTC staining; 2) increased the neurological deficit from 2.4 ± 1 to 3.1 ± 0.64 (p = 0.036) at 24h post-tMCAO, as evaluated by the Bederson scale; 3) reduced the survival rate from ~80% to ~60% at 72h post-tMCAO (p=0.18). As inflammation is one of the major factors contributing to secondary brain injury, we characterized the immune cell population by fluorescence-activated cell sorting (FACS) and examined the cytokines/chemokines production by cytokine array in the ischemic and non-ischemic hemisphere of CT and Tg-hCBS *Cbs*$^{-/-}$ mice at 24h post-tMCAO. We found that HHcy increased the number of infiltrated neutrophil (NØ) from 1448 ±208.1 in CT mice to 2550 ± 361.8 in Tg-hCBS *Cbs*$^{-/-}$ mice (p=0.0468) and the number of the inflammatory Ly6C^{hi} monocyte (MC) from 580.4 ± 162.2 to 1268 ± 232 in the ischemic hemisphere. HHcy did not significantly alter the number of NØ, Ly6C^{hi+mid} MC, Ly6C^{lo} MC and lymphocyte (Lym) in the blood samples that were collected at 24h post-tMCAO. HHcy also increased several leukocyte-recruiting cytokines/chemokines, including ICAM1, CCL2, CCL3 and CXCL1 in the ischemic hemisphere of Tg-hCBS *Cbs*$^{-/-}$ mice, as measured by cytokine array. In vivo, we confirmed that HHcy increased ICAM1 in mouse brain microvascular endothelial cells (MBMEC) that were isolated from the ischemic hemisphere of Tg-hCBS *Cbs*$^{-/-}$ mice, as determined by FACS. In vitro, DL-Hcy (50μM, 24h) upregulated ICAM1, and to a lesser extent, E-selectin and P-selectin in the condition

of normoxia, as well as in the condition of oxygen-glucose deprivation (4h) and subsequent reoxygenation (20h) (an in-vitro model of ischemic/reperfusion injury) on the cultured primary human brain microvascular endothelial cells (HBMEC). Considering that ICAM1 is a well-established key molecule that mediates NØ and MC recruitment, we hypothesized that HHcy-induced ICAM1 upregulation led to enhanced NØ and MC infiltration, and subsequent exacerbated-brain injury at 24h post-tMCAO. Using MC-adhesion assay, we found that there was an increase in the number of both THP-1 monocytic cells and human primary peripheral monocyte (HPBMC) that adhere to the DL-Hcy-treated (50μM, 24h) HBMEC monolayer. Using MC trans-endothelial migration assay, we found that Hcy promoted the migration of MC across HBMEC, with or without the presence of CCL2. In vivo, the peritoneal injection of ICAM1-blocking antibody (2mg/kg) directly after reperfusion attenuated HHcy-exacerbated and stroke-induced brain injury.

Conclusion: HHcy exacerbated stroke-induced brain injury by promoting endothelial activation, as well as inflammatory NØ and MC infiltration, partially via upregulating the ICAM1 of MBMEC.

ACKNOWLEDGEMENTS

I would first like to express my appreciation to my mentor Dr. Hong Wang and co-supervisor Dr. Xiaofeng Yang for providing me the precious opportunity to receive advanced scientific training in USA and to conduct my dissertation work in their labs, allowing my intellectual growth. Their dedication to science and strong spirit inspired and drive me towards scientific research. Their guidance throughout the training process enabled me to achieve something that I wouldn't have thought possible before meeting them.

I must also thank my committee members: Dr. Asby, Dr. Persidsky Yuri, Dr. Jun Yu, Dr. Satoru Eguchi and Dr. Binzhou. They helped guide me through my thesis project, giving me precious suggestions for my study. I would especially like to thank Dr. Ashby for always being helpful at every step in this Ph.D. program. I would also especially like to thank Dr. Yuri for helping me develop the method of isolating mouse brain microvascular endothelial cells. I would especially like to thank Dr. Eguchi for his kindness being my committee member. I would like to thank Dr.Yu for his precious suggestions for my thesis writing and presentation. I would like to thank Dr. Zhou kindly accept the invitation as my thesis external examiner.

I would also like to thank a few of my colleagues, especially my dear friend Ramon Cueto, for their aid in my graduate studies, sharing their time and wisdom with me. I would like

to thank our lab manager for her help throughout these years. I would like to thank Huimin for providing precious mouse for my experiment.

Finally, I would like to thank my family for their love and support during my life.

DEDICATION

To my dearest family

TABLE OF CONTENTS

LIST OF FIGURES

LIST OF TABLES

LIST OF ABBREVIATIONS

ACK	Ammonium-Chloride-Potassium
APC	Allophycocyanin
B6	Vitamin B6
B12	Vitamin B12
BBB	Blood brain barrier
BCA	Bicinchoninic acid
BFGF	Basic fibroblast growth factor
BHMT	Betaine homocysteine S-Methyltransferase
BMEC(s)	Brain microvascular endothelial cell(s)
BP	Base pair
BW	Body weight
CAT	Catalog
$CaCl_2 \cdot 2H_2O$	Calcium chloride dehydrate
CBF	Cerebral blood flow
CBS	Cystathionine β synthase

CCA	Common carotid artery
CCL	Chemokine Ligand
CCR2	C -C chemokine receptor type 2
CXCL	Chemokine (C-X-C motif) ligand
CXCR	CXC chemokine receptors
CDNA	Complementary DNA
CD	Cluster of differentiation
CSE	Cystathionine gamma-lyase
CSF	Colony stimulating factor
CSPPT	China Stroke Primary Prevention Trial
CT	Control
CVDs	Cardiovascular diseases
CXCL	Chemokine C-X-C motif ligand
CYS	Cysteine
DAPI	4', 6-diamidino-2-phenylindole
DBPS	Dulbecco's Phosphate-Buffered Saline
DMEM	Dulbecco's modified eagle medium
DNA	Deoxyribonucleic acid
DNMT	DNA methyltransferase
EAE	Encephalomyelitis
EB	Evans blue

ECA	External carotid artery
ECGS	Endothelial cell growth supplement
EC(s)	Endothelial cell(s)
EDTA	Ethylenediaminetetraacetic acid
EGF	Epithelial growth factor
EGM	Endothelial growth medium
ERα	Estrogen receptor alpha
FA	Folic acid
FACS	Fluorescence-activated cell sorting
FITC	Fluorescein isothiocyanate
FSC	Forward-scattered light
HAEC(s)	Human aortic endothelial cell(s)
HBMEC(s)	Human brain microvascular endothelial cell(s)
HBSS	Hank's Balanced Salt Solution
Hcy	Homocysteine
HF	High fat
HHcy	Hyperhomocysteinemia
HM	High methionine
HOPE2	Heart Outcomes Prevention Evaluation-2 Study
HRP	Horseradish Peroxidase
HUVEC	Human Umbilical Vascular Endothelial Cell

ICA	Internal carotid artery
ICAM1	Intracellular cell adhesion molecule-1
IFNγ	Interferon-gamma
IgG	Immunoglobulin G
IL	Interleukin
IP	Intraperitoneal
I/R	Ischemia/Reperfusion
IS	Ischemic hemisphere
KCL	Potassium chloride
KH_2PO_4	Monopotassium phosphate
LFA1	Lymphocyte function-associated antigen 1
LPS	Lipopolysaccharides
LYM	Lymphocyte
LY6C	Lymphocyte Ag 6C
MAEC(s)	Mouse aortic endothelial cell(s)
MAC1	Macrophage-1 antigen
MC/MΦ	Monocyte/macrophage
MET	Methionine
MG	Microglia
MNC(s)	Mononuclear cell(s)
MS	Methionine synthase

MTHFR	Methylenetetrahydrofolate reductase
NIS	Non-ischemic hemisphere
NLR	Neutrophil lymphocyte ratio
NØ	Neutrophil
NORVIT	Norwegian vitamin trial
OGD	Oxygen glucose deprivation
PBS	Phosphate buffered saline
PCA	Posterior cerebral artery
PComA	Posterior communicating artery
PCR	Polymerase chain reaction
PE	Phycoerythrin
PE-Cy	Phycoerythrin-Cyanine
PFA	Paraformaldehyde
PGE	Prostaglandin E
PMCAO	Perminent middle cerebral artery occlusion
PSA	Penicillin, streptomycin, and amphotericin
PSGL1	P-selectin glycoprotein ligand 1
QRT-PCR	Quantitative real-time PCR
RAG	Recombination activating gene
ROS	Reactive oxygen species
rtPA	Recombinant tissue plasminogen activator

SAH	S-adenosylhomocysteine
SAM	S-adenosylmethionine
SDS	Sodium dodecyl sulfate
SEARCH	Study of the effectiveness of additional reductions in cholesterol and homocysteine
SELE	E-selection
SELP	P-selection
SEM	Standard error of the mean
SPW	Spleen weight
SSC	Side-scattered light
STZ	Streptozotocin
Tg-hCBS	Human transgenic CBS
THP-1	Human acute monocytic leukemia cells
TMCAO	Transient middle cerebral artery occlusion
TTC	2, 3, 5-Triphenyltetrazolium chloride
VCAM1	Vascular cell adhesion protein 1
VEGF	Vascular endothelial growth factor
VLA4	Very Late Antigen-4
VISP	Vitamin Intervention for Stroke Prevention
VITATOPS	Vitamins to prevent stroke
WBC	White blood cell count

WENBIT	Western Norway B vitamin intervention trial
WT	Wild type

CHAPTER 1

BACKGROUND INTRODUCTION

HHcy is a risk factor for cardiovascular disease

Chemical features of Hcy

Homocysteine (Hcy) was first discovered by Butz and Du Vigneaud in 1932, and is defined as a sulfur-containing amino acid with a similar structure to that of cysteine (Cys) and methionine (Met) (**Figure 1**). Hcy shares the same free sulfur hydro group (-SH) with cysteine, but differ from cysteine by its additional methylene bridge (-CH2-) and from methionine by the lack of a methyl group (-CH3) attaching its sulfur atom(S). These structure differences account for some of the distinctive biological properties of these three sulfur-containing amino acids. For example, Cys and Met are two of the 20 canonical amino acids that are incorporated into proteins, while Hcy is normally a non-protein amino acid.

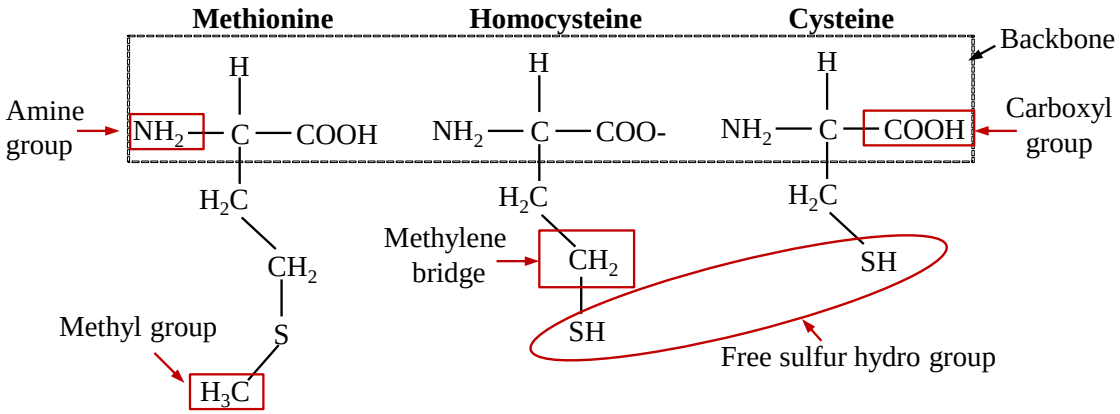

Figure 1. The chemical structure of sulfur-containing amino acids: methionine, homocysteine and cysteine. Homocysteine is a sulfur-containing amino acid, as are methionine and cysteine. It shares a free sulfur hydro group (-SH) with cysteine, but differs from cysteine by its additional methylene bridge (-CH2-) and from methionine by the lack of a methyl group (-CH3) attaching its sulfur atom (S).

Hcy metabolic cycle

Hcy is not obtained from dietary intake. It is biosynthesized from Met as a by-product of biological methylation reactions (**Figure 2**). Firstly, Met reacted with ATP, thereby generating S-adenosylmethionine (SAM) in the presence of S-adenylyl-methionine synthase. SAM served as a methyl donor, thereby transferring the methyl group to a targeted molecule and becoming S-adenosylhomocysteine (SAH). This reaction was catalyzed by methyltransferases (MTs), the activity of which was regulated by its substrate, SAM. With a higher affinity for the MT-active site than SAM, SAH serves as a competitive inhibitor of SAM. The intracellular ratio of SAM/SAH is determined as an index of transmethylation potential(Kerr, 1972). SAH was further reversibly hydrolyzed to Hcy and adenosine. The generated Hcy can be either recycled back to Met through a 'remethylation pathway', or converted into Cys through a 'transsulfuration pathway'.

The remethylation pathway exists in all tissues, with a higher activity in the liver and the kidney. There are two distinct pathways for the remethylation of Hcy back to Met: one is catalyzed by methionine synthase (MS) and the other is catalyzed by betaine-homocysteine

methyltransferase (BHMT) restricted in the liver. The functional activity of MS strictly relies on the methyl donor N5-methyl tetrahydrofolate (5-MTHF) and cofactor cobalamin (vitamin B12). 5-MTHF came from 5, 10-methylenetetrahydrofolate (5, 10-CH2-THF), which was converted from THF: a folate derivate that relies on human dietary intake. This process was catalyzed by the enzyme 5, 10-methyltetrahydrofolate reductase (MTHFR). In contrast, BHMT used betaine as a methyl donor and its activity is independent of B12.

The transsulfuration pathway occurs exclusively in the liver, kidney, small intestine and pancreas, and is not found or very lowly expressed in the human cardiovascular system. It was dependent on the rate-limiting enzyme cystathionine β-synthase (CBS), which can irreversibly condense Hcy with serine in the presence of cofactor pyridoxine (B6) to cystathionine, which is finally converted to cysteine, ammonia and α-ketobutyrate by B6-dependent enzyme cystathionine γ-lyase. In the liver and kidney, ~50% of Hcy is used for the production of Cys(Jacobsen, Catanescu, Dibello, & Barbato, 2005), which is a precursor for the production of glutathione and utilized in the synthesis of proteins, such as taurine.

Under normal conditions, these two pathways work synergistically to maintain body Hcy at low levels. In a Met-deficient diet, remethylation will be dominant and ~50% of the Hcy will be remethylated into Met, while in high-Met diets, more Hcy will degrade by the

transsulfuration pathway. In addition to the degrading systems, elevated Hcy in a cell will be pumped into extraocular and plasma, and excreted out through urine.

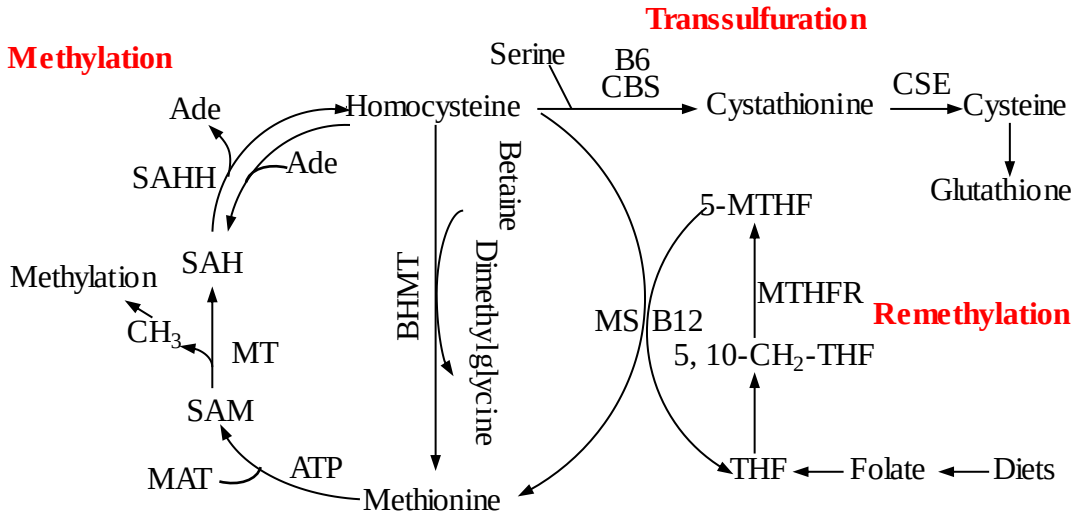

Figure 2. Hcy metabolic cycle. Hcy is generated from Met by the removal of its methyl group during the cellular methylation process. Hcy can be either converted to Cys via the transsulfuration pathway or recycled into methionine via the remethylation pathway. The transsulfuration pathway is catalyzed by CBS, which requires B6 as a cofactor, while the remethylation pathway is catalyzed either by MS, which requires B12 as a cofactor, or by BHMT. Increased Hcy can react with adenosine and contribute to the accumulation of SAH: a potent inhibitor of MT. Abbreviations: Ade, Adenosine; ATP, Adenosine triphosphate; BHMT, Betaine-homocysteine methyltransferase (liver restricted); Bet, Betaine; CBS, Cystathionine-β-synthase; CSE, Cystathionine γ-lyase; Hcy, Homocysteine; MAT, Methionine adenosyl transferase; MT, Methyltransferase; 5-MTHF, 5-methytetrahydrofolate; 5,10-CH2-THF, 5, 10-methylenetetrahydrofolate; MS, Methionine synthase; MTHFR, Methylenetetrahydrofolate reductase; Met, Methionine; SAM, S-

adenosylmethionine; SAH, S-adenosylhomocysteine; SAHH, S-adenyl-L-homocysteine hydrolase; THF, Tetrahydrofolate.

HHcy definition

In blood, 70-80% of Hcy is bound with albumin and 20-30% is present as homocysteine-cysteine-mixed disulfide or homocysteine (dimer of homocysteine). Only1-2% exists as free Hcy (Mudd et al., 2000). The majority of clinical studies involving Hcy have relied on the measurement of total Hcy (tHcy), including all forms mentioned above. In humans, the physiological level of total Hcy level (tHcy) is 3-15 μmol/. tHcy>15 μmol/L is considered to be a medical condition called HHcy. 31-100 μmol/L tHcy is defined as intermediately elevated and >100 μmol/L as severely elevated. Moderately elevated-plasma Hcy levels are the most common and highly prevalent within the general population (**Table 1**). HHcy does not need to exist permanently. It has been reported that up to 50% of subjects have a

normal fasting-plasma Hcy level and only develop HHcy after HM loading(Bostom et al., 1995).

A. Stage of HHcy

Plasma Hcy (μM)	Mild (15~30μM)	Moderate (30~100μM)	Severe >100 μM

B. Composition of total Hcy (tHcy)

Composition	%
Protein bound bHcy	70-80% (mostly albumin bounded)
Non-protein bound(fHcy):	20-30%:
Free Hcy	1~2%
Homocystine (Hcy-Hcy)	~1%
Hcy-Cys disulfide (Hcy-S-S-Cys)	20%

Table 1. Definition of HHcy and composition of plasma tHcy. A) HHcy that refers to plasma tHcy levels is >15μmol. The stage of HHcy is defined according to the grade of plasma tHcy levels. **B**) Hcy exists in plasma in protein-bound and non-protein-bound forms (consisting of free Hcy, Hcy-Hcy and Hcy-S-S-Cys). Abbreviations: tHcy, Total homocysteine; HHcy, Hyperhomocysteinemia.

Cause of HHcy

The elevation of tHcy can be caused by the genetic defect of key Hcy-metabolism enzymes, including MTHFR, CBS, MR and BHMT. The tHCY levels corresponding to major types of gene mutations in humans are summarized in **Table 2**. Among these gene variants, the MTHFR 677C→T variant is recognized as the most common genetic cause of mild to moderate HHcy (Isotalo, Wells, & Donnelly, 2000). The mutation of MTHFR and CBS has been found to be frequently associated with increased risk of cardiovascular disease

(CVD), such as stroke, coronary artery disease (CAD), hypertension and thromboembolism. On the contrary, the mutation of MR and BHMT in humans has not been found to be significantly associated with an elevation of tHcy. Moreover, the mutation of MR and BHMT has been found to be more closely associated with cancer and brain disease, but not with CVD.

In general population, HHcy commonly arise from nutritional deficiencies of folate, vitamin B6 and vitamin B12, which are critical for the maintenance of MTHFR and CBS activity, as mentioned above. A methionine-rich diet, renal disease, thyroid dysfunction, cancer, psoriasis, diabetes, various drugs, alcohol, tobacco, coffee, older age and

menopause are also shown to be associated with moderate HHcy. Severe HHcy is rare and most commonly caused by homozygous deficiency of CBS, termed 'homocystinuria'.

Genes	Mutation	Plasma tHcy level (μM)	Mutation phenotype	PMID#
MTHFR	C677T: CC CT TT	 13.97±7.6 15.66±10.8 29.32±23.5	TT: Plasma Hcy↑ CAD ↑ Schizophrenia↑ CVD & hypertension↑ Spina bifida↑ **Stroke↑**	22470444 24903192 22411217 10791559 17344026 27378745
	A1298C: AA AC CC	 12.53 ± 1.43 12.04 ± 1.45 14.24 ± 1.54	CC contributes to HHcy in combination with C677T or low folate intake	17344026
CBS	T883C: TT TC CC	 9.91+/-0.36 9.62+/-0.25 9.65+/-0.5	CC: Hypertension↑ **stroke↑**	 25120587 21917271
	844ins68	15.13+/-9.75 12.66+/-8.01	Breast cancer↑ Schizophrenia↑	21917271 19906435
	C1397T (missense)	~167	Thromboembolism	10780316
	C1265T(missense)	~167	Thromboembolism	10780316
	Deficiency	50~100(neonate) >100(adult)	Arteriosclerosis Mental retardation Thromboembolism Ectopia lentis Hepatosteatosis Skeletal abnormalities Mortality	20301697 3872065
MS	A2756G: AA AG GG	 10.1±0.22 9.5±0.28 9.5±0.	Breast cancer Digestive system cancer Neural tube defect	24166605 23613867 23438943
	Deficiency	NA	Encephalopathy	3872065
BHMT	G742A: GG GA AA	 10.1±0.22 9.5±0.28 9.5±0.	Down syndrome Head and neck squamous cell carcinoma	23645037 21630102
CSE	NA	NA	NA	NA

Table 2. Plasma Hcy level in humans with a gene defect of Hcy major-metabolism enzymes: MTHFR, CBS, MS, BHMT and CSE. Change of plasma Hcy levels in humans

with the most common gene mutation and the observed pathologic phenotype. Abbreviations: BHMT, Betaine-homocysteine methyltransferase; CAD, Cervical artery dissection; CBS, human cystathionine-β-synthase; CSE, Cystathionine-γ-lyase; Hcy, Homocysteine; MTHFR, Methylenetetrahydrofolate reductase; MS, Methionine synthase; NA, unclear. Red frames emphasize the discoveries from Dr. Wang's laboratory.

Mouse model of HHcy

In order to study the role of HHcy in human disease, several animal models of HHcy have been developed, using animal species such as baboons, monkeys, minipigs, rabbits, rats and mice. The murine model of HHcy has an advantage over others due to the availability of many transgenic and gene-targeted strains. HHcy can be induced in mice via dietary modifications, genetic approaches, and combinations of dietary and genetic interventions. Commonly used dietary modifications include adding Hcy to drinking water; increasing the dietary content of Met, which is converted to Hcy after the methylation reaction; decreasing the dietary content of vitamin B6, which promotes the CBS-dependent conversion of Hcy to cystathionine; and decreasing the dietary content of folate and vitamin B12, which mediate the MTHFR-dependent conversion of Hcy back to Met. The drawback of diet-induced HHcy is that the elevation of Hcy is simultaneously accompanied by alterations in other metabolites such as Met, SAM and SAH, which have been shown to have adverse effects on vascular functions. The genetic model of HHcy included mice with a depletion of genes encoding MTHFR, CBS, MS, BHMT and CSE, as well as transgenic

mice that express the human CBS gene. The limitation of genetic HHcy is that the observed alternation of the vascular function may be due to other functions of the gene, rather than to the elevation of Hcy. Many experiments combine the dietary and genetic manipulations in order to generate mice with a wide range of plasma tHcy levels. The most frequently used mice models of HHcy, and their corresponding plasma Hcy level and pathology phenotype are summarized in **Table 3**. As it shows, *Cbs*$^{+/-}$ mice with plasma Hcy ~13.5 μM represent a model of mild HHcy. MTHFR$^{-/-}$ mice and *Cbs*$^{+/+}$ mice that are fed with an HM diet have plasma Hcy ~32μM and ~22μM, thereby representing a model of moderate HHcy. *Cbs*$^{+/+}$ mice that are fed with an HM diet have plasma Hcy ~90μM, thereby representing a model of moderate to severe HHcy. *Cbs*$^{-/-}$ mice, Tg-hCBS *Cbs*$^{-/-}$ mice, Tg-I278T *Cbs*$^{-/-}$ mice, Tg-I278T/T424N *Cbs*$^{-/-}$ mice and Tg-S466L *Cbs*$^{-/-}$ mice all have plasma Hcy>100μM, thereby representing a model of severe HHcy. *Cbs*$^{-/-}$ mice have a high neonatal lethality, thereby circumventing its use in the adult stage. The high neonatal lethality in *Cbs*$^{-/-}$ mice was found to be due to the lack of the *Cbs* protein, but not to the elevated Hcy. This is because Tg-I278T *Cbs*$^{-/-}$ mice, Tg-I278T/T424N *Cbs*-/- mice which expressed dysfunctional transgenic human CBS but developed severe HHcy did not have the high neonatal lethality that was observed in *Cbs*$^{-/-}$ mice(L. Wang et al., 2005). Compared to Tg-I278T *Cbs*$^{-/-}$ mice, Tg-I278T/T424N *Cbs*$^{-/-}$ mice and Tg-S466L *Cbs*$^{-/-}$ mice, Tg-hCBS *Cbs*$^{-/-}$ mice have a normal inserted human CBS CDNA, driven by a zinc-inducible metallothionein promoter. By adding $ZnSO_4$ into drinking water, the human CBS gene is expressed and HHcy is prevented. While withdrawing $ZnSO_4$ shut off CBS gene

expression and induced HHcy (Cheng et al., 2011). Therefore, Tg-hCBS *Cbs*$^{-/-}$ mice represent an ideal and currently the only conditional HHcy model. Tg-hCBS *Cbs*$^{-/-}$ mice that receive an Streptozotocin (STZ), High fat (HF) diet, or those with a depletion of ApoE, LDLR genes represent a model of both HHcy and metabolic disorder, which frequently

occur simultaneously in CVD patients. The observed phenotypes in these HHcy mice strongly suggest that HHcy plays an important role in CVD pathogenesis.

Genes	Manipulation	Plasma tHcy Level(μM)	Phenotype	PMID#
MTHFR	*MTHFR*$^{-/-}$	33.1 ± 4.1(M) 31.5 ± 6.8(F)	Epilepsy, vascular disease, methylation capacity, retardation, aortic lipid deposition, exacerbate lipid accumulation in ApoE deficiency	11181567
			Cerebellar defect	15979267
			Increased susceptibility to mild neonatal stress	20532821
			Impaired retinal function	20532821
	MTHFR$^{+/-}$	5.4 ± 1.0	Appear normal	
Cbs	*Cbs*$^{+/-}$	13.5 ± 3.2	Normal growth	7878023
			BBB permeability↑ leukoaraiosis, fornix inflammation↑, and cognitive impairment	23696861
	Cbs$^{-/-}$	203.6±65.3	Neonatal lethality, growth retardation, liver hypertrophy, multinucleated hepatocytes with lipid droplets	7878023
			Lung fibrosis	17543941
			Infertility	22617046
			Fat loss	22096601
			Hepatosteatosis, skeletal abnormalities, ocular disease, endothelial dysfunction	20971760
	Cbs$^{+/+}$, HM diet	23.5 ± 5		16189268
	Cbs$^{+/-}$, HM diet	98.4 ± 22	BBB permeability↑& leukocyte adhesion↑	22628578
	Cbs$^{+/+}$, HM diet	~22	EC dysfunction	25352635
	Cbs$^{+/-}$, HM diet	~88	EC dysfunction	
	Cbs$^{+/+}$, HM diet + STZ	~53	Potentiate HG-induced EC dysfunction	
	Cbs$^{+/-}$, HM diet + STZ	~173	Potentiate HG-induced EC dysfunction	
	Cbs$^{-/-}$*ApoE*$^{-/-}$	210.4±80	Atherosclerosis↑	12506016
	Cbs$^{-/+}$*ApoE*$^{-/-}$, HF+HM	154.9±90	Atherosclerosis↑	12506016
	Cbs$^{+/-}$*LDLR*$^{-/-}$, HM	244.6±50	Inflammatory MC↑, atherosclerosis↑	22628578
	Tg-hCBS Cbs$^{-/-}$	169.5±3.5	hCBS with normal CBS activity	21653942
	Tg-hCBS Cbs$^{-/-}$,*ApoE*$^{-/-}$, HF	107 ± 31	Inflammatory MC↑, atherosclerosis↑	25008174
	Tg-hCBS Cbs$^{-/-}$*ApoE*$^{-/-}$,*HF,STZ*	182 ± 20	Inflammatory MC↑, atherosclerosis↑	25008174
	Tg-I278T Cbs$^{-/-}$	~250	Lack CBS enzyme activity, low body weight and adiposity, facial alopecia, osteoporosis, liver steatosis.	15972722
	Tg-I278T/T424N Cbs$^{-/-}$	~274		15972722
	Tg-S466L Cbs$^{-/-}$	142±55	Lack AdoMet inducibility	18454451
MS	*MS*$^{+/-}$	9.7(F), 5.9(M)	Hematocrits	11158293
BHMT	*BHMT*$^{-/-}$	50.8±5.96	Fatty liver, hepatocellular carcinomas, altered choline metabolites	21878621
CSE	*CSE*$^{-/-}$, HF	140±5	H_2S↓, atherosclerosis↑	23704252
	CSE$^{-/-}$, cysteine deficient diet	165±7.1	Growth retardation	21310231
			Hypertension, VSMC proliferations↑, cardiac dysfunction	20051385

Wang lab models

Table 3. Plasma Hcy level in mice with a gene defect of Hcy major-metabolism enzymes: MTHFR, CBS, MS, BHMT and CSE. Various genetic and diet-induced HHcy animal models, and the observed pathologic phenotype. Abbreviations: BHMT, Betaine-homocysteine methyltransferase; CBS, human cystathionine-β-synthase; *Cbs*, Mouse cystathionine-β-synthase; CSE, Cystathionine-γ-lyase; Hcy, Homocysteine; HM, High methionine; HF, High fat; MTHFR, Methylenetetrahydrofolate reductase; MS, Methionine synthase; STZ, Streptozotocin. Red frames emphasize the discoveries from Dr. Wang's laboratory.

EC and MC are the major cellular target-mediating HHcy-related CVD

Despite HHcy being a well-established independent risk factor for CVD, the exact cellular mechanisms remain unclear. EC and MC are two frequently identified cellular targets of Hcy/HHcy (**Figure 3**).

EC injury and growth inhibition have been regarded as the primary mechanisms underlying Hcy-related CVD(Cheng, Yang, & Wang, 2009). Endothelium is the monolayer of EC's lining at the innermost layer of the vessel and heart. Compared to other cell types, CBS is relatively absent in EC. Moreover, endothelium is the first layer directing contact plasma, which have a far higher Hcy compared to other tissues, with the exception of the liver. Therefore, EC/Endothelium is one of the most vulnerable cell types in HHcy. EC/Endothelium is well known for its critical role in regulating vasomotor function, thrombosis, vessel permeability and blood-cell trafficking. Attacking the EC/Endothelium

layer has been demonstrated to be the initial and key event in CVD pathogenesis. Reported Hcy/HHcy-induced EC injury include EC activation, EC dysfunction and EC apoptosis/pyrotosis. EC activation is a pro-inflammatory and pro-coagulant state of the EC that is characterized by the upregulation of adhesion molecules and the release pro-inflammatory cytokines. It results in an increase of interactions with leukocytes, thereby facilitating their recruitment into inflammatory sites. The characteristics of Hcy-induced EC activation differ in different subtypes of EC. In human aortic EC (HAEC), Hcy-induced EC activation was featured by the upregulation of VCAM1, and by the increased production of CCL2 and IL8 (Poddar, Sivasubramanian, DiBello, Robinson, & Jacobsen, 2001). In human saphenous vein EC (HSVEC), Hcy-induced EC activation was marked by the upregulation of ICAM1 and by the increased production of IL6(Dalal, Parkin, Homer-Vanniasinkam, & Nicolaou, 2003). In human umbilical vein EC (HUVEC), Hcy-induced EC activation was characterized by the upregulation of ICAM1 and by the increased production of CXCL16 (Postea, Koenen, Hristov, Weber, & Ludwig, 2008). The characteristics of Hcy-induced activation of human brain microvascular EC (HBMEC) is unknown. However, several studies using bend3 cell, a rat microvascular-EC cell line, found an upregulation of ICAM1 by Hcy. The activation of different subtypes of EC by Hcy leads to the increase of leukocyte-EC adhesion: an initial and critical step for the infiltration of leukocyte into inflammatory sites. When EC inflammatory activation is accompanied with impaired endothelium-dependent vessel relaxation, the status is defined as EC dysfunction, which is the best characterized as Hcy/HHcy-induced EC injury.

Dysfunctional EC predisposes thrombosis formation, leukocyte adhesion and the development of CVD, such as coronary artery disease (CAD), and stroke and atherosclerosis (AS). In the presence of severe HHcy, EC can go through programed cell death, termed pyrop-apoptosis (Xi et al., 2016). Under normal conditions, the loss of EC can be repaired by reendothelialization, which can also be impaired by Hcy/HHcy via the inhibition of EC proliferation (Jamaluddin et al., 2007). In summary, Hcy/HHcy can promote the development of CVD by injuring the EC and by the inhibition of post-injury reendothelialization.

Enhanced leukocyte recruitment has been observed in aorta, leading to the development of HHcy-induced AS. Current evidence suggests that the enhanced leukocyte recruitment into HHcy-induced atherogenic lesion is not only due to the EC injury, but also to HHcy-induced systemic immune response (D. Zhang et al., 2012). Indeed, HHcy was not only found to be connected to CVD, but is also frequently associated with inflammatory disease, such as rheumatoid arthritis, inflammatory bowel disease and psoriasis, as well as other inflammation-related diseases, such as neurodegenerative disease(Durga, van Tits, Schouten, Kok, & Verhoef, 2005). Our lab clearly demonstrated that severe HHcy may promote inflammatory MC differentiation in both hyperlipidemia and a type1 diabetic mouse, accompanied with increased infiltration of inflammatory Ly6C^{hi} MC in atherogenic lesion and more severe AS(Fang et al., 2014; D. Zhang et al., 2012).In addition to promoting the differentiation of inflammatory Ly6C^{hi} MC, Hcy may also directly activate

MC. For example, Hcy may enhance the generation or secretion of various pro-inflammatory cytokines/chemokines, such as TNFα, IL6, CCL2(Capasso et al., 2012), IL-8(Zeng, Dai, Remick, & Wang, 2003) and CCL5(Sun, Wang, Zhang, Zeng, & Wang, 2005) IL1β(Su, Huang, Pai, Liu, & Chang, 2005) in human monocytic cell lines (THP-1) and primary human peripheral MC(Dai et al., 2008; G. Wang, Siow, & O, 2001). In line with in-vitro studies, the elevation of CCL2, IL6 and IL8 was also found in various mouse models of HHcy. In summary, HHcy promoted the leukocyte recruitment indirectly by injuring EC, or directly by promoting MC activation and the differentiation of inflammatory Ly6C^{hi} MC.

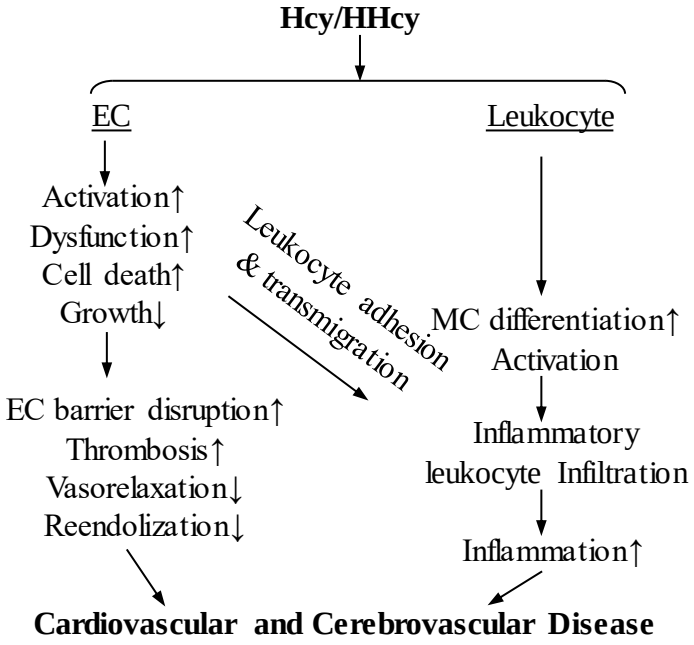

Figure 3. Potential cellular mechanisms underlying Hcy/HHcy-induced cardiovascular and cerebrovascular disease. EC and leukocyte are two cell types frequently found targeted by Hcy/HHcy. Hcy/HHcy induces EC injury, including EC

activation, EC dysfunction and EC cell death, thereby leading to increased EC barrier disruption, thrombosis, inflammation by increasing leukocyte recruitment, and by decreasing vasorelaxation and reendolization. Hcy/HHcy-induced inflammatory MC differentiation and leukocytes activation also play a critical role. Abbreviations: EC, Endothelial cells; Hcy, Homocysteine; HHcy, Hyperhomocysteinemia; MC, Monocyte.

DNA hypomethylation, excitotoxicity and oxidative stress are major molecular mechanisms that are involved in HHcy-related CVD

The exact molecular mechanisms underlying HHcy-induced cellular pathology and CVD are incompletely understood. Proposed molecular mechanisms involve DNA hypomethylation, excitotoxicity and oxidative stress (**Figure 4**).

The role of DNA hypomethylation in HHcy-related CVD−In mammals, DNA is a process that adds a methyl group to five positions of the cytosine of DNA. In adult somatic cells, DNA methylation typically occurred in a CpG dinucleotide, and it was reported that 60% and 90% of all CpGs were methylated in mammals. Unmethylated CpGs were often grouped in clusters, termed CpG islands, which often existed in many genes' five regulatory regions. Methylation of CpG sites in the promoter of a gene usually repressed gene expression. DNA methylation was catalyzed by DNA methyltransferase, which transferred methyl groups from S-adenosylmethionine to cytosine residues. It consisted of DNMT1, DNMT3a and DNMT3b. DNMT1 was the 'maintenance' methyltransferase, which was responsible for copying DNA methylation patterns to the daughter strands

during DNA replication. DNMT3a and DNMT3b were the de novo methyltransferases that created DNA methylation patterns in early development. DNMT1/3a/3b activity may be inhibited by SAH. The SAM/SAH ratio has been considered to be a positive indicator of DNA methylation. Our lab initially proposed Hcy-induced DNA hypomethylation as the main biochemical mechanism by which Hcy/HHcy induces vascular injury. As shown in figure 1, Hcy is catalyzed from SAH by AHCY and SAH is catalyzed from SAM after transferring the methyl group to target molecules. Under normal conditions, when the Hcy level is low and able to be removed efficiently, the methionine cycle favors the Methionine-SAM-SAH-HCY direction. However, in HHcy conditions, the direction can go backward, thereby resulting in an accumulation of SAH and a decrease of the SAM/SAH ratio. Abundant evidence has demonstrated a significant increase of SAH and a decrease of the SAM/SAH ratio in HHcy patients. For instance, CVD patients with HHcy also presented higher levels of SAH and a lower SAM/SAH ratio in plasma, accompanied with DNA hypomethylation(Castro et al., 2003). Folic-acid treatment lowered plasma Hcy and was accompanied by an increased SAM/SAH ratio(Stam et al., 2005). Our lab also clearly demonstrated a significantly increased SAH, and a decreased SAM/SAH ratio in the plasma of both genetically and HM diet-induced HHcy mice, both with and without hyperlipidemia and diabetes (Fang et al., 2014; D. Zhang et al., 2012). In in-vitro study, treating HAEC with Hcy caused the intracellular accumulation of SAH but not SAM, as demonstrated by two-dimensional thin layer chromatography analysis (H. Wang et al., 1997). The Hcy/HHcy-elevated SAH and Hcy/HHcy-decreased SAM/SAH ratio may

contributed to the inhibition of DNMT activity. Our lab found that the activity of DNMT1 but not that of DNMT3a/3b was decreased in HUVEC, HAEC and primary mouse MC treated with Hcy (Fang et al., 2014; Jamaluddin et al., 2007). The Hcy-induced inhibition of DNMT1 activity has been found to contribute to the hypomethylation of the promoter CpG Island of cyclin A (Jamaluddin et al., 2007), ICAM1 (unpublished data) and CD40 (Yang et al., 2016), and to the transcriptional downregulation or upregulation of these genes. The overexpression of DNMT1 prevents the Hcy-induced upregulation of ICAM1 in HAEC and CD40 in MC, and the downregulation of cyclin A1 in HUVEC. In conclusion, Hcy-induced DNA hypomethylation occurs by increasing SAH and inhibiting DNAMT1 activity, thereby resulting in the upregulation of ICAM1 and CD40, and the downregulation of cyclin A.

The role of excitotoxicity in HHcy-related CVD −The hypothesis that Hcy was an excitatory amino acid begins with Lipton SA's findings: Hcy acted as an agonist at the glutamate binding site of the N-methyl-D-aspartate receptor (NMDAR), the activation of which can lead to excessive calcium (Ca^{2+}) influx, oxidative stress and increased neuron-cell death (Lipton et al., 1997). The NMDA antagonist, MK801, or antioxidants could block Hcy-induced neuron-cell death. Neurotoxicity that was mediated by the activation of the NMDA receptor was dependent upon the condition of ischemia (Siesjo, Bengtsson, Grampp, & Theander, 1989). In physiological conditions, concentrations of the excitatory neuro-transmitters, such as glutamate, aspartate, cysteine and Hcy were found very low in

the cerebrospinal fluid, compared to plasma. For example, the detected Hcy level was only 0.02 μmol/L in cerebrospinal fluid, which was 500 times lower than the 10μmol/L that was usually detected in plasma (McCully, 2009). However, in stroke there was a significant elevation of excitatory neuro-transmitters, such as GABA, glycine, taurine, L-glutamate and L-aspartate(Sergeant & Meyns, 1997). If Hcy experienced the same increase as glutamate did in the ischemic brain, it is possible that Hcy exacerbated stroke-induced brain injury by increasing neuron vulnerability to excitotoxicity through the activation neuron NMDA. NMDA glutamate receptors were also detected and widely expressed in cultured rat cerebral-endothelial cells, aortic endothelial cells and other peripheral vasculature (Chen et al., 2005; Krizbai et al., 1998). Hcy/HHcy was found able to impair brain-EC tight junction by reducing claudin-5 expression (Beard, Reynolds, & Bearden, 2011).

The role of oxidative stress in HHcy-related CVD−Oxidative stress is a condition that is defined as an imbalance between ROS production and antioxidant-scavenging capacity. It has also been regarded as one of the major mechanisms underlying Hcy-induced risk of CVD, starting from the observation in studies that antioxidants such as Vitamin C and vitamin E can effectively block HHcy-impaired vascular EC dysfunction in humans (Chambers, Obeid, & Kooner, 1999; Nappo et al., 1999; Ong, 1976). Our lab demonstrated that superoxide was increased Hcy-treated EC, mediating calpain-induced eNOS and EC dysfunction (Cheng et al., 2015), and caspase1-mediated EC apoptosis/proptosis (Xi et al., 2016). Increased ROS was also observed in MC of hyperlipidemia mice with genetic

HHcy. Inhibition of ROS by apocynin or superoxide dismutase (SOD) can block Hcy-induced MC differentiation (D. Zhang et al., 2012). It has also been demonstrated that Hcy-induced oxidative stress was a key mediator of cerebral EC dysfunction (Dayal et al., 2004). Reported mechanisms underlying Hcy-induced oxidative stress include the following: 1) Hcy autoxidation, 2) inhibition of antioxidant enzymes such as SOD, glutathione peroxidase or heme oxygenase -1, 3) eNOS uncoupling, 4) mitochondria dysfunction and 5) NADPH oxidase activation. NADPH oxidase has been consistently identified as the major source of ROS. But the specific isoform involved was cell-type and species specific. For example, in cultured HUVEC, Hcy treatment increased membrane translocation and the expression level of P47phox, resulting in cell apoptosis and upregulation of VCAM1 (Carluccio et al., 2007; Dong et al., 2005; Sipkens et al., 2013). In bend3 cells, Hcy increased the mRNA level of NOX4, which may be involved in MMP activation, mitochondria toxicity and EC dysfunction (Kamat, Kalani, Tyagi, & Tyagi, 2015; Tyagi et al., 2009). The exact molecular mechanism participating in Hcy-induced NADPH oxidase activation is unclear. P38 MAPK activation, PKC activation and NDMA

activation were reported in VSMC/MG, HUVEC and bend3 cells treated with Hcy respectively.

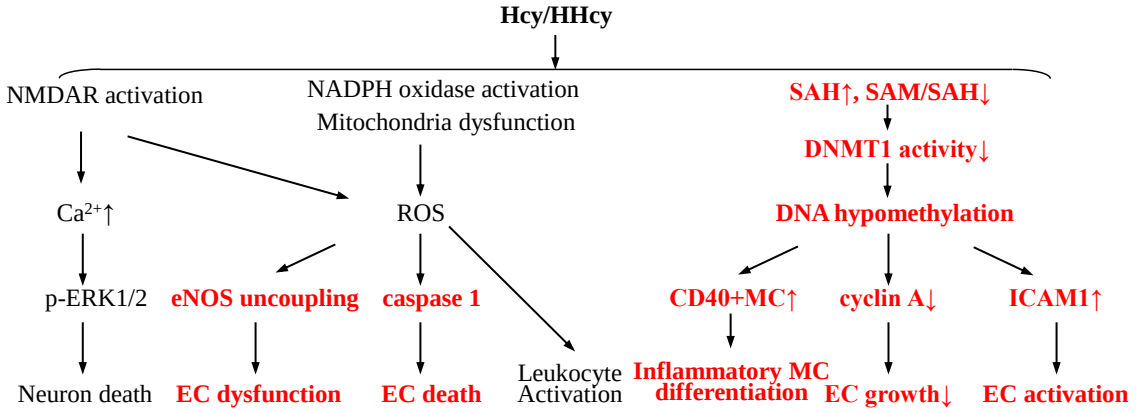

Figure 4. Proposed molecular mechanisms underlying HHcy-induced EC, leukocyte and neuron pathology. Hcy/HHcy can directly activate NMDAR, leading to calcium (Ca^{2+}) influx, subsequent ERK1/2 phosphorylation and neuron-cell death. Hcy/HHcy also increase ROS generation by promoting NADPH oxidase activation or mitochondria dysfunction, thereby leading to EC dysfunction via inducing eNOS uncoupling, or to EC death via acting-caspase1 or leukocyte activation. Moreover, Hcy/HHcy induces DNA hypomethylation by increasing SAH, decreasing the SAM/SAH ratio and decreasing subsequent DNMT1 activity, thereby resulting in inflammatory MC differentiation via increasing CD40+MC, to EC-growth inhibition via decreasing cyclin A transcription and to EC activation via upregulating ICAM1. Abbreviations: EC, Endothelial cells; ENOS, endothelial constitutive nitric oxide synthase; DNMT, DNA methyltransferase; Hcy, Homocysteine; HHcy, Hyperhomocysteinemia; ICAM1, Intercellular adhesion molecule 1; MC, Monocyte; NMDAR, N-methyl-D-aspartate receptor; NADPH, Nicotinamide

adenine dinucleotide phosphate; SAM, S-adenosylmethionine; SAH, S-adenosylhomocysteine. Words highlighted in red indicate discoveries from our laboratory, led by Dr. Hong Wang.

HHcy lowering therapies

In humans, the elevation of plasma Hcy can be prevented by a low-HM diet, and by the dietary supplement of folic acid, B12, betaine and B6. Low-HM diet reduces the source of Hcy. Folic acid and B12 help Hcy remethylated back to Met by MS. Betaine help Hcy remethylated back to Met by BHMT. B6 facilitates the conversion of Hcy to Cys by CBS. It has been reported that 0.5-5 mg folic acid daily can alone reduce the blood Hcy level by 25% and that 0.5 mg B12 daily resulted in an additional reduction of 7%. A daily 16.5 mg B6 does not have additional effects("Lowering blood homocysteine with folic acid based supplements: meta-analysis of randomised trials. Homocysteine Lowering Trialists' Collaboration," 1998).The effect of folic acid alone or combined with B12 and/or B6 on plasma Hcy level is summarized in **Table 4**. As it shows, a low dose of folic acid (0.8mg) alone is sufficient to lower plasma by Hcy >2 μM or >20%. Betaine has also been shown to be an effective strategy for lowering Hcy. It has been reported that the supplementation with 4 g/d of betaine for six weeks can lower the plasma Hcy level by ~1.23μmol/L(McRae, 2013). However, betaine intake is only effective when body Met is present in small quantities. Betaine therapy is therefore usually accompanied with a low-Met diet. The specific strategy can vary according to the cause of HHcy. Nutritional inadequacy caused

by HHcy can be simply corrected by adding folic acid, B12, betaine and B6. In CBS deficiency-induced HHcy, high doses of B6 plus folic acid and betaine have been suggested. For those who do not respond to B6, a low-Met diet plus betaine and folic acid is the only available therapy.

Stroke is the leading cause of long-term disability

Epidemiology of stroke

Stroke is the third most common cause of death and the leading cause of serious long-term disability in the adult population (Capasso et al., 2012). In the USA, over 795,000 people have a stroke every year, 18,500 of which (1/4) occur in people who have had a previous stroke. Annually, 130,000 people die as the result of stroke (Mozaffarian et al., 2015). Stroke can be divided into ischemic stroke which constitutes 87% of stroke, and hemorrhagic stroke which accounts for the remaining 13%. Ischemic stroke is caused by the blockade of a blood vessel from an atherosclerotic or blood clot while hemorrhage stroke is caused by the rupture of a vessel, mostly due to hypertension. Irrespective of the cause, both types of stroke finally lead to blood-flow cut-off, after which brain cells die due to the deprivation of oxygen and nutritional supply. Well-identified risk factors for stroke include stroke history, atrial fibrillation, high cholesterol, hypertension, diabetes and HHcy. In this study, we focus on the ischemic stroke due to its far higher incidence.

Pathologic events in acute phase of ischemic stroke

When a brain artery is blocked, the blood flow of the central region that is supplied by the affected artery is reduced to less than 20% of the baseline. As brain tissue is very highly demanding of oxygen and glucose, this central region goes through severe energy failure within minutes, resulting in anaerobic glycosis, lactic acidosis and failure of Na^+/K^+-ATPase. Failure of Na^+/K^+ pumps cause neuronal depolarization, intracellular Ca^{2+} overload and the subsequent release of neurotoxic substances, such as excitatory neurotransmitters, ROS, lytic enzymes and inflammatory mediators, which together cause neuronal necrosis. These cascade processes occur so quickly that there is practically no chance to rescue this area, which is described as the 'infarct core' (**Figure 5**). In the area surrounding the infarct core, the blood flow has been reported to be reduced to ~40% of the baseline due to its receiving partial blood flow from collateral arteries. This extent of blood-flow reduction is not sufficient to cause severe energy failure but able to induce neuronal dysfunction and brain microvascular injury. This area is termed the 'penumbra' and can be rescued back to become healthy tissue if the blood flow is restored on time (within 4.5h for humans). However, the penumbra is very vulnerable, as it is subjected to a wave of deleterious metabolic processes that are propagated from the infarct core, as well as to immune-cell invasion from circulation, leading to the expansion of the ischemic core and the exacerbation of initial brain injury. Mice stroke results from middle cerebral artery occlusion (MCAO) and the striatum is usually the infarct core. The neurons' deaths occur

rapidly and mostly are necrotic. In contrast, the cortical infarction is more delayed, and accompanied with a prolonged and biphasic opening of the blood brain barrier, and inflammatory cell infiltration, followed by a progressing neuron-cell death.

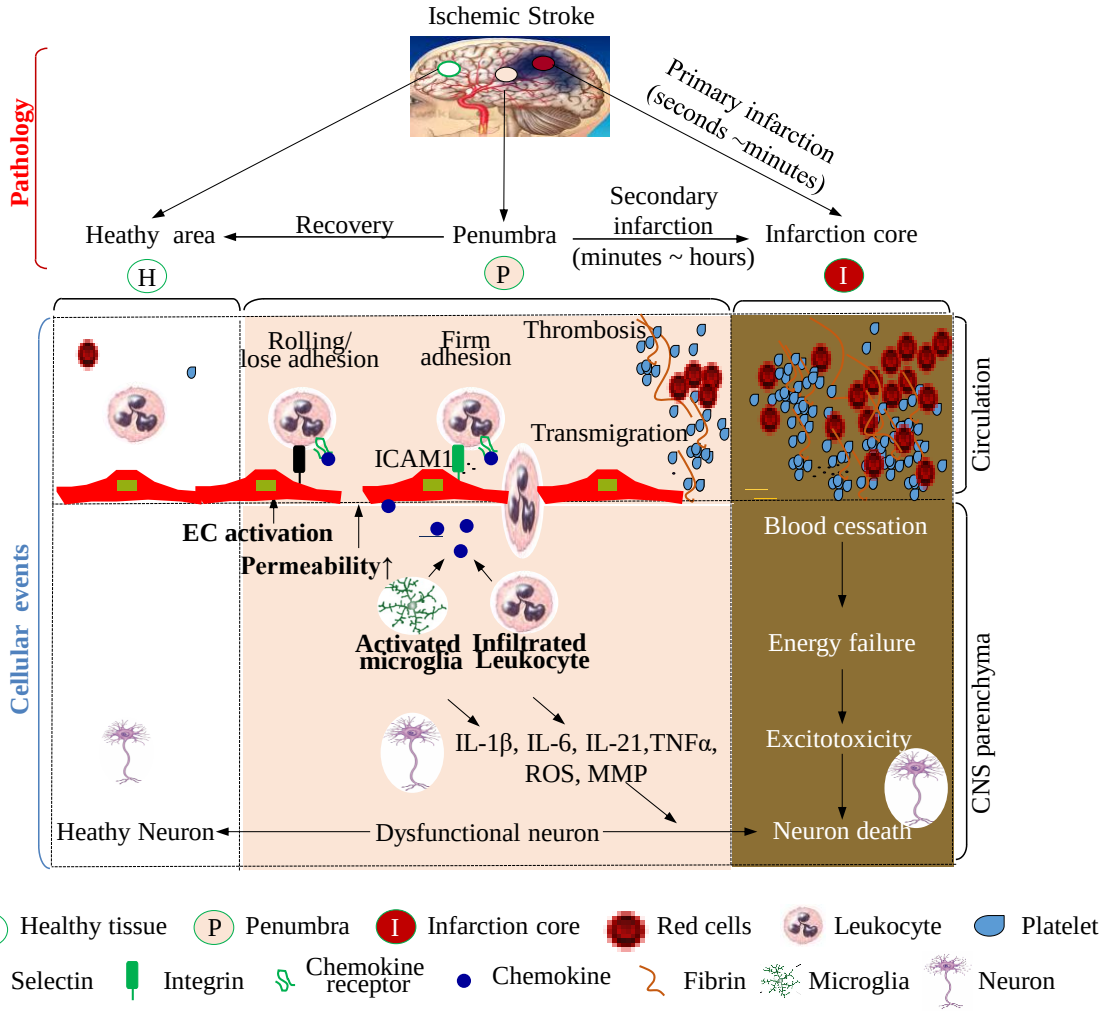

Figure 5. Major pathological and cellular events in the acute phase of ischemic stroke.

In the case of stroke, the brain can be divided into three different areas (healthy, penumbra and infarction core). The healthy area is that with normal blood flow and without injury. The penumbra is the area surrounding the infarction core and has a partial decrease of blood

supply because it still receives blood from collateral arteries. The infarction core is the area with complete cessation of the blood flow and death of neurons, and develops immediately (within seconds to minutes) following the stroke. The penumbra contains injured but viable neurons, which can be recovered to healthy tissue with timely reperfusion. In contrast, without or with delayed reperfusion, the penumbra will become irreversible infarct tissue, described as 'secondary infarction growth'. Major cellular events that promote secondary infarction growth include the increase of brain-endothelial cells' permeability, activation of brain-endothelial cells, activation of resident microglia cells and infiltration of leukocyte. Activated EC upregulates adhesion molecules, including E-selectin and P-selectin, which mediate the leukocyte rolling and loose adhesion, and VCAM1 and ICAM1, which mediate leukocyte firm adhesion and transendothial migration. Activated EC, microglia and infiltrated leukocyte will secrete chemokines such as ccl2 and ccl3 to attract more leukocyte infiltrating into the penumbra. Infiltrated leukocytes also produce proinflammatory cytokines (IL1β, IL6, IL21 and TNFα), and proteolytic enzymes MMP and ROS, which together promote the dysfunction neuron into death neuron. Within the infarction core, severe cessation of blood flow leads to energy failure, which results in excitotoxicity and finally to neuron-cell death. The lines with arrows indicate permissive actions. Abbreviations: BBB, Blood brain barrier; EC, Endothelial cells; MG, Microglia; ROS, Reactive oxygen species.

Brain inflammation mediates stroke-induced brain injury

Accumulating evidence suggest that inflammation contributes to secondary brain injury. The brain's inflammatory response after stroke is initially triggered by the inflammatory mediators that are released from the necrotic neurons in the infarct core. It is characterized by the activation of microglia (MG) and the peripheral leukocyte influx into the cerebral parenchyma (**Figure 5**). However, the temporal profile and roles of different leukocyte subsets infiltrating into the brain are distinct and summarized as follows:

The role of MG activation in stroke-induced brain injury − MG is the 'resident macrophage' of the brain. In physiological conditions, MG plays an important role in the phagocytosis of developing/adult neurons and in monitoring their synapse. In pathologic conditions, it has been demonstrated to be involved in many brain diseases, such as experimental allergic encephalomyelitis (EAE)(Horstmann et al., 2016), multiple sclerosis (Jack, Ruffini, Bar-Or, & Antel, 2005), neurodegenerative disease(Plaza-Zabala, Sierra-Torre, & Sierra, 2017)and stroke(Patel, Ritzel, McCullough, & Liu, 2013). In the rodent tMCAO model, MG activation occurred within minutes after MCAO, preceding any type of circulation-derived infiltration of immune cells (Kennedy, 1992), the number of which increased as early as within 2h and lasting up to 16 weeks. Activated MG developed macrophage-like capabilities including phagocytosis, cytokine production, antigen presentation and secretion of matrix metalloproteinases (MMP). These events acted on the brain EC, thereby inducing an increase of BBB permeability, the upregulation of adhesion

molecules and finally triggering circulating-leukocytes rolling, adhesion and infiltration into the ischemic area (Patel et al., 2013). Activated MGs induced in stroke were shown be either detrimental or neuroprotective, depending on the subtype of MG(Tang & Le, 2016). M1 phenotype MG is regarded as a malefactor, being characterized by reduced phagocytosis, activation via toll-like receptors or interferon-γ and secretion of pro-inflammatory cytokines, such as TNFα, IL1β and IL6, as well as other potential cytotoxic molecules, such as NO and ROS. M2 phenotype MG, on the other hand, was considered to be a benefactor, being characterized by activation by IL4 or IL13 and secreting factors that are critical for angiogenesis and matrix remodeling. In stroke, whether MG is activated into M1 or M2 phenotype is temporally dependent. In the in-vitro model of the ischemia, Hu demonstrated that, in the early stage of the ischemic condition, MG was mainly activated into neuroprotective M2 phenotype, while in the later stage, MG was transformed into M1 phenotype(Hu et al., 2012). However, in human stroke, it is unclear how the temporal profile for activated MG switches from M2 to M1. Current study into Hcy's effect on MG is limited and only one study has demonstrated that Hcy promoted MG proliferation and activation through an oxidative stress-related mechanism (Zou et al., 2010). However, it is unknown whether Hcy induces MG proliferation and activation, and whether M1/M2 phenotypes switch in stroke disease settings.

The role of MC infiltration in stroke-induced brain injury − MC is one of the predominant types of immune cells that infiltrate into the brain after stroke. In the brain, circulatory-

derived MC is distinct from MG by its higher expression level of CD45 (Hammond et al., 2014). In both the transient MCAO and permanent MCAO models (Chu et al., 2014), MC began infiltrating into the brain as early as within 3h, peaking at around 72h and subsequently slowly regressing until two weeks after. Compared to permanent MCAO, transient MCAO has been shown to have a higher percentage of infiltrated MC among all infiltrated leukocytes at 24h post-tMCAO. Infiltrated MC was located around the microvesel at an early point in time and subsequently invaded into the brain parenchymal. The role of MC in stroke remains incompletely understood. In clinical study, it has been demonstrated that the baseline absolute-blood MC count was positively associated with 30-day mortality (Walsh et al., 2015). In mice experiments with the focal-ischemic model, blocking MC invasion by using $CCR2^{-/-}$ mice or $CCL2^{-/-}$ mice effectively reduced stroke-induced neuron injury and neurological deficit(Dimitrijevic, Stamatovic, Keep, & Andjelkovic, 2007; Hughes et al., 2002). MC was a heterogeneous population of cells with different functions. In mice, cell-surface expression levels of Ly6C MC were divided into $Ly6C^{+}$ MC (further divided into $Ly6C^{hi}$ + $Ly6C^{mid}$) and $Ly6C^{-}$ MC (also known as $Ly6C^{lo}$). In humans, MC was divided into the classical subset ($CD14^{++}CD16^{-}$), the intermediate subset ($CD14^{++}CD16^{+}$) and the non-classical subset ($CD14^{+}CD16^{++}$)(Yang, Zhang, Yu, Yang, & Wang, 2014). According to the biological function, mouse $Ly6C^{+}$MC or human classical/intermediate MCs were considered to be inflammatory MC which has a high expression level of CCR2 and a low expression level of CX3CR1, whereas $Ly6C^{-}$MC or non-classic MC were anti-inflammatory MC which has a low expression level of CCR2

and a high expression level of CX3CR1. Inflammatory MC have a higher capacity to produce ROS, TNFα and IL1β in response to LPS, while anti-inflammatory MC had a reduced phagocytic ability, producing high levels of anti-inflammatory cytokine IL10 and low levels of TNFα in response to LPS(Yang et al., 2014). In the acute phase of ischemic stroke, both the $Ly6C^+$ and $Ly6C^-$ subsets were found to be significantly increased in the ischemic brain. However, the absolute $Ly6C^+$MC numbers that were accumulated in the brain were several folds higher than $Ly6C^-$MC, suggesting that $Ly6C^+$MC was the predominant MC subset that infiltrated into the ischemic brain (Miro-Mur et al., 2016). It was unclear whether the detected ischemic brain $Ly6C^-$MC derives from the transmigration of circulatory $Ly6C^-$MC or from the differentiation of already infiltrated brain $Ly6C^+$MC. However, adoptive transferred $CD45.1^+Ly6C^+$ did not differentiate into $Ly6C^-$MC at least within 24h after MCAO. After 24h, however, $Ly6C^+$MC gradually downregulated Ly6C, and upregulated F4/80, arginase-1 and YM-1, thereby becoming an M2-like macrophage(Miro-Mur et al., 2016). Despite the appropriate characterization of different MC subset infiltrations after stroke, the exact contribution of each MC subsets in stroke remains elusive. In a mice intracerebral hemorrhage stroke model, both $CCR2^{-/-}$ mice and WT mice receiving $CCR2^{-/-}$ hematopoietic cells transplantation have a better motor function than WT or chimeric WT mice, accompanied with significantly less $Ly6C^+$MC. This study supports the hypothesis that $Ly6C^+$MC mediates stroke-induced brain injury(Hammond et al., 2014). However, a recent study had opposite findings, suggesting that mice receiving INCB3344, a selective CCR2 antagonist, have significantly less

Ly6C$^+$MC infiltration but markedly worse functional outcomes and larger infarct volumes compared to vehicle-treated mice at 24h after tMCAO(Chu et al., 2015). Therefore, further experiments need to be conducted in order to confirm the exact role of Ly6C$^+$MC within 24h after stroke. As our lab has demonstrated that HHcy promotes the inflammatory Ly6C$^+$MC differentiation, it would be interesting to investigate how HHcy affects the inflammatory Ly6C$^+$MC infiltration and Ly6C$^+$MC differentiation after stroke.

The role of NØ infiltration in stroke-induced brain injury − Within 15min after stroke, circulatory NØ begins to attach cerebral EC by binding EC-adhesion molecules, including P selectin (SELP)/E, selectin (SELE) and VCAM1/ICAM1 via its EC-interacting molecules PSGL1/ESL1 and LFA1/VLA4. Around 6h after stroke, NØ can be detected in the brain microvesel and the infiltration begins, peaking at around day 1-3 and subsequently rapidly declining to a normal level at around day 4-7 (Gronberg, Johansen, Kristiansen, & Hasseldam, 2013). It continues to be debated whether NØ or MC invades into the brain first, but there is consensus that both NØ and MC are the predominant infiltrated leukocytes within 24h after stroke. The numbers of accumulated NØ in the infarct area, as well as the number of NØ in blood were found to be positively correlated with the severity of brain injury and neurological deficit after ischemic stroke(Buck et al., 2008). Depleting NØ or blocking its adhesion to/transmigration across the brain EC effectively reduced stroke-induced brain injury. For example, it has been shown that the anti-PMN leukocyte-depleting antibody, which depleted ~90% of NØ without affecting

other leukocytes counts as effectively reduced, stroke-induced, IL1β-exacerbated brain injury in the tMCAO mice model (Erba, Fadel, & Famula, 1991). NØ damaged the brain by releasing ROS (superoxide, hypochlorous acid), proteases (MMP, elastase, cathepsin G and proteinase 3) and pro-inflammatory cytokines (IL1β, IL6, IL8 and TNFα)(Jickling et al., 2015). Compared to other immune cells, NØ had the highest ROS generation, together with MMP9, which was the key molecule mediating the disruption of the blood brain barrier (BBB) by degrading EC tight-junction molecule claudin5, basal lamina and type IV collagen. NØ adhesion in microvasculature may also accelerate thrombosis. Altogether, these events result in reduced reflow and thus worse ischemic damage. Study into Hcy's effect on NØ is limited. It has been demonstrated that Hcy may promote NØ adhering to peripheral EC by stimulating its ROS generation, but our study will be the first to test the effect of HHcy on NØ recruitment during stroke.

Role of Lymphocyte (Lym) infiltration in stroke-induced brain injury − Compared to NØ and MC, Lym was previously regarded to be relatively late in infiltrating immune cells in stroke. However, recent studies have demonstrated that the temporal prolife of T-cell recruitment varied in subtypes of T cells. $CD4^+$ T-helper cells were recruited in the ischemic brain as early as 4h post-MCAO and peaked at 24h post-MCAO, while $CD8^+$ cytotoxic T cells infiltrated around day three post-MCAO. Other types of T cells, such as regulatory T cells, accumulated after day three post-MCAO and persisted in the ischemic hemisphere for up to 30 days(Stubbe et al., 2013). T cells were detrimental in the acute and

subacute phases of stroke. This finding was supported by evidence showing that mice with wither $CD4^+$ T cell or $CD8^+$ T cell deficiency had a reduced infarction volume and neurological deficit compared to WT mice, at 24h post-MCAO. Adoptive transfer of either $CD4^+$ or $CD8^+$ T cells to $RAG1^{-/-}$mice, which lack both T and B Lym equally, fully restored the susceptibility for stroke. B cells did not mediate early ischemic-brain damage 24hafter tMCAO, because the adoptive transfer of B cells into $RAG1^{-/-}$mice did not restore the susceptibility of $RAG1^{-/-}$ mice to stroke (Kleinschnitz et al., 2010). It is currently unclear which the mechanisms underlie T-cell mediated brain injury at early stroke. A recent study demonstrated that IL21 generated in $CD4^+$T cells may account for the early detrimental effect of recruited T cells (Clarkson et al., 2014). IL21-deficiency mice had significantly reduced infarct volume and neurological deficit. IL21 from $CD4^+$ T cells mediates stroke-induced brain injury by promoting neuron autophagy and implying the recruitment of both $CD4^+$ and $CD8^+$ T cells.

Peripheral inflammatory response is triggered by stroke and involved in stroke-induced brain injury

In addition to inducing brain-specific immune responses, ischemic stroke also dynamically triggers peripheral immune responses that can either be deemed to be adaptive cerebroprotective reactions that limit cerebral inflammation, or adjunctive detrimental events that exacerbate cerebral inflammation. Alternations of the systemic immune response, such as exacerbating the pro-inflammatory response by the administration of

Lipopolysaccharides (LPS) or IL1 can aggravate stroke-induced brain damage or neuroinflammation(McColl, Rothwell, & Allan, 2007). One of the characteristics of stroke-induced systemic immune response is the change in number of circulatory leukocytes. In patients with ischemic stroke, the elevated white blood cell count (WBC) on admission has been associated with stroke severity and poor functional outcome (Audebert, Rott, Eck, & Haberl, 2004), (Furlan, Vergouwen, Fang, & Silver, 2014). Compared to the cell count of other leukocytes in blood, the NØ count is the most meaningful in predicting stroke prognosis. Elevated NØ is an early indication of ischemic brain injury, and is associated with larger infarction volume and higher mortality. On the contrary, the Lym count was found to be decreased in the acute phase of ischemic stroke, which is inversely associated to poor outcome. In addition to the absolute number of NØ or Lym, the NØ to Lym ratio (NLR) recently emerged as an independent marker by which to predict the stroke prognosis (Xue et al., 2016). NLR was observed to be elevated for ischemic stroke patients after admission. Higher NLR predicted higher neurological deficit and mortality, and recurrent ischemic stroke, independently of infarction volume (Tokgoz, Keskin, Kayrak, Seyithanoglu, & Ogmegul, 2014) (Qun et al., 2017; Tokgoz et al., 2013). Compared to the NØ or Lym count, NLR was more adequate in predicting the stroke-hemorrhagic transformation(Guo et al., 2016). The total MC count has not been found to be changed in stroke patients. However, the number of blood-classical MCs ($CD14^{++}CD16^{-}$) that are equivalent to rodent pro-inflammatory $Ly6C^{hi}$ MC was found to be significantly increased at two days after the onset of stroke, while the number of non-classical MCs

($CD14^{+}CD16^{++}$) that was equivalent to rodent anti-inflammatory $Ly6C^{low}$ MC was found to be decreased (Kaito et al., 2013). Classical MC has also been reported to be positively associated with poor outcome and high morality in all types of stroke, while non-classical MC had the opposite effect (Kaito et al., 2013). In the mice tMCAO model, the temporal profile of circulatory response was different. The number of pro-inflammatory NØ and $Ly6C^{hi}$ MC was found to be increased within 6h after MCAO and subsequently decreased below pre-ischemic levels at 24h post-MCAO (Kim, Yang, Beltran, & Cho, 2014). In severe stroke, the number of all types of leukocytes in blood has been shown to dramatically decrease at 24h post-MCAO. This phenomenon was considered to be stroke-induced immunosuppression. Our study further investigates the effect of ischemic stroke on the blood cell count of NØ, Lym, $Ly6C^{low}$MC, $Ly6C^{hi}$ MC and NLR in an HHcy setting.

Brain-EC activation is required for circulatory immune cells' recruitment

Leukocyte recruitment to the microvasculature is the rate-limiting step in stroke-induced brain inflammation. The recruitment process was highly coordinated and dependent on the interaction of adhesion molecules that were expressed on the brain microvascular endothelial cells (BMEC), including intercellular adhesion molecule 1 (ICAM1), vascular cell-adhesion protein (VCAM1), selectin E (SELE), selectin P (SELP) and EC-interacting molecules expressed on circulatory leukocytes such as P-selectin glycoprotein ligand1 (PGSL1), E-selectin ligand1(ESL1), Lym function-associated antigen-1(LFA1) and macrophage-1 antigen (Mac1). Normally, adhesion molecules' expressions in the BMEC

level were far lower than in peripheral EC. ICAM1 and VCAM were constitutively expressed, while SELE and SELP were only induced. In response to ischemia/reperfusion injury, brain EC was activated and characterized by upregulation of SELE, SELP, VCAM1 and ICAM1. SELP was found to be upregulated as early as 15min following ischemia injury, while SELE induction occurred around 2h after ischemia. Upregulation of ICAM1 was reported at around 4h after ischemia(Yilmaz & Granger, 2008). Circulatory leukocytes constitutively express a high level of ESL1, PGSL1, LFA1 and Mac1, which may also be further induced after stroke. The leukocyte-recruitment process began with a low affinity process, manifested as rolling, which was mediated by the interaction between PGSL1 and SELE/SELP, followed by a high-affinity binding that was manifested as firm adhesion and mediated by the interaction between LFA-1/VLA4 with ICAM1/VCAM1, and finally the transmigration of leukocyte across BMEC. Blocking or knockout of SELE, SELP and ICAM1 has been shown to be protective in stroke by reducing the infiltration of leukocytes (Yilmaz & Granger, 2008).

However, VCAM1 appeared to be dispensable, as blocking VCAM1 with antibodies did not reduce the infarction volume, neurological deficit, or mortality after stroke(Justicia et al., 2006). When EC activation progressed into more severe EC injury, such as cell death, and water and other toxic-plasma constituents such as thrombin or tPA entering the brain, thereby causing vasogenic edema, direct neuron damage and more severe leukocyte influx. As described above, it has been well established that Hcy/HHcy may induce EC activation

and injury in a no-stroke setting. We hypothesize that HHcy also activates EC after stroke and will identify the responsible adhesion molecule that is involved in HHcy-induced brain EC activation.

DNA methylation, excitotoxicity and oxidative stress participated in stroke-induced brain injury

The role of DNA methylation in stroke-induced brain injury − Emerging evidence suggests that DNA methylation plays a role in the pathophysiology of stroke. Clinical studies have reported that patients with stroke exhibited global DNA hypomethylation in blood. In addition, longitudinal analyses show that people with global DNA hypomethylation are at higher risk of incident-ischemic heart disease and stroke(Baccarelli et al., 2010). However, the global blood DNA-methylation status did not differ between subtypes of ischemic stroke, including large-artery atherosclerosis (LAA), small-artery disease (SAD) and cardio-aortic embolism (CE)(Soriano-Tarraga et al., 2014). In experimental studies, the increase of DNA-methylation levels has been observed in mildly ischemic brains of wild type (WT) mice at 12h after 30-min MCAO(Endres et al., 2000). Mice with a reduced DNMT level or those administrated with DNMT inhibitor 5-aza-2'-deoxycytidine developed less infarction volume after a 30-min MCAO and 12h of reperfusion. However, with severe ischemic brain injury induced by a longer time (two h) of MCAO occlusion and 22h of reperfusion, the DNA methylation of the ischemic brain had not changed and reducing the DNMT level or inhibiting DNMT activity did not reduce stroke-induced

infarction. The same research group using mice with neuronal-specific know-down or knockout of DNMT1 found that infarct volume was less in mice with a reduced level of neuronal DNMT1, but not in mice with total neuronal DNMT1 depletion. The results from these two studies suggest that the role of DNA methylation in stroke-induced brain injury was cell-type and ischemic injury-severity dependent (Endres, Fan, Meisel, Dirnagl, & Jaenisch, 2001; Endres et al., 2000). A recent study using the same mice-stroke model confirmed the elevation of brain DNA methylation and the protein level of DNMT1/3a in the ischemic brain. Interestingly, in $Ins2^{+/-}$ Akita mice, a type 1 diabetic model, both the brain DNMT1 protein and global DNA-methylation level were significantly decreased after 40min of MCAO and 24h of reperfusion (Kalani, Kamat, & Tyagi, 2015), thereby suggesting that the role of DNA methylation in stroke was also disease specific. The mechanisms by which DNA methylation contributes to stroke pathology are incompletely understood. It has been demonstrated that DNA hypomethylation occurs and participates in the transcriptional regulation of the estrogen receptor α (ERα) gene after 24h of MCAO. This occurred selectively in female rats, indicating that the role DNA hypomethylation in stroke is also gender dependent and may explain why sex affects stroke response (Westberry, Prewitt, & Wilson, 2008). Our lab has established abundant evidence showing that the DNA hypomethylation was induced by Hcy/HHcy in cultured HAEC and was accompanied with decreased DNMT1 activity. Moreover, increase of SAH and decrease of the SAM/SAH ratio has been observed in the brain of our Tg-hCBS *Cbs*$^{-/-}$ mice. It is

therefore possible that HHcy-altered brain-DNA methylation plays a role in stroke-induced brain injury.

The role of excitotoxicity in stroke-induced brain injury −As described above, after the onset of ischemic stroke, neurons were deprived of energy, hereby leading to dramatically reduced ATP generation and subsequent loss of Na^+/K^+ ATPase function, followed by membrane depolarization. This resulted in the activation of voltage-gated calcium channels and the release of excitatory amino acids (particularly glutamate) into the extracellular compartment. Excess glutamate over-activated calcium-permeable NMDAR on postsynaptic cells, which finally induced neuron-cell death. This phenomenon was termed "Excitotoxicity" in stroke. In rat-experiment stroke, glutamate is detected in high concentrations in the penumbra. In clinical studies, plasma concentration of glutamate is correlated with early neurological deterioration. Over-activated NMDAR by excess glutamate can induce neuron-cell death through several mechanisms. Firstly, NMDAR stimulation triggers the calcium-dependent and calpain-dependent proteolysis of NCX3, p35, STEP61, insig1 and mGluR1, thereby leading to neuron-cell death. In addition to the activation of the calpain pathway, NMDAR-mediated calcium overload caused mitochondrial dysfunction, thereby leading to the subsequent activation of the mitochondrial and caspase-dependent apoptosis pathway. As Hcy has been identified as the agonist of NMDAR, it would be interesting to detect whether Hcy experiences the same

increase as glutamate in ischemic brain and exacerbates stroke-induced brain injury by NMDAR-mediated excitotoxicity.

The role of oxidative stress in stroke-induced brain injury − Oxidative stress has been considered to be the main mechanism mediating stroke-induced brain injury. Excess ROS executed their detrimental effects through direct oxidation, and damage of macromolecules, lipids, protein and DNA, thereby leading to neuron-cell death. ROS in ischemic tissue also play an important role in MMP activation, which degrade laminin and the tight junction of EC, thereby leading to increased BBB permeability and dysfunction. Increased ROS production has been observed in activated MG, infiltrated leukocytes, BMEC and in neurons themselves. Sources of ROS include mitochondria, xanthine oxidase, NOS and NADPH oxidase. NADPH oxidase was recently identified as the major enzyme source of ROS in stroke. It has seven isoforms, and NOX1, NOX2 and NOX4 were the major isoforms expressed in the brain. In a normal brain, NOX1 is primarily expressed in neurons and astrocyte. NOX4 is mainly detected in neurons and BMEC (Vallet et al., 2005). NOX2 is highly localized in the neuron and MG of the cerebral cortex, and in the hippocampal CA1 region, as well as in BMEC (Q. G. Zhang et al., 2012). After stroke, the mRNA, and the protein levels of NOX2, NOX4and NOX1 were found to increase in neurons, astrocytes and BMEC, especially in the penumbra area. NOX2 from infiltrated leukocyte also constituted a major source of ROS in the ischemic brain. The role of ROS from different NOX isoforms in stroke has been greatly explored in knockout (KO)

animals in the mice stroke model. NOX2-/- was found to reduce infarction volume and BBB-disruption hemorrhagic transformation in the acute phase of stroke in the mice tMCAO, but not in the permanent MCAO model of several research groups. Bone-marrow transplantation experiments suggest that both peripheral and brain-residential NOX2 contribute to the exacerbation of stroke-induced brain injury, but that NOX2 from infiltrated immune cells played a more important role. Interestingly, $NOX2^{-/-}$ also downregulated ICAM1of BMEC and reduced NØ infiltration after stroke, thereby indicating that NOX2-derived ROS may be involved in NØ transmigration across BMEC. $NOX4^{-/-}$ has also been shown to be neuroprotective by reducing infarct volume, BBB permeability and mortality, in both the tMCAO and permanent MCAO models, disregarding the sex and age of mice. The role of NOX1 in stroke continues to be debated.

Stroke therapies

Currently, the only FDA-approved therapy for stroke in the acute phase is to recover the cerebral blood flow through recombinant tissue-plasminogen activator (rtPA)-mediated thrombolysis. However, the time windows are quite narrow and require that patients receive treatment no later than 4.5h after the onset of stroke. After this time, the 'clot' becomes too firm for rtPA to dissolve it, BBB disruption is likely to have occurred and the delivered rtPA may penetrate into the perivascular compartment, causing neuron damage and hemorrhage transformation. Moreover, this therapy is accompanied with reperfusion-induced brain injury. Because of the narrow time window for therapy, only ~1.8% of stroke

patients in the USA are able to receive this treatment. During the past decades, many efforts have been made and over 1,000 potential stroke therapeutics have been developed and tested in preclinical cerebral-stroke models, but only one tenth of them have made it to clinical trials. The common concept for all of these stroke strategies is, if possible, the immediate and timely recovering of the cerebral blood flow, in combination with strategies that prevent the penumbra from becoming part of the infarct core. The major strategies are preventing excitotoxicity, preventing oxidative stress and preventing inflammatory response.

Mouse model of ischemic stroke

The animal model of stroke is a procedure by which a cerebral event (ischemia or hemorrhage) similar to human stroke is provoked in order to investigate the pathophysiologic mechanisms of strokes and potential therapeutic interventions. Ischemic stroke model can be further divided into global and focal ischemia. Global ischemic model involves a permanent unilateral carotid-artery ligation with indicated times of exposure to a hypoxic environment. Compared to focal ischemic model, it is easier to perform but has less clinical relevance, because less than 1% of stroke patients suffer global cerebral ischemia that is mainly caused by cardiac arrest. For focal ischemia, several methods have been developed, each of which has its own advantage and disadvantage. Most models target the middle cerebral artery (MCA) and it has been reported that 80% of ischemic strokes were involved in MCA territory. Major focal ischemic stroke models include Tamura

MCAO, intraluminal monofilament-induced MCAO, thrombotic MCAO and photochemical MCAO **(Figure 6)**. Tamura MCAO is induced by electrocoagulation and produces consistent infarct lesion. However, the occlusion is permanent, whereas in human stroke, cerebral vessel occlusion is seldom permanent, as most cases of human ischemic stroke have spontaneous or thrombolytic therapy-induced reperfusion (Mhairi Macrae, 1992). In addition, this model requires complex surgical skills and craniotomy, which causes extensive traumatic surgical damage and affects intracranial pressure after the dura is removed. Therefore, a reversible and relatively noninvasive method was developed by introducing the intraluminal suture to occlude MCA. It does not require craniotomy but produces an infarct lesion that is similar in reliability to the Tamura MCAO method, as long as parameters such as temperature and filament type are well controlled. It is flexible for studying both permanent and transient MCAO. Another advantage is that the ischemic intervals can be freely chosen according to the needs of experiment. Based on similar concepts, thromboembolic MCAO was developed by intraluminal injection of clots or microsphere, instead of using filament. The occlusion of MCAO is not limited to proximal site and can be applied to distal MCAO by using smaller particles or thrombi and produces smaller lesion, similar to human stroke s(Carmichael, 2005). However, this modified method is not comparable to filament occlusion with regard to the efficiency of occlusion, the variability of infarct lesion and unachievable reperfusion. Despite the advantage of filament-induced MCAO over Tamura MCAO or intraluminal thrombotic MCAO, the model is associated with risk of subarachnoid hemorrhage and high mortality. Transection

of the ECA caused mastication and swallow-muscle ischemic, thereby resulting in eating difficulty and severe weight loss, and affecting the behavior assessment(Watson, Parker, & Slack, 1988). The large infarct lesion does not represent most of the human stroke infarction that is involved in small lesion. Photochemical MCAO can be a less invasive method, inducing small infarct lesion. Briefly, rose-bengal or other photosensitive dyes are injected intravenously and irradiated within minutes through the intact skull, thereby generating singlet oxygen, focal endothelial damage, platelet activation, followed by simultaneous microvascular occlusion throughout the irradiated area. However, this model only induced microvascular insult with little penumbra and reperfusion occurred in patients. In our study, we adopt the filament MCAO model based on the following: 1) it is relatively non-invasive, 2) it can be permanent or transient and best suitable for studying brain inflammation, 3) it generates reproducible lesions, 4) it has the flexibility of ischemic interval control and 5) it is the most frequently used model.

In the filament-induced transient MCAO mice model, occlusion time is the first determinant of infarct lesion size. In C57BL/6 mice, it was reported that 8min of occlusion was able to induce damage to striatum and hippocampus. An occlusion of 30min can produce rapid infarction in the striatum and delayed infarction in overlying cortex, while 60-120min caused widespread, simultaneous damage in both striatum and cortex. Despite the fact that 8min of MCAO is sufficient to cause damage, reproducible infarct volume after tMCAO required at least 30min of MCAO. Therefore, in the mice tMCAO model,

the most frequently used durations of suture occlusion are 30min and 60min. The infarct lesion can be detected by triphenyl tetrazolium chloride (TTC) staining at 6h after MCAO and reaches its peak at 24h. The reported infarct volume for wild type C57BL/6 mice after 60min of occlusion and 23h of reperfusion was 47.5 ± 25 mm^3 (22.2 ± 13.7, % of hemisphere). Moderate neurological deficits were observed, including circling gait, moderate hypo-mobility, forelimb flexion and spinning by tail suspension (Lee, Hong, Park, Lee, & Chang, 2014; Park et al., 2014). The great standard derivation of infarct volume across different research groups may be caused by the use of a different anesthesia method, type of filament, length of filament insertion(Zhang, Guo, Yang, Wen, & Shen, 2012), surgical time, sterile control and housing condition, especially the temperature control, which should maintain mouse core temperature at 37.0±0.5°C. Other critical confounding factors include blood gas, glucose level, blood pressure, cerebral blood flow and cerebral vascular anatomy. Abnormal CBF caused by surgery procedure can be used as a criterion by which to exclude animals that are not useful. On the other hand, a different alternation of CBF caused by other factors, such as treatment or genetic defect, can be an explanation for different infarct lesion or neurological deficit. Cerebral vascular anatomy examination is of great importance when study is involved in indifferent strains of mice or in mice with genetic manipulation, as differences have been observed in the cerebral vascular anatomy. Examining anatomy includes examining the intactness of the Willis Circle and the patency of posterior communicating artery (PComA), which connects

carotid and vertebrobasilar circulation. Abnormalities in these anatomies affected CBF and subsequently also stroke-induced brain damage in tMCAO model (Kitagawa et al., 1998).

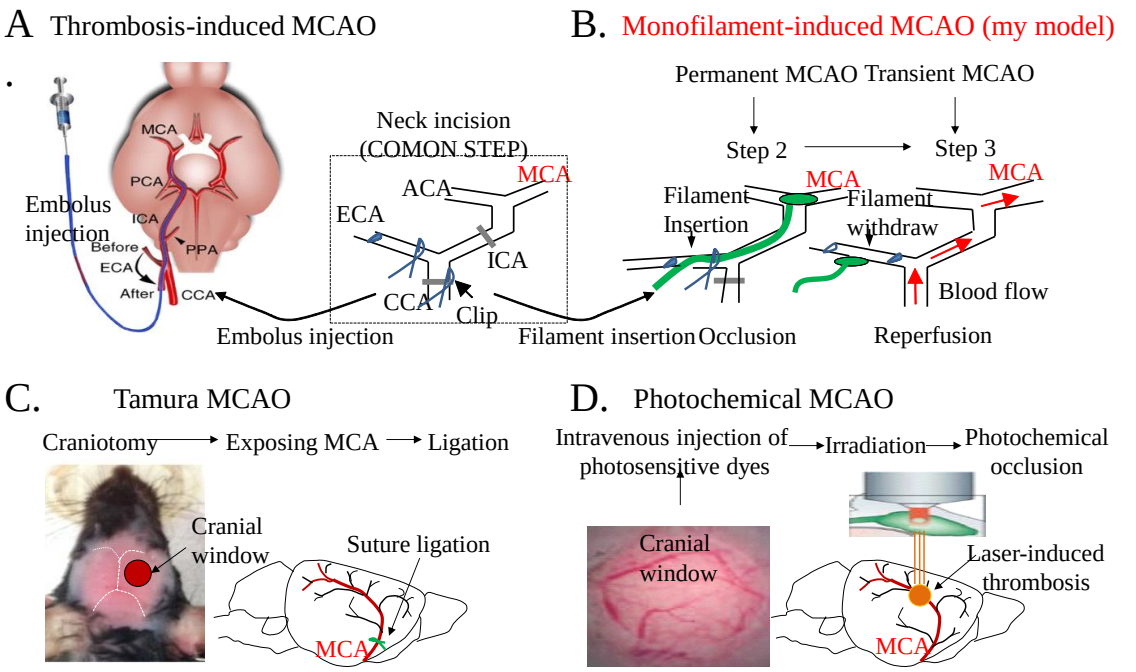

Figure 6. Mouse models of focal ischemic stroke. There are four acceptable mouse models of middle cerebral artery occlusion (MCAO) that produce focal ischemic stroke: A) Thrombotic MCAO: Embolus was injected through the ICA to the origin of MCA, B) Monofilament-induced MCAO: Instead of embolus, filament was inserted through ICA to the origin of MCA. Filament can be withdrawn to recover the blood flow and thereby the reperfusion injury, C) Tamura MCAO: MCA was exposed by opening a hole in the skull and ligated to induce permanent ischemia, and D) Photochemical MCAO: A cranial window was created by drilling a hole in the skull of the MCA-supplied area and covering it with a glass. After intravenous injection of photosensitive dyes, the selected branch of MCA vessel was irradiated, thereby leading to photochemical occlusion. Abbreviations:

ACA, anterior cerebral artery; CCA, Common carotid artery; ECA, External carotid artery; ICA, Internal carotid artery; MCAO, Middle cerebral artery occlusion; MCA, middle cerebral artery; PCA, Posterior cerebral artery.

HHcy is an independent stroke risk factor

HHcy as an independent risk factor of CVD was first proposed by McCully in 1969. He found that children with homocystinuria have a high incidence of premature CVD. However, in that decade, the cholesterol-heart-attack theory was dominant and little attention was dedicated to Hcy. In 1976, Wilcken and Wilcken published the first clinical study on coronary artery patients supporting Dr. McCully's theory, as the number of clinical and mechanistic studies within the field of Hcy research increased exponentially during that time. Abundant epidemiologic studies were conducted, most of which demonstrate a positive correlation of Hcy and the risk of CVD, including myocardial infarction (MI), AS and stroke (**Table 4**). JAMA's meta-analysis from 2002 clearly demonstrated that an 3μmol/L increase of plasma Hcy level was associated with 24% higher risk of stroke and 15% higher risk of MI. However, whether HHcy was simply a biomarker or a causal factor remained debated, though results from genetic studies favored the latter hypothesis. As shown in **Table 2**, gene mutation leading to higher plasma Hcy level was found to be correlated with increased risk of CVD. Because gene defect was defined after birth, any association in between should be considered to be the cause effect of the gene. To further confirm the causal role of Hcy as a risk factor of CVD, many Hcy-lowering clinical trials

with B vitamins were initiated during the last decades. The best-known trials include the SEARCH, Vitamin Intervention for Stroke Prevention (VSIP), Heart Outcomes Prevention Evaluation (HOPE2), VISTOP and CSPPT (**Table 5**), all of which were designed for secondary prevention and conducted among patient populations with preexisting cardiovascular disease. Initial results of these four large clinical trials have not shown a beneficial effect of folic acid (FA) supplementation for prevention of CVD, despite the fact that FA supplements significantly reduce the Hcy level. However, post-hoc analysis of VISTOP2, HOPE2 do suggested a reduction of stroke risk for certain patients. For example, the post-hoc subgroup analysis of the HOPE2 study found that tHcy-lowering therapy had larger treatment benefit for patients aged younger than 69 years. The post-hoc analysis of the VISTOP2 study revealed that Hcy-lowering therapy only benefited patients who did not take an antiplatelet. The meta-analysis by Huo suggested that FA supplementation significantly reduced the risk of stroke, particularly among patients with low folate level and not taking statins. The most convincing data suggesting that Hcy-lowering therapy does reduce the risk of stroke is from the most recent clinical trial, CSPPT. Unlike all other Hcy-lowering clinical trials, CSPPT was specially designed for primary prevention. It recruited patients with hypertension but without a history of stroke and MI. Stroke is the primary outcome, together with hemorrhagic stroke, while MI and all-caused death were secondary outcomes. Moreover, CSPPT was conducted in China with low dietary folate intake and participants whose folate level is 50% lower than in the VISP study. Another unique aspect of the CSPPT was the low percentage of participants'

concomitant use of lipid-lowering drugs and antiplatelet agents. CSSPT also considered the confounding factor, namely polymorphism of MTHFR 677T. This trial found that, compared to participants receiving enalapril alone, participants receiving enalapril/FA therapy significantly reduced the relative risk of first stroke, namely by 21%, without changing the risk of hemorrhagic stroke, MI and all-caused death. Interestingly, all these clinical consistently demonstrated the benefit for stroke but not for other CVDs, thereby raising the possibility that FA supplementation may be more effective for stroke prevention than for other cardiovascular outcomes.

Study	Time	Age	Case NO.	Subjects	Area	Hcy level (μm)	Risk factor association	PMID#
BRHS	1995	40~59	225	General population	UK	13.7 VS 11.9	RF:All stroke	7475822
ZES	1998	64~84	878	General population	Netherlands	Mean:15.8	RF:All stroke, CHD	9848881
FHS	1999	61~77	165	Elderly population	USA	Quartile analysis	RF:All stroke in elderly people	10475888
BIP	2003	66~81	105	Patients with CAD	Israel	16.4VS14.3	RF: Ischemic stroke	12624283
NOMAS	2004	59~79	2939	Multiethnic population	USA	Mean:10.2	RF: Ischemic stroke	15345803
KIHD	2005	46~64	1015	Population without Stroke history	Finland	Mean:10.9	RF: All stroke, stronger in Ischemic stroke	16079645
NSHDS	2011	50~75	381	Stroke patients	N. Swedish	Quartile analysis	RF: Hemorrhagic stroke	21631392
FHS	2016	52~70	3224	Elderly population	USA	Quartile analysis	RF: Ischemic stroke	27558379

Table 4. Epidemiologic studies for HHcy association with CVD. All studies, consisting of different subjects from different areas, consistently demonstrated a positive correlation between plasma Hcy level and CVD risk, particularly stroke. Abbreviations: BRHS, British regional heart study; BIP, Bezafibrate infarction prevention study; CAD, Coronary artery disease; CVD, Cardiovascular disease; FHS, Framingham heart study; Hcy, Homocysteine; KIHD, Kuopio ischemic heart disease; NOMAS, Northern Manhattan

study; NSHDS, Northern Sweden health and disease; PMID, PubMed ID; RF, risk factor; ZES, Zutphen elderly study.

	Study	Time	Case#	Area	Subjects (disease)	Therapy	Hcy levels	Findings	PMID#
	Secondary prevention trial:								
Negative findings	VISP	2004	1827	USA	Stroke	FA(2.5mg)+VitB6(25mg)+Vit B12(0.4 mg)	2μM↓	No benefit for vascular outcome	14762035
	HOPE2	2006	2758	USA&CA	Vascular disease	FA(2.5mg)+VitB6(50mg)+Vit B12(1mg)	3.2μM↓	No benefit for CVD death and MI	16531613
	NORVIT	2006	3749	NW	Myocardial infarction	FA(0.8mg)+VitB6(40mg)+Vit B12(0.4mg) or FA(0.8mg)++VitB12(0.4mg) or VitB6(40mg)	27%↓	No benefit for the risk of recurrent CVD	16531614
	WENBIT	2008	3096	NW	Coronary artery disease or aortic valve stenosis	FA(0.8mg)+VitB6(40mg) FA(0.8mg)+VitB12(0.4mg) VitB6(40mg)	30%↓	No benefit for mortality or CVD events	18714059
	VITATOP	2010	8164	USA	All type of stroke	FA(2mg)+VitB6(25mg)+Vit B12(0.5mg)	2μM↓	No benefit for preventing recurrent stroke	20688574
	WENBIT	2010	348	NW	Coronary artery disease or aortic valve stenosis	FA(0.8mg)+VitB6(40mg) FA(0.8mg)+VitB12(0.4mg) VitB6(40mg)	22%↓	No benefit for angiographic progression of CAD	20494665
	SEARCH	2010	6033	UK	Myocardial infarction	FA (2mg)+B12 (1mg)	3.8μM↓	No benefit for major vascular events	20571015
Positive findings	VISP (post hoc)	2005	2155	USA	Stroke	FA(2.5mg)+VitB6(25mg)+Vit B12(0.4 mg)	3μM↓	Reduced risk of all stroke by 21%	16239629
	HOPE2 (post hoc)	2009	5522	USA&CA	Vascular disease	FA(2.5mg)+VitB6(50mg)+Vit B12(1mg)	2.2μM↓	Reduced risk of all stroke , promoting recovery	19228852
	VITATOP (post hoc)	2012	1463	USA	Stroke without antiplatelet intake	FA(2.5mg)+VitB6(25mg)+Vit B12(0.4 mg)	2μM↓	Reduced risk of stroke but not MI in patients without taking antiplatelet	22554931
	Primary prevention trial:								
	CSPPT	2015	29190	China	Hypertensive patients	FA(0.8mg)+Enalapril(10 mg)	2μM↓	Reduced first IS by 21% in hypertensive patients taking enalapril	25771069
	Population study:								
	CDC cohort study	2006	Nation wide	USA&CA	General population	FA fortification	>2μM↓	Stroke related mortality↓	16534029

Table 5. Major Hcy-lowering clinical trials and population study in CVD. Secondary prevention trials including VISP, HOPE2, NORVIT, WENBIT, VITATOP and SEARCH demonstrated that Hcy-lowering therapy reduced the risk of stroke in CVD populations without FA fortification, renal disease, commitment to antiplatelet-drug intake, or B-vitamins malabsorption. As the only primary-prevention trial, CSPPT showed that Hcy-

lowering therapy also reduced the risk of stroke in general populations without CVD. Abbreviations: VSIP, Vitamin intervention for stroke prevention; VITATOPS, Vitamins to prevent stroke (VITATOPS); HOPE2, Heart outcomes prevention evaluation; WENBIT, Western Norway B vitamin intervention trial; SEARCH, Study of the effectiveness of additional reductions in cholesterol and homocysteine; NORVIT, the Norwegian vitamin trial; CSPPT, China stroke primary prevention trial; Hcy, Homocysteine; CVD, Cardiovascular disease; CAD, Coronary artery disease; AVS, Aortic valve stenosis; MI, Myocardial infarction; FA, Folic acid; Vit, Vitamin, PMID, PubMed ID.

In addition to the risk factor of stroke, accumulating evidence suggests that Hcy affected stroke severity and prognosis (**Table 6**). As is shown, plasma-Hcy level in acute phase of stroke (with 24h) was associated with severe neurological deficit (Wu et al., 2013) and long-term mortality. However, it remains unclear whether Hcy is a pure biomarker of stroke severity in the acute phase. Currently, limited experimental studies have been conducted. Decades ago it was demonstrated that FA deficiency-induced HHcy increased the stroke infarct lesion and neurological function in the mouse-transient middle cerebral artery occlusion (tMCAO) model. Recently, another group using a rat HHcy model that was induced by directly feeding Hcy compound found that mildly elevated Hcy

exacerbated stroke-induced cortical neuron injury via promoting neuronal autophagy in the same tMCAO model.

Time	Subjects (disease)	Case#	Findings	PMID#
Negative Findings:				
2005	Acute stroke	775	Hcy was higher in stroke patients, no correlation with stroke severity	16388364
2008	Acute ischemic stroke	69	No difference in Hcy levels, not correlated with short term outcome	18620594
2009	Ischemic stroke	198	HHcy had a better 3 month outcome	19185985
2009	Acute ischemic stroke	267	Hcy was not correlated with functional disability after stroke	19062047
2015	Ischemic stroke	792	Hcy-lowering did not improve neurological function after IS	26643782
Positive Findings:				
2009	Vascular disease	258	Hcy-lowering reduced fatal stroke, increased tendency of recovery	19228852
2013	Acute ischemic stroke	977	Hcy (>15μmol/L) predicted 1-year poor outcome	24023414
2013	Acute ischemic stroke	189	Hcy was independent predictors of short-term outcome and mortality	23816540
2013	Acute ischemic stroke	977	Patients with plasma Hcy>15um had poor outcome	25265507
2013	Ischemic stroke	198	HHcy increased long-term mortality	23735372
2014	Acute ischemic stroke	396	HHcy predicted early neurological deterioration	24448992
2014	Acute stroke	3695	HHcy was independent risk factors for prognosis of AIS	24174694
2015	Acute ischemic stroke	1342	HHcy predicted severer neurological deficit and higher IS recurrence	26256006
2015	Hemorrhagic stroke	69	HHcy was associated with larger hematoma volume	25620712
2015	Acute ischemic stroke	809	HHcy was associated with higher white matter hyperintensity burden	25795555
2015	Acute ischemic stroke	3309	HHcy was associated with poor prognosis in women only	26910818
2015	Acute ischemic stroke	3799	HHcy was associated with stroke-related long term mortality	26199315
2016	Acute ischemic stroke	644	HHcy predicted severer neurological deficit in elderly patients	27096104
2016	Acute ischemic stroke	194	HHcy predicted severer neurological deficit and higher incidence of intracerebral hemorrhage in patients receiving tPA	27629768
2016	Acute ischemic stroke	112	Hcy level is associated with cerebral microbleeds after AIS	27629768

Table 6. Case-control studies for HHcy's association with stroke prognosis. Both negative and positive results were generated in all of the published studies. However, most recent studies have suggested that a higher plasma Hcy level predicted worse stroke outcomes, including stroke-related mortality and neurological deterioration. Abbreviations: Hcy, Homocysteine; HHcy, Hyperhomocysteinemia; VD, Vascular disease; AS, Acute stroke; AIS, Acute ischemic stroke; IS, Ischemic stroke; ICH, intracerebral hemorrhage; CT, Computed tomography; PMID, PubMed ID; Coronary artery disease; CHD, chronic heart disease; tPA, tissue plasminogen activator.

CHAPTER 2

MATERIAL AND METHODS

Tg-hCBS *Cbs*$^{-/-}$ mice

All animal experiments were performed in accordance with the Institutional Animal Care and Use Committee (IACUC) guidelines, with authorization for the use of laboratory animals and approved by the experimental animal committee of Temple University. The transgenic Tg-hCBS *Cbs*$^{-/-}$ mice were established by Dr. Kruger's laboratory in Fox Chase Cancer Center and used for experiments. Briefly, the mice have a C57BL/6 background with an inserted human CBS cDNA, controlled by a zinc-inducible metallothionein promoter (**Figure 7A**), and with a mutated mice *Cbs*$^{-/-}$ gene in which exon 3 and exon 4 was deleted (**Figure 7B**). In order to circumvent the high neonatal lethality that occurred in *Cbs*$^{-/-}$ mice, Tg-hCBS *Cbs*$^{-/-}$ mice will be fed with 25mM ZnSO4-containing water during pregnancy and lactation, thereby inducing the human CBS gene expression. After four weeks, ZnSO4-containing water was withdrawn to shut off the human CBS gene expression and to induce the development of HHcy for another 10 weeks (**Figure 7C**). 100µl blood was withdrawn from the tail vein at two weeks before surgery to measure the plasma Hcy level, which was 151 ± 25µM in Tg-hCBS *Cbs*$^{-/-}$ mice and therewith significantly increased compared to their sibling CT ($P<0.001$). No difference was observed between Tg-hCBS *Cbs*$^{+/+}$ and Tg-hCBS *Cbs*$^{+/-}$ mice (5.5 ± 2.1µM vs5.5 ± 2.2µM).

Before surgery, the mice were group-housed (five per cage) on a 12h light-dark cycle, with access to food and water in a temperature and humidity-controlled environment. The mice were fed with standard rodent chow diet (0.67% methionine; 5001; Labdiet, Saint Louis, MO). Male mice aged 12-16 weeks were chosen for study. Experimental mice were defined as Tg-hCBS *Cbs*$^{-/-}$ mice and their littermates, either with a Tg-hCBS *Cbs*$^{+/-}$ or Tg-hCBS *Cbs*$^{+/+}$ background, were selected as control (CT) mice.

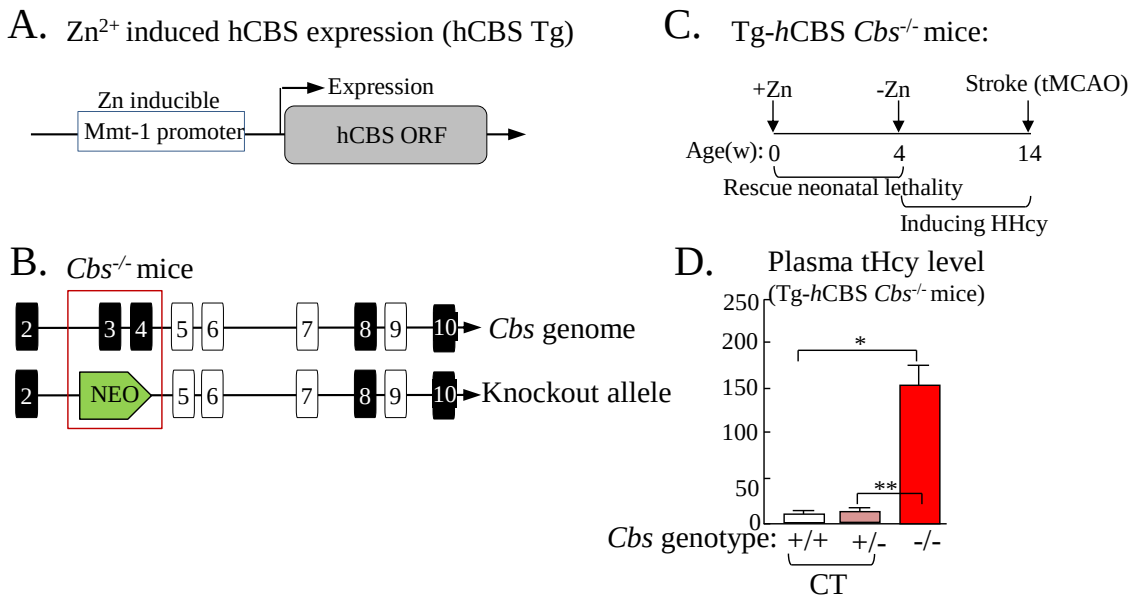

Figure 7. HHcy mouse model in this study. A) Zn^{2+} induced hCBS expression (hCBS Tg). ORF indicates hCBS open-reading frame. hCBS is driven by the zinc-inducible metallothionein (Mmt-1) promoter. **B**) *Cbs*$^{-/-}$ mice. Black box indicates exon, while open box indicates intron. Neo gene replaces the exon 3 and 4 in the same orientation of *Cbs* gene. **C)** Tg-hCBS *Cbs*$^{-/-}$ mice. Maternal mice are fed with Zn-containing water to induce the expression of hCBS, in order to prevent the neonatal lethality that occurred in *Cbs*$^{-/-}$ mice. After four weeks, Zn-containing water was withdrawn to shut off the expression of

hCBS, in order to induce HHcy in Tg-hCBS *Cbs*$^{-/-}$ mice. **D**) Plasma tHcy level. Blood was withdrawn from the tail vein to measure the plasma tHcy levels of Tg-hCBS *Cbs* mice at two weeks before tMCAO. Abbreviations: ACA, Anterior cerebral artery; CCA, Common carotid artery; ECA, External carotid artery; ICA, Internal carotid artery; MCAO, Middle cerebral artery occlusion; MCA, Middle cerebral artery; NEO, Neomycin-positive selection marker; ORF, Open reading frame; PCA, Posterior cerebral artery; tMCAO, Transient middle cerebral artery occlusion.

Mouse genotype

Mice were genotyped for specific genes that are of interest with polymerase chain reaction (PCR), followed by agarose gel separation of the products. Mouse tail or ear tissue was collected at postnatal day 10 and digested with 600µl of tissue-lysis buffer [10mM tris (pH 8.0), 100mM sodium chloride (NaCl), 10mM ethylenediaminetetraacetic acid (EDTA, pH 8.0) and 0.5% sodium dodecyl sulfate (SDS)] containing 0.4mg/ml proteinase K at 55°C overnight. Tissue lysate was centrifuged at 13,000rpm for 20min. Supernatant-containing genomic DNA was collected and DNA was precipitated in 100% ethyl alcohol and dissolved in distilled deionized water at 37°C overnight.

Mouse-genomic DNA was amplified with specific primer sets by PCR. Genotyping for the mouse *Cbs* allele was performed using a three-primer PCR system developed by the Loscalzo Laboratory. The three primers that were used are 5'-GAAGTGGAGCTATCAGAGCA-3' (forward primer), 5'-

TGGCTCTTGGTTCTGAAACC-3' (reverse primer, WT) and 5'-GAGGTCGACGGTATCGATA-3' (reverse primer, KO). The PCR condition was 94°C for 1 min, 60°C for 1min and 72°C for 1 min, for a total of 30 cycles. The wild-type allele gives an 800 bp product, whereas the deleted allele gives a 450 bp product. Human CBS allele was examined using a primer pair developed by the Kruger Laboratory. The two primers that were used are 5'-ATGTAGTTCCGCACTGAGTC-3' (forward primer) and 5'-AGTGGGCACGGGCGGCACCA-3' (reverse primer). The human CBS-gene product is 380 bp. The PCR condition is 94°C for 30s, 60°C for 30s and 72°C for 30s, for a total of 30 cycles. The PCR products were separated by 2% agarose gel and examined by a Foto-analyst image system (Hartland, WI).

Plasma and brain Hcy, SAM, and SAH measurement

After sacrifice, mouse blood was withdrawn by puncturing a syringe into the heart. The blood was then immediately centrifuged at 3000 rpm for 15min in order to obtain plasma. The brain was harvested, and cut into left and right hemisphere. The hemispheres were weighted, added with corresponding volume (1µl per 1 mg tissue) of 0.1M perchloric acid (PCA), homogenized and sonicated. The samples were the immediately centrifuged at 13000rpm for 20min in order to obtain the brain extract. A total of 50µl plasma or brain extract was then batched, frozen and transported to Baylor Institute of Metabolic Disease. Hcy, SAM and SAH were determined by liquid chromatography-electrospray ionization (ESI) tandem mass spectrometry (LC-ESI-MS/MS), as previously described.

Transient focal cerebral ischemia model

Mice were carefully shaved on the neck one night before surgery and anesthetized with 2% isoflurane in 30%O_2/70% N_2O gas mixture via a facemask, using the V-10 Anesthesia system. Body temperature was monitored with the rectal probe and maintained at 37 °C by placing the mice on the thermo-controlled rodent blanket throughout the procedure. Lubricant ophthalmic ointment was applied to both eyes and eyelids were closed to prevent eye desiccation during the surgical process. Under aseptic conditions, a midline incision was made on skin and a midline neck incision was made with scissors between the manubrium and the jaw. The skin and underlying submandibular glands were pulled laterally to exposure the right common carotid artery (CCA), external carotid artery (ECA) and internal carotid artery (ICA). The right proximal CCA was carefully isolated from the vagus nerve and clamped. The ECA was dissected from carotid bifurcation into lingual and maxillary arteries. A distal permanent ligation was made at ~3mm from carotid bifurcation with 6-0 silk suture and a proximal loose ligation was made directly right of the carotid bifurcation. The ICA was dissected and a loose ligation was made at ICA, as far as possible from carotid bifurcation. A hole was cut between the proximal and distal ligation at ECA. A silicone-coated monofilament (6-0, length 20 mm, coating length 5-6 mm, tip diameter with coating 0.27±0.02 mm, Doccol Co, Cat#602156PK10) was then inserted and gently advanced into the distal ICA, 10-12 mm distal to the carotid bifurcation, thereby occluding the MCA at the junction of the Circle of Willis. The filament was then tied in place and the

clamp at CCA was removed. After 1h of cerebral ischemia, the monofilament was retracted to allow reperfusion for 23h. Reperfusion was confirmed by an immediate increase in regional cerebral blood flow (rCBF), which reached at least ~80%, of the pre-ischemic level. Sham-operated mice received an identical procedure, with the exception that no filament was inserted. All animals were administered 1mL of sterile 0.9% saline via a subcutaneous injection for rehydration after surgery. Mice were monitored until they regained consciousness and returned to their cages with free access to mashed food and water.

A laserPro Blood Perfusion Monitor (TSI Inc., Shore-view, MN, USA) was used to quantify rCBF before MCA occlusion, during MCAO and after reperfusion. Briefly, the left side skin of the head was cut and the skull was exposed. A microfiber-laser Doppler probe (1mm diameter) was attached under the skull with the tip pointing to the core area, supplied by the MCA (4 mm lateral and 2 mm posterior of bregma). Changes of rCBF were recorded as a percentage of the baseline value (before MCA occlusion). The ischemia was considered adequate if rCBF showed a sharp drop no greater than 25% of the baseline level. The reperfusion was considered effective if rCBF had greater than 75% of baseline value after reperfusion.

Mice were excluded if (1) Mice died during surgical procedure; (2) Insufficient occlusion (>25% of the baseline) and insufficient reperfusion (<75% of the baseline) occurred; (3)

Excessive bleeding occurred during surgery; and (4) Hemorrhage was found in the brain slices or at the base of the Circle of Willis during post-mortem examination.

Intracranial vasculature investigation

Mice were anesthetized with ketamine (100mg/kg, IP.) and xylazine (10 mg/kg, IP). After thoracotomy was performed, a cannula was introduced into the ascending aorta through the left ventricle. Transcardial perfusion fixation was performed with 2 ml saline and 2 ml of 3.7% formaldehyde. Carbon lampblack (Thermo Fisher Scientific, CAT# C198-500) in an equal volume of 20% gelatin in ddH_2O (1ml) was injected through the cannula. The brains were removed and fixed in 4% PFA overnight at 4°C. The Circle of Willis was examined and photographed under a dissection microscope. Posterior communicating arteries (PComA) were identified as anastomoses connecting the vertebrobasilar arterial system to the Circle of Willis and ICA. Development of PComA in both hemispheres was examined and graded on a scale of 0-3: 0) no connection between anterior and posterior circulation; 1) anastomosis in capillary phase (present but poorly developed); 2) small truncal PComA; 3) truncal PComA.

Infarction volume measurement

Triphenyltetrazolium chloride (TTC) staining was used to detect infarct lesion. Briefly, mice were sacrificed by CO_2 and the brain was carefully removed from the skull, avoiding brain damage by the sharp bone. The harvested brain was washed with ice-cold Hanks'

Balanced Salt solution (HBSS) and then transferred into a mice-brain matrix. The brain was cut into 1mm thick coronary slices using razor blades and using bregma as position zero. A total of six slices can be obtained. Each brain slice was carefully transferred to a petri dish containing 1% TTC (Sigma-Aldrich, Cat# T8877-5G) in HBSS, maintained at 37°C in a heater. Gentle stirring of the slices was used to ensure even exposure of the surfaces to staining. After 30 min, TTC solution was drained, HBSS were added to wash the brain slice twice and 4% paraformaldehyde fixative (PFA) was added to fix the slices for 24h. Brain slices were scanned into a computer file for image analysis.

The size of the brain lesion was measured by using Image J software. Briefly, the entire non-ischemic hemisphere area and the non-infarct area (red) of ischemic hemisphere from each section were circled out, and each of the areas was measured. Infarct area was calculated by subtracting the non-infarct area of ischemic hemisphere from the area of the non-ischemic hemisphere area. Infarction areas on each section were summed and multiplied by section thickness (1mm) in order to attain the total infarction.

General neurological function evaluation

General neurological deficit was assessed by using the Bederson scoring system: 0) no deficit, 1) forelimb flexion, 2) decreased resistance to lateral push, 3) unidirectional circling, 4) no movement or death. Neurological assessment was evaluated by an observer blinded to experimental groups.

Evans blue extravasation assay

Evans Blue (EB) is a 961Da dye that is strongly bound to the albumin fraction of proteins and makes a high molecular weight complex (68.5 kDa). Under physiologic conditions, EB-bound albumin does not permeate the intact BBB. At 6h before sacrifice, mice were weighted and injected peritoneallly (IP) with 2% EB in 0.9% saline (4mL/kg of body weight). The mice were then transcardially perfused with 50 ml ice-cold phosphate-buffered saline (PBS), and the brain was dissected and divided into left and right hemisphere. The hemispheres were homogenized in 1 ml PBS, sonicated and centrifuged (30 min, 13000 rcf, 4°C). 500µl supernatant was collected and an equal amount of 50% trichloroacetic acid was added. After incubation in a 4°C refrigerator overnight, the mixture was centrifuged (30 min, 13000 rcf, 4°C) and the supernatant was collected for EB measurement by using a spectrophotometer at 610 nm. The amount of EB was quantified according a standard curve. The results are presented as (µg of EB)/(g of tissue).

Brain and blood mononuclear-cells isolation and FACS analysis

After mice were sacrificed, blood was withdrawn by cardiac puncture. 200µl blood was pipetted and added into a 1.5ml Eppendorf tube containing 5ul 0.5M EDTA for later mononuclear cells (MNCs) isolation and fluorescence-activated cell sorting (FACS) analysis. The mice were then transcardially perfused with 50ml ice-cold PBS. Brains were harvested, washed with 10ml ice-cold PBS in a petri dish, and then divided into left and right hemisphere. Each hemisphere was placed in a 40 mm cell strainer placed in a 50ml

tube on ice, homogenized with the back of a sterile 3 ml syringe while simultaneously adding the ice-cold PBS (~30ml). The cell strainer washed with the PBS solution was clear and centrifuged for 10min at 500g. Suspension was removed and the pellet was re-suspended with 4ml of 30% Percoll (GE Healthcare Life Sciences, Cat# 17-0891-01). 4ml of 70% Percoll was then very slowly added on the top (clear interface should be visible between the 30%-70% junction) and centrifuged at 500g for 30min at 18°C. Centrifuge was stopped with no brake in order to avoid the disturbance of the interface. The layer of debris on the top of the tube was then removed and the MNCs located at the 30%-70% interface (2ml) were transferred into a 15ml conical tube containing 10ml PBS. Cell suspension was mixed thoroughly and centrifuged at 500g for 10min at 18°C. The pellet was re-suspended in 1 ml of FACS buffer (2% fetal bovine serum in PBS) and 20µl cell suspension was pipetted into 80 µl PBS in order to count the total cell number with a hemocytometer. Left cell suspension was centrifuged at 1000rpm for 5min at 4°C. The pellet was re-suspended with FACS buffer containing corresponding. For the blood, the leukocytes were firstly purified by using red blood cell lysis buffer (155mmol/L NH_4Cl, 10mmol/L $KHCO_3$ and 3mmol/L EDTA) and centrifuged at 1000rpm for 5min at 4°C. Red blood cell lysis buffer was removed and cell pellet was washed three times with 1ml PBS. 20 µl cell suspensions were pipetted into 80 µl PBS in order to count the total cell number with a hemocytometer. Finally, the leukocytes were re-suspended in the same staining buffer as that used for brain MNCs analysis. Both brain MNCs and blood leukocytes were incubated with antibodies for 30min at 4°C in darkness. After staining,

cells were analyzed by means of a LSRII flow cytometer (BD Biosciences, Franklin Lakes, NJ and USA) and FlowJo software (Tree Star Inc., Ashland, OR, USA).

Gating strategy in FACS analysis

Briefly, cell debris and intact cells were identified by forward scatter (FSA) and sideward scatter (SSA). The total intact cells were gated out and divided into four distinct populations according to CD11b and CD45 expression level: Lym ($CD11b^{-}CD45^{hi}$), circulation-derived myeloid leukocyte cells ($CD11b^{+}CD45^{hi}$), resident MG ($CD11b^{+}CD45^{lo}$) and other cells, including neuron/astrocyte/oligodendrocyte ($CD11b^{+}CD45^{-}$). Circulation-derived myeloid leukocyte cells were further gated with Ly6G marker to identify NØ ($CD11b^{+}CD45^{hi}Ly6G^{+}$) and MC ($CD11b^{+}CD45^{hi}Ly6G^{-}$). MC was then divided into three subsets by the expression level of Ly6C: $Ly6C^{lo}$MC, $Ly6C^{mid}$MC and $Ly6C^{hi}$ MC. Positive gates were determined by matched IgG controls and single-staining FACS microbeads were used to determine the compensation parameters.

MC depletion with clodronate liposome

Clodronate liposomes (FormuMax Scientific, Cat# F70101C-A) were intraperitoneally injected at 48h before tMCAO and PBS liposome was used as the control. Different doses of clodronate liposomes (5μl/g, 10μ/g and 15 μ/g) were firstly tested in evaluating the efficiency of blood MC depletion, as determined by flow cytometry via counting the number of MC, defined as $CD11b^{+}SSC^{low}$.

Mouse brain cytokine array

The expression profile of inflammatory cytokines was performed with a Mouse Cytokine Antibody Array (R&D mouse cytokine array-panel A kit, Cat# ARY006) containing 40 different cytokines. 24h after sham procedure or MCAO, the brains of Tg-hCBS *Cbs*$^{-/-}$, and CT mice were harvested. Olfactory bulb, cerebellum, brain stem and meninges were removed. Obtained brain tissue was then homogenized with kit-provided 1 x cell lysis buffer with protease-inhibitor cocktail. After extraction, samples were spun down and supernatant was used for the experiment. The protein concentration was determined for each sample by BSA assay and diluted at 300µg total proteins in 1 x blocking buffer. The samples contained four groups: CT mice with sham surgery, Tg-hCBS *Cbs*$^{-/-}$ mice with sham surgery, CT mice with tMCAO and Tg-hCBS *Cbs*$^{-/-}$ mice with tMCAO. For each group (three mice per group), samples were pooled together and incubated with the array membrane pre-coated with 40 different antibodies overnight at 4°C. After washing in the washing buffer, membranes were incubated with biotin-conjugated antibodies overnight. After washing, membranes were incubated with horseradish peroxidase-conjugated streptavidin diluted in the blocking buffer for 2h. Signal detection was performed by exposing membranes to x-ray film and the obtained results were analyzed with Image J software.

Mouse brain microvascular EC single cell suspension and FACS analysis

After mice were sacrificed, the brain was harvested and immediately placed in ice-cold HBSS. Cerebellum, meninges, brainstem, choroid plexus and large superficial blood vessels were removed. The remaining brains were further divided into left and right hemisphere, weighted, and diced in 4 ml of ice-cold HBSS per gram of tissue. Diced tissues were further homogenized with a Potter-Thomas homogenizer (0.25mm clearance), using 20 up-and-down strokes at 400 rpm. The resulting homogenate was centrifuged at 1000g for 10min. Supernatant was discarded and a small sample of the pellet was used as whole cortex homogenate control. The remaining pellet was re-suspended with ~5ml of 17.5% dextran (Sigma, Cat#31392) and centrifuged for 15min at 4400g at 4°C. Supernatant containing a layer of myelin was removed and the pellet was re-suspended in ~5ml of HBSS containing 1% BSA. The suspension was further broken up in a petri dish using a 10ml pipet and passed through a 10μm mesh-nylon filter. The resulting filtrate was again passed through a 40μm mesh-nylon filter and centrifuged at 4000g for 10min at 4°C. Afterward, supernatant was discarded, and the pellet, which contains mostly brain microvasculature, was digested and incubated with 2.5mL collagenase (Type 1a, 1mg/mL) for 30min in a 37°C water bath inside a 15mL tube. Every 10min during incubation, the tube was gently agitated to further dissolve the tissues. After incubation, 2.5 ml of 10%FBS/DMEM was added to the tube. The resulting tissue/cell suspension was filtered through a 100μm strainer into a 50mL tube and the filtered cell suspension was centrifuged at 1500 rpm for 5min. After removal of the supernatant, the cell pellet was washed and

then re-suspended in serum-free DMEM. Cells were then incubated with monoclonal antibodies to CD31 (anti-CD31–PE, BD Pharmingen, Cat# 553373) and monoclonal antibodies to CD45 (anti-CD45–APC, BD Pharmingen, Cat# 555485) for 20min. CD31 is a maker for EC. CD45 labeling is used to gate out leukocytes which can also be $CD31^+$.

Primary human brain microvascular endothelial cells culture

Passage 2 primary HBMEC were purchased (Neuromic, Cat#HECO2-T25) and cultured with ENDO-Growth Media (Neuromic, Cat#MED001). In some experiments, 50μM adenosine and 10μM erythro-9-(2-hydroxy-3-nonyl)-adenine (EHNA) were added to the medium. The HBMEC used in this study were passages 9-10. For adhesion-molecule and cytokine-array analysis, treatments were applied at ~80% confluence and cells were harvested at indicated time points.

Primary human peripheral blood mononuclear cells isolation

Blood was drawn from healthy donors recruited by the Thrombosis Center at Temple University. 50ml of whole blood was collected into a 50ml tube containing 7.5ml anti-coagulant buffer (85mM sodium citrate, 71.4mM citric acid and 111mM glucose). 25ml whole blood was overlaid with 25ml 1077-histopaque (Sigma, CAT#10771) and centrifuged at 400g for 45min in room temperature. Red blood cells (RBCs) are found at the bottom of the tube, with a 'buffy coat' of granulocytes on the top of the RBCs, followed by a layer of mononuclear cells (MNCs).

In-vitro model of ischemia/reperfusion

Ischemia-like conditions in vitro were induced by oxygen and glucose deprivation (OGD) and reperfusion-like conditions in vitro were induced by reoxygenation. After cells reached ~80% confluence, the medium was replaced with DMEM without glucose and Hcy treatment was applied. For the hypoxia group, cultures were transferred to a hypoxia incubator chamber (Stem cell technologies, Cat#27310), infused with a gas mixture containing 5% CO_2, 95% N_2 and incubated at 37°C. For the normoxia group, cultures were incubated at 37°C under 5% CO_2 and 95% air. After 1 or 4h of normoxia or hypoxia incubation, HBMEC were harvested and the surface-adhesion molecules' expressions were determined by FACS. The results represented the effect of Hcy on HBMEC-adhesion molecules under normal or ischemic conditions. To further test effect of Hcy on HBMEC adhesion molecules under conditions of both ischemia and reperfusion, cultured cells which have undergone 4h hypoxia incubation were switched back to oxygenated ENDO-growth media for another 20h.

HBMEC cytokine array

~80% confluence HBMEC were replaced with fresh ENDO growth media added 50μM adenosine and 10μM erythro-9-(2-hydroxy-3-nonyl)-adenine (EHNA). Cells were then treated with DL-Hcy (50μM) for 24h. Cells and culture supernatant were then collected for analysis and the samples were divided into four groups: CT/cell lysis group, Hcy/cell lysis group, CT/culture supernatant group and Hcy/culture supernatant group. Each group

consists of pooled samples from three separated culture dishes. Equal amounts of cell lysis protein (300ug) and equal volumes (1 ml) of each culture supernatant were incubated with the pre-coated Human XL Cytokine Array nitrocellulose membranes spotted with 105 different antibodies to human cytokines (R&D, Cat# ARY022b) overnight at 4ºC. Membranes were then washed three times with 1 × wash buffer and incubated with Streptavidin-HRP for 30min at room temperature. Finally, cytokines were detected by film exposure and development. The densitometric analysis of dot blots was performed using Image J software.

MC-EC static adhesion assay

THP-1 cells (Human acute monocytic leukemia cell line; American Type Culture Collection, Cat# ATCC® TIB-202™) and fresh isolated HPBMC were used for this assay. First, THP-1 cells or HPBMC were stained with 2μM calcein AM fluorescence dye (Invitrogen, Cat# c3099) for 30min at 37ºC. THP-1 cells or HPBMC ($1x10^6$ cells/mL) were suspended in complete RPMI 1640 medium and complete M199 medium (1:1), and added to HBMEC monolayer. After 1h of incubation at 37ºC, unattached THP-1 cells or HPBMC were removed by carefully washing the cells three times with PBS supplemented with $CaCl_2$ and MgCl2. Fluorescence was measured with a microplate fluorescence reader (FLx800, Bio-tek) at 494nm/517nm.

MC trans-endothelial migration assay

Boyden-chamber assay was used for trans-endothelial migration assay, which refers to the migration of HPBMC across a monolayer of HBMEC. The Boyden chamber assay was performed using the Neuro Probe 48 well Micro Chemotaxis chamber (Cat#AP48) and a filter membrane containing 5µm pores. The filter membrane needed to be coated with 0.2% gelatin for 1h. The lower chamber wells were firstly filled with THP-1 medium containing CCL2 (0ng/ml, 50 ng/mL or 100 ng/mL). After the chamber apparatus was assembled, 50,000 HBMEC cells in 50µL THP-1 medium were seeded into the upper chambers. These cells were allowed to adhere to the membrane surface for 4h before treatment, using 500µM DL-Hcy for 24h in the incubator. The following day, the old medium was carefully removed from the upper chambers and 50,000 freshly isolated HPBMC in50µL of THP-1 medium were added to each of the upper wells. The apparatus was incubated for 3h, after which the apparatus was disassembled and the membrane was stained using HEMA3 staining in petri dishes. The membrane was transferred to a glass slide with the migrated cells facing down and adhering EC were carefully wiped off using cotton swabs. The slide was sealed using xylene:permount, covered with a cover slip and allowed to dry at 4°C. Three randomly selected locations in each well were imaged at 200x. The migrated cells were counted in each image and the three cell counts were averaged for a cell count that was representative of the entire well.

Statistical analysis

Data were expressed as the mean of replicate measurements or the mean normalized values of multiple experiments ± standard error of the mean (SEM). For comparisons between two groups, two-tailed Student t test (α=0.05) was used for the evaluation of statistical significance. For comparison across multiple groups, one-way ANOVA was used.

CHAPTER 3

RESULTS

HHcy worsens stroke prognosis

Monofilament tMCAO stroke model validation

In order to investigate the effect of HHcy on stroke-induced brain injury, we firstly established the monofilament tMCAO mice focal-ischemic stroke model, as described in Figure 6B. The success of the model was confirmed by a dramatic CBF reduction after inserting the filament and by the complete restoration of CBF after withdrawing inserted filament in the MCA-supplied area, as determined by the Laser speckle flowmetry image (**Figure 8C**). Observed infarct lesion assessed by TTC staining and moderate neurological deficit, such as forelimb flexion and circling behavior, assessed by Bederson score scaling were also proof of the model's success.

Cerebral vascular anatomy and CBF change before, during and after MCAO were normal in Tg-hCBS Cbs$^{-/-}$ mice

It has previously been reported that cerebral-vascular anatomy difference in mice strain with genetic manipulation greatly affected the CBF, which can significantly influence the stroke outcome in mice. Therefore, we investigated the normality of cerebral vascular anatomy, including the intactness of the Willis Circle and the patency of the posterior communicating artery (PComA) in Tg-hCBS *Cbs*$^{-/-}$ mice. Cerebral vasculature was

revealed by intracardiac administration of carbon black. We found that the Willis Circle was intact in Tg-hCBS *Cbs*$^{-/-}$ mice and that PComA is present with an equivalent degree of patency between CT and Tg-hCBS *Cbs*$^{-/-}$ mice ((2.33 ± 2.47 vs 2.66 ± 2.57, p=0.52) (**Figure 8B**). The reading of CBF was obtained with laserPro Blood Perfusion Monitor before, during and after MCAO. The value of CBF was expressed as a percentage of the baseline value 100%. We found that, in all mice subjected to MCAO, CBF was reduced to ~20%. CBF was not different between CT and Tg-hCBS *Cbs*$^{-/-}$ mice during MCAO (14.1 ± 8.4% vs 11.6 ± 6.4%, p=0.57). 20min after reperfusion, all mice restored CBF back to ~85%. CBF was not different between CT and Tg-hCBS *Cbs*$^{-/-}$ mice at 20min post-MCAO (14.1 ± 8.4% vs11.6 ± 6.4%, p=0.57) (**Figure 8D**).

Core body temperature and body weight were not different between CT and Tg-hCBS Cbs$^{-/-}$ *mice before and after MCAO*

It is also well known that body temperature (BT) greatly affects the development of infarction volume (Barber, Hoyte, Colbourne, & Buchan, 2004). Therefore, mice BT were maintained by placing mice on a thermal blanket. The rectal temperature (RT) of mice was taken at 10min before, during and at 24h after MCAO. There was no statistically significant difference in RT during the indicted time frame between CT and Tg-hCBS *Cbs*$^{-/-}$ mice (**Figure 8E**). It has also been reported that body weight (BW) after tMCAO is significantly reduced and the extent of BW reduction has been correlated with stroke severity (Scherbakov, Dirnagl, & Doehner, 2011). Therefore, BW was recorded 10min before and

24h post-tMCAO. In line with previous studies, all mice subjected to tMCAO had significant weight loss, ranging from 4%-11% at 24h post-tMCAO, compared to their BW before surgery. The BW of Tg-hCBS *Cbs*$^{-/-}$ mice before surgery was slightly less than the BW of CT mice (22.33 ± 0.22 g vs23.04 ± 0.46 g, p=0.19). The BW of Tg-hCBS *Cbs*$^{-/-}$ mice at 24h post-MCAO was not different from the BW of CT mice (20.34 ± 0.29 g vs 20.44 ± 0.42 g, p=0.84) (**Figure 8F**).

Spleen weights were not different between CT and Tg-hCBS Cbs$^{-/-}$ *mice at 24h post sham or tMCAO*

Spleen atrophy has been reported to occur after tMCAO, and is involved in brain and systemic immune response, which contribute to stroke-induced brain injury(Offner et al., 2006; Pennypacker & Offner, 2015). In line with these previous studies, the spleen weight (SPW) was found to be significantly decreased in mice subjected to tMCAO, compared to sham-operated animals at 24h after surgery (0.052 ± 0.003 vs 0.786 ± 0.002 in CT mice, p=0.0016; 0.056 ± 0.002 vs 0.086 ± 0.007 in Tg-hCBS *Cbs*$^{-/-}$ mice, p=0.0002). However, SPWs were not significantly different between CT and Tg-hCBS *Cbs*$^{-/-}$ mice, in both the

sham group (0.078 ± 0.002 vs 0.086 ± 0.006, p=0.35) and the tMCAO group (0.052 ± 0.003 vs 0.056 ± 0.002, p=0.29) (**Figure 8G**).

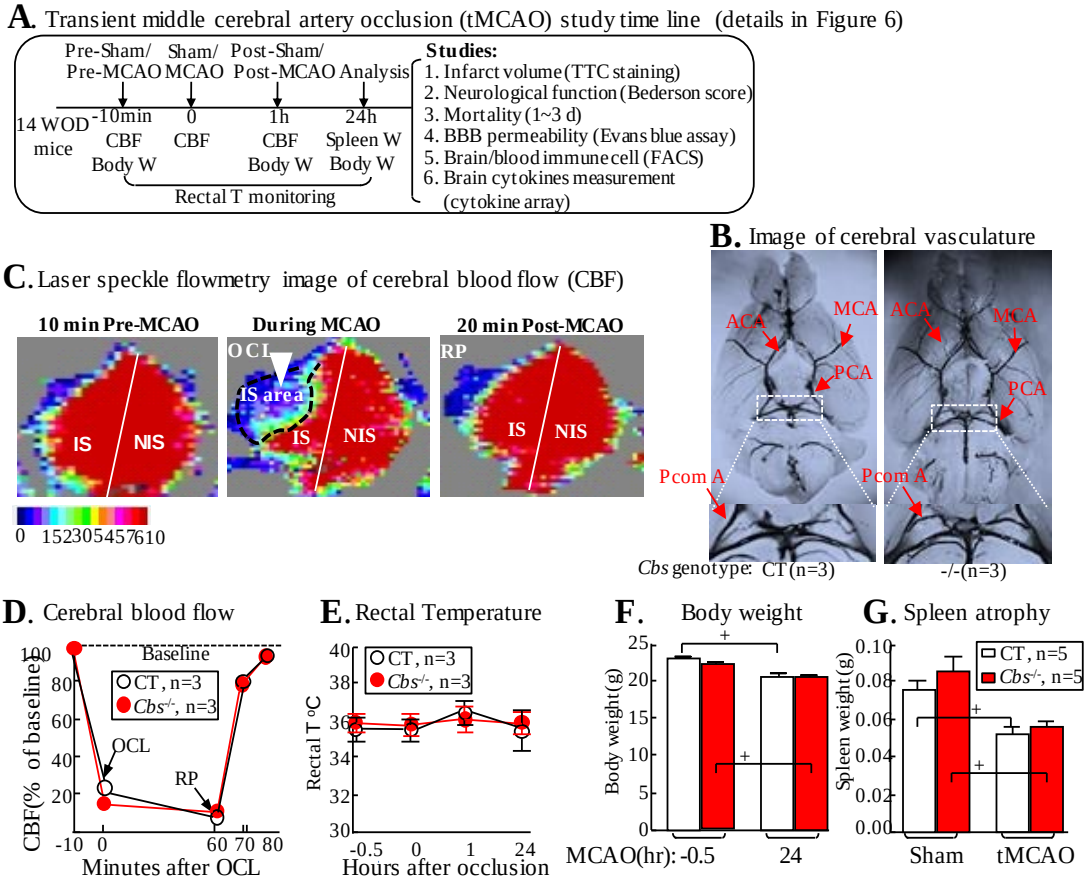

Figure 8. Study design and basic parameter determination (cerebral vasculature, CBF, RT, BW and SPW). A) tMCAO study timeline. The MCAO procedure was performed on 14-week-old mice. After 1h of MCAO, reperfusion (post-MCAO) was induced for another 23h. Mice were then scarified for designated analysis. **B)** Image of cerebral vasculature. Arrows indicate ACA, MCA and PCA. High magnification images (framed area) demonstrated the presence of the PComA. There is no difference with regard to the cerebral vasculature between CT and Tg-hCBS *Cbs*$^{-/-}$ mice. **C**) The laser speckle

flowmetry image of CBF. The perfusion image of the whole brain was captured at 10min before MCAO, during MCAO and at 20min after MCAO. A red color indicated high CBF, while a blue color indicated low CBF. A white arrow pointed to the ischemic area. Filament insertion-mediated MCAO induced a dramatic decrease of CBF in the operated hemisphere, while filament withdrawal induced reperfusion recovery of the blood flow. **D**) CBF. CBF value was determined by a laser Doppler flowmeter at 10min before MCAO, during MCAO and at 20min after MCAO. Occlusion caused a >70% decrease of basal CBF and reperfusion recovered back >80% of basal CBF. **E**) RT. RT was monitored and maintained at 36 ± 0.5 °C by using a heating pad throughout the surgical procedure. The RT is no different between CT and Tg-hCBS *Cbs*$^{-/-}$ mice throughout the entire study procedure. **F**) BW. tMCAO induced a significant decrease of BW after 24h. BW is not significantly different between CT and Tg-hCBS *Cbs*$^{-/-}$ mice before tMCAO and at 24h post-tMCAO. **G**) SPW. tMCAO induced a significant decrease of Spleen weight at 24h post-tMCAO, but sham surgery did not. BW was not significantly different between CT and Tg-hCBS *Cbs*$^{-/-}$ mice receiving either sham surgery or tMCAO. Data were expressed as mean ± SEM; +, $P<0.01$; Student's t test. Abbreviations: ACA, Anterior cerebral artery; CBF, Cerebral blood flow; Hcy, Homocysteine; HHcy, Hyperhomocysteinemia; IS, Ischemic hemisphere; MCAO, Middle cerebral artery occlusion; MCA, Middle cerebral artery; NIS, Non-ischemic hemisphere; PCA, Posterior cerebral artery; PComA, Posterior communicating artery.

HHcy increased infarct volume at 24h post-MCAO in Tg-hCBS Cbs$^{-/-}$ mice

Infarction volume was a good predictor of stroke outcome. In stroke patients, infarction volume assessed within 72h onset of ischemic stroke was an independent predictor of stroke outcome at 90 days (Vogt, Laage, Shuaib, & Schneider, 2012). In this study, infarct lesion was detected by using TTC staining at 24h post-MCAO. We found that after 1h of ischemia and 23h of reperfusion, all mice develop a moderate-severe infarct lesion involving the striatum and cortex (**Figure 9B**). Infarct volumes were larger in Tg-hCBS *Cbs*$^{-/-}$ mice than in CT mice (42.3 ± 4.9 mm^3 vs 53.5±10.5 mm^3, p = 0.055) (**Figure 9C**). No infarct lesion was detected in mice receiving sham procedure.

HHcy increased neurological deficit at 2h post-MCAO in Tg-hCBS Cbs$^{-/-}$ mice

Infarction lesion detected by TTC staining only reflects the extent of brain cell death, but not the impairment of neuronal function. Neurological deficit may better reflect the extent of functional impairment of the neurons that were still alive after stroke and is also a superior indicator of infarction volume in evaluating the recovery from stroke. In this study, Bederson-score scaling as described in the legend of **Figure 9** was used to evaluate the general neurological deficit, which mainly reflects the motor function. In line with a larger infarct volume, Tg-hCBS *Cbs*$^{-/-}$ mice also develop a worse neurological deficit than CT

mice at 24h post-MCAO (3.1 ± 0.64 vs 2.4 ± 1, p = 0.036) **(Figure 9D)**. No infarct lesion was detected in mice receiving sham procedure.

HHcy decreased survival rate at 3 days post-MCAO in Tg-hCBS Cbs$^{-/-}$ mice

Mortality was a predictor of stroke outcome and may be dependent of infarction volume and neurological deficit. In this study, the survival number of mice was recorded at one, two and three days post-MCAO. The survival rate was analyzed by using the Log-rank (Mantel-Cox) test. We found that there was a trend of decrease in survival rate in Tg-hCBS *Cbs$^{-/-}$* mice at three days post-MCAO (Log-rank test, p=0.18). There is no mice death in the shame group (**Figure 9E**).

HHcy increased BBB permeability at 24h post-tMCAO in both the ischemic and non-ischemic brains of Tg-hCBS Cbs$^{-/-}$ mice

Increased BBB permeability was associated with the expansion of infarct lesion. Here, we determine whether HHcy will exacerbate stroke-induced BBB disruption. BBB permeability was assessed by Evans blue assay and expressed as μg of Evans blue extravasation per g of brain tissue. We found that BBB permeability was significantly higher in the ischemic (IS) hemisphere than in the non-ischemic (NIS) hemisphere in CT mice (7.66 ± 0.66 vs 5.1± 0.057. P=0.0185). BBB permeability was significantly higher in

the NIS hemisphere (6 ± 0.11 vs 5.1 ± 0.57, P=0.006) of Tg-hCBS *Cbs*$^{-/-}$ mice than in the corresponding hemisphere of CT mice (**Figure 9F**).

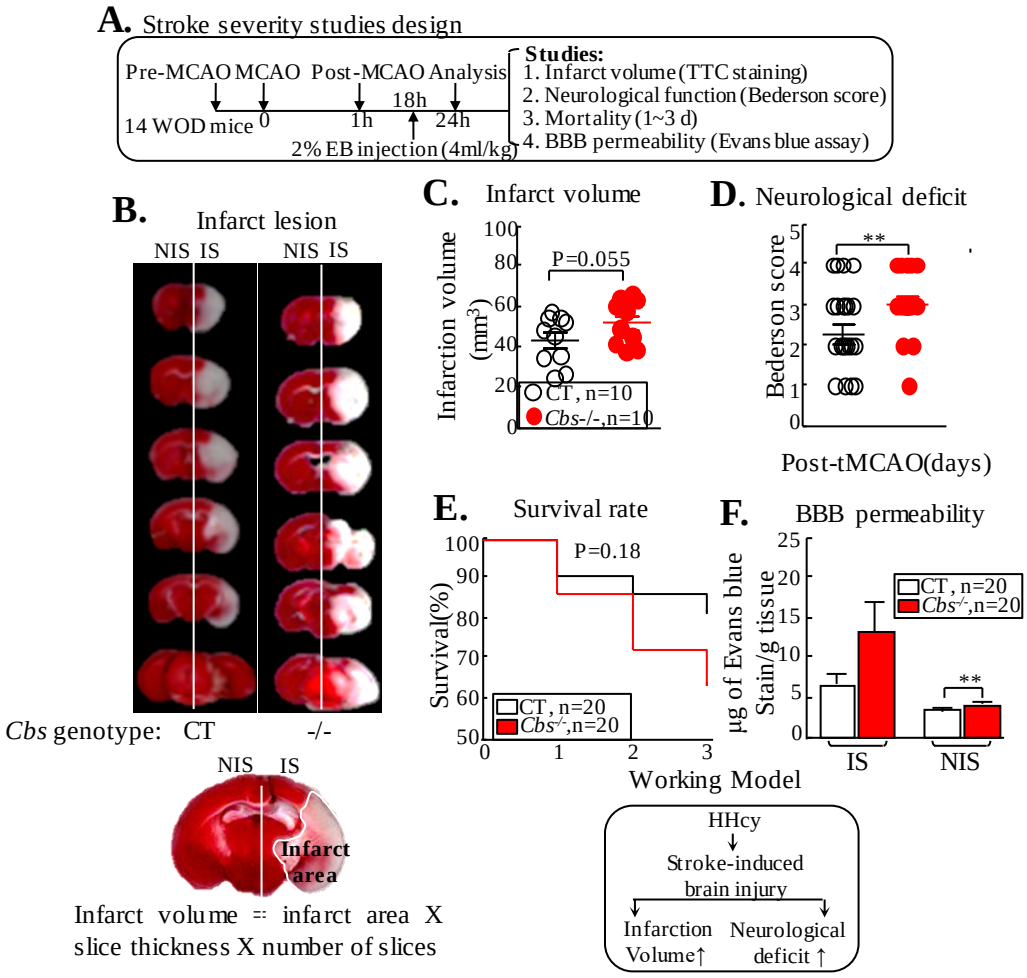

Figure 9. HHcy worsens stroke-induced brain damage and potentiated neurological deficit at 24h post-tMCAO. **A**) Stroke-severity study design. **B**) Image of infarct lesion. Representative image of TTC-stained 1mm brain slices from CT and Tg-hCBS *Cbs*$^{-/-}$ mice. The circle area on the coronal slice indicates ischemic infarction and the infarct volume was quantified using image J and calculated with the formula shown below. **C**) Infarct

volume. Tg-hCBS *Cbs*$^{-/-}$ developed larger infarction volume than CT mice after tMCAO. **D**) Neurological deficit. The neurological-deficit score was graded with the Bederson-score scale, in which 4 represents the most severe neurological deficit. Tg-hCBS *Cbs*$^{-/-}$ mice worsen stroke-induced neurological deficit. **E**) Survival rate. Survival rate was displayed using the Kaplan–Meier curve and analyzed using the Log-rank (Mantel-Cox) test. Survival rate was less in Tg-hCBS *Cbs*$^{-/-}$ than CT mice from 3 days post-tMCAO. **F**) BBB permeability. BBB permeability was evaluated by leakage of Evans blue (EB) dye in NIS and IS hemisphere. 2% EB (4ml/kg) was intraperitoneally injected 6h before the sacrifice of mice. Leaked EB was extracted from homogenized brain tissue and the amount was measured using a spectrophotometer at 610 nm. The exact amount of EB was quantified according to a standard curve. *Cbs*$^{-/-}$ mice promoted stroke-induced elevation of BBB permeability in both the NIS and IS hemispheres. Data were expressed as mean ± SEM; **, $P<0.05$, Tg-hCBS *Cbs*$^{-/-}$/tMCAO vs CT/tMCAO; student's t test. Abbreviations: BBB, Blood brain barrier; CT, Control; HHcy, Hyperhomocysteinemia; IS, Ischemic hemisphere; NIS, None ischemic hemisphere; tMCAO, Transient middle cerebral artery occlusion; TTC, 2, 3, 5-Triphenyltetrazolium chloride.

HHcy exacerbated stroke-induced brain injury partially via promoting brain-EC activation and inflammatory cells infiltration

HHcy aggravated brain NØ and inflammatory MC infiltration in Tg-hCBS Cbs$^{-/-}$ mice

It has been known that inflammatory response contributed to secondary brain injury after stroke. However, less is known about how HHcy affects the inflammatory response to stroke. This study aims to define the characteristics of brain immune cells Tg-hCBS *Cbs*$^{-/-}$ mice at 24h post-tMCAO. One of the established protocols in evaluating the numbers of infiltrating leukocytes and resident MG cells is based on the two-color quantitative and qualitative FACS analysis of CD45^{+}CD11b^{+}cell population (**Figure 10B**). First, we analyzed the effect of tMCAO alone on brain inflammatory response in CT mice. We found that at 24h post-MCAO the number of most brain immune cells, including NØ, total MC, Lym, Ly6C^{hi} MC, Ly6C^{mid}MC, Ly6C^{lo}MC and MG were significantly greater in the IS hemisphere than in the NIS hemisphere (~3 fold, ~2.7 fold, ~1.8 fold, ~2.43, ~2.93 fold, ~1.94 fold and ~2 fold respectively). MG was the only cell type with a greater cell number in the NIS hemisphere of tMCAO/CT mice than in the brain of sham/CT mice. These data suggested that NØ and MC were the predominant leukocytes and that inflammatory Ly6C^{hi}MC Ly6C^{mid}MC were the predominant MC subset infiltrating into the IS hemisphere (**Figure 10C**). We then analyzed how HHcy affected these events in the NIS and IS hemisphere of Tg-hCBS *Cbs*$^{-/-}$ mice. We found that the number of NØ and MC was ~1.75 fold ($P<0.05$) and ~1.5 ($P<0.05$) greater in the IS hemisphere of Tg-hCBS *Cbs*$^{-/-}$ mice

than in the IS hemisphere of CT mice. In the MC subset, the number of Ly6C^{hi}MC and Ly6C^{mid}MC was ~3 fold ($P<0.01$) and ~1.8 ($P=0.056$) greater in the IS hemisphere of Tg-hCBS *Cbs*$^{-/-}$ mice than in the ischemic hemisphere of CT mice. The number of Ly6C^{lo} MC in the IS hemisphere was not different between CT and Tg-hCBS *Cbs*$^{-/-}$ mice, thereby indicating that HHcy preferentially exacerbated stroke-induced recruitment of inflammatory MC subset into the IS hemisphere. HHcy did not further increase the number of stroke-induced MG in the IS hemisphere of Tg-hCBS *Cbs*$^{-/-}$ mice. In conclusion, HHcy increased the number of brain NØ and inflammatory MC in the IS hemisphere of Tg-hCBS *Cbs*$^{-/-}$ mice. We also tested the effect of stroke and HHcy on the brain immune cell composition (**Figure 10D**). First, we found that the percentage of Lym among brain immune cells or infiltrated leukocytes was greatly decreased in both the IS and NIS hemispheres of all mice. This was possibly due to the relatively inert response of Lym in the acute phase of stroke, compared to other more actively responding MGs and leukocytes. Second, we found that the percentage of NØ and MC among brain immune cells, the percentage of NØ among leukocytes and the percentage of Ly6C^{hi}MC among total MC were also significantly higher in the IS hemisphere of Tg-hCBS *Cbs*$^{-/-}$ mice. These were consistent with the above findings, which indicated that NØ and inflammatory MC were the main leukocytes recruited into the IS hemisphere after tMCAO and affected by HHcy.

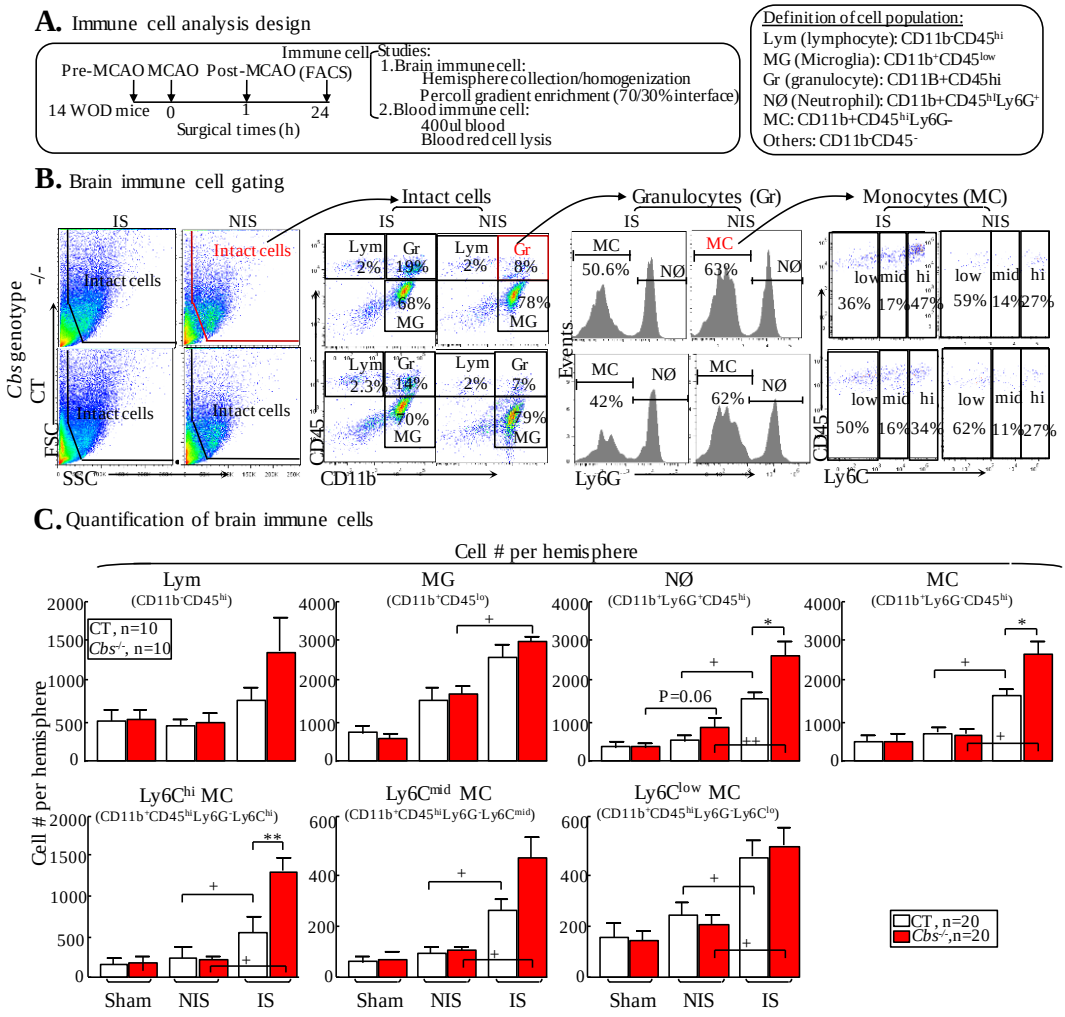
A. Immune cell analysis design
Pre-MCAO MCAO Post-MCAO (FACS)
14 WOD mice
0
1
24
Surgical times (h)
Immune cell Studies:
1.Brain immune cell:
Hemisphere collection/homogenization
Percoll gradient enrichment (70/30% interface)
2.Blood immune cell:
400ul blood
Blood red cell lysis
Definition of cell population:
Lym (lymphocyte): CD11b-CD45hi
MG (Microglia): CD11b+CD45low
Gr (granulocyte): CD11B+CD45hi
NØ (Neutrophil): CD11b+CD45hiLy6G+
MC: CD11b+CD45hiLy6G-
Others: CD11b-CD45-
B. Brain immune cell gating
Intact cells
Granulocytes (Gr)
Monocytes (MC)
IS
NIS
Cbs genotype
-/-
CT
FSC
SSC
Intact cells
Lym 2%
Gr 19%
68% MG
Lym 2%
Gr 8%
78% MG
Lym 2.3%
Gr 14%
70% MG
Lym 2%
Gr 7%
79% MG
CD45
CD11b
Events
MC 50.6%
NØ
MC 63%
NØ
MC 42%
NØ
MC 62%
NØ
Ly6G
low 36%
mid 17%
hi 47%
low 59%
mid 14%
hi 27%
low 50%
mid 16%
hi 34%
low 62%
mid 11%
hi 27%
Ly6C
C. Quantification of brain immune cells
Cell # per hemisphere
Lym
(CD11b-CD45hi)
MG
(CD11b+CD45lo)
NØ
(CD11b+Ly6G+CD45hi)
MC
(CD11b+Ly6G-CD45hi)
CT, n=10
Cbs-/-, n=10
P=0.06
Ly6Chi MC
(CD11b+CD45hiLy6G-Ly6Chi)
Ly6Cmid MC
(CD11b+CD45hiLy6G-Ly6Cmid)
Ly6Clow MC
(CD11b+CD45hiLy6G-Ly6Clo)
Sham
NIS
IS
CT, n=20
Cbs-/-,n=20

D. Brain immune cell composition

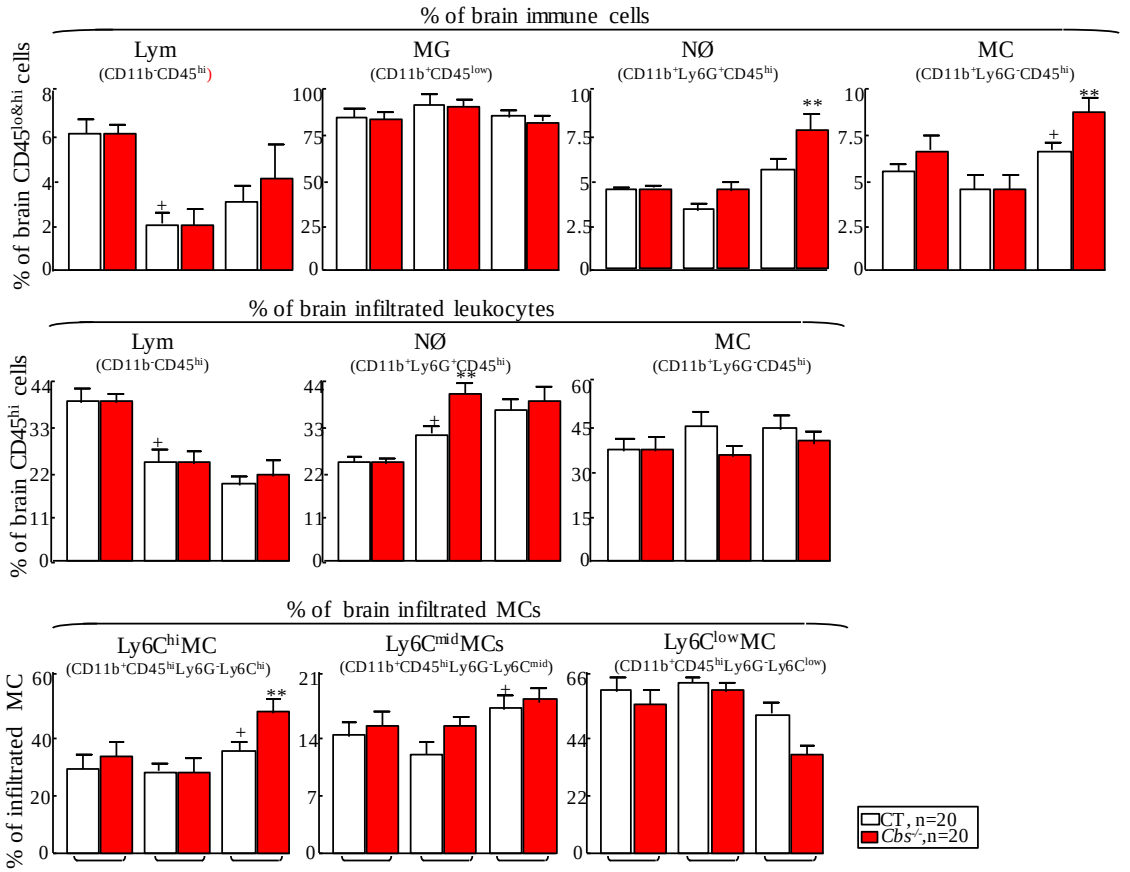

Figure 10. HHcy potentiated stroke-induced NØ and inflammatory MC infiltration in the IS hemisphere at 24h post-tMCAO. A) Immune cell analysis design. **B**) Brain immune cell gating. Representative dot plots and gating strategies for analyzing immune cells of both the NIS and IS hemisphere of CT and Tg-hCBS *Cbs*$^{-/-}$ mice at 24h post-tMCAO. **C**) Quantitation of brain immune cells. The absolute number of infiltrated leukocyte subsets and resident MG per hemisphere was calculated as the total counted isolated total cells multiplied by the corresponding percentage of total intact cells. HHcy potentiated stroke-induced NØ and inflammatory MC infiltration in the IS hemisphere at 24h post-tMCAO. **D**) Brain immune cell composition. Data were shown as mean ± SEM;

**, P<0.05, Tg-hCBS *Cbs*$^{-/-}$/tMCAO vs CT/tMCAO; +, P<0.05, IS vs NIS; Student's t test. Abbreviations: CT, Control; FACS, Fluorescence-activated cell sorting; Gr, Granulocyte; HHcy, Hyperhomocysteinemia; IS, Ischemic hemisphere; Lym, Lymphocyte; MG, Microglia; MC, Monocyte; NØ, Neutrophil; NIS, None ischemic hemisphere; tMCAO, Transient middle cerebral artery occlusion.

HHcy did not significantly alter the blood-immune cell number or composition in Tg-hCBS Cbs$^{-/-}$ *mice*

It has been well known that ischemic stroke greatly modulates systemic inflammatory responses, which may reversely influence the stroke prognosis. Therefore, we characterized the blood immune cells simultaneously with the brain immune cell analysis. The gating strategy is described in **Figure 11A**. First, we examined the effect of tMCAO on the cell number of various blood leukocytes, and found that the number of NØ, total MC and Lym all show a decreasing trend in the blood of tMCAO mice compared to that of sham mice. Within MC, the number of Ly6C^{hi}MC and Ly6C^{mid}MC was ~4 fold, and ~2 fold less in the blood of tMCAO mice compared to that of sham mice (not significant). The number of Ly6C^{lo}MC was not changed by tMCAO. The reason for why the number of blood NØ, total MC and Lym decreased was unclear. However, two studies using the same tMCAO also demonstrate a similar phenomenon, which may be caused by the shift of blood leukocyte into the brain. We then examined the effect of HHcy on the cell number of various blood leukocytes in Tg-hCBS *Cbs*$^{-/-}$ mice with sham or with tMCAO invention and

found that the number of various leukocytes in blood were not different between CT and Tg-hCBS *Cbs*$^{-/-}$ mice receiving sham procedure. However, HHcy showed an increasing trend for the number of all leukocytes or MC subset in the blood of Tg-hCBS *Cbs*$^{-/-}$ mice receiving tMCAO ($P>0.5$), thereby suggesting that HHcy exacerbated systemic inflammatory response (**Figure 11B**). We also tested the effect of stroke and HHcy on the blood immune cell composition (**Figure 11C**) and found that the percentage of NØ significantly increased, while the percentage of Lym significantly decreased in both CT and Tg-hCBS *Cbs*$^{-/-}$ mice at 24h post-tMCAO. This also suggests that the NLR ratio increased after MCAO. These data were in line with many human studies which had demonstrated that higher NLR was associated with poor stroke prognosis. HHcy did not change the percentage of NØ, MC and Lym with or without MCAO. However, we did observe a trend of increase in the percentage of Ly6C^{hi}MC and a decreased percentage of Ly6C^{low}MC in the blood of Tg-hCBS *Cbs*$^{-/-}$ mice with either sham or tMCAO. The data were in line with our lab's finding, showing that severe HHcy promoted peripheral inflammatory MC differentiation. Interestingly, the percentage of Ly6C^{hi}MC was significantly higher ($p<0.05$) and Ly6C^{lo}MC was significantly lower ($p<0.05$) in the blood

of MCAO mice than in the blood of sham mice, thereby suggesting that, like HHcy, stroke also promoted peripheral inflammatory MC differentiation.

A. Blood immune cell gating strategy

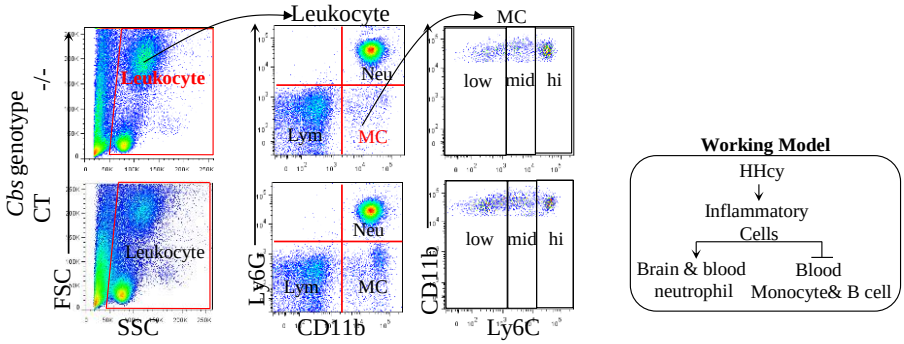

B. Blood myeloid cell subpopulations

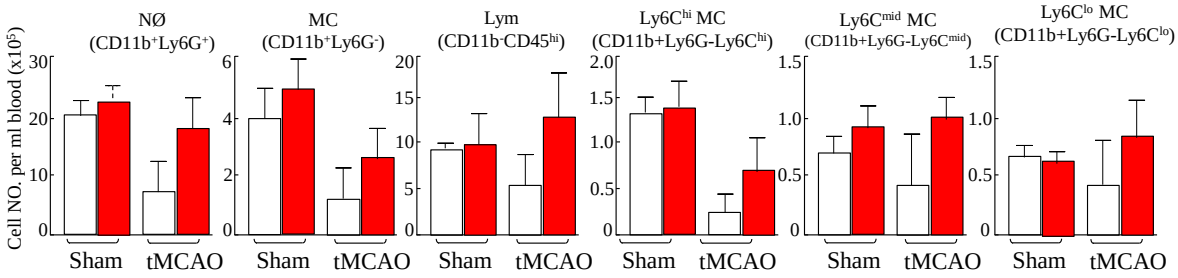

C.

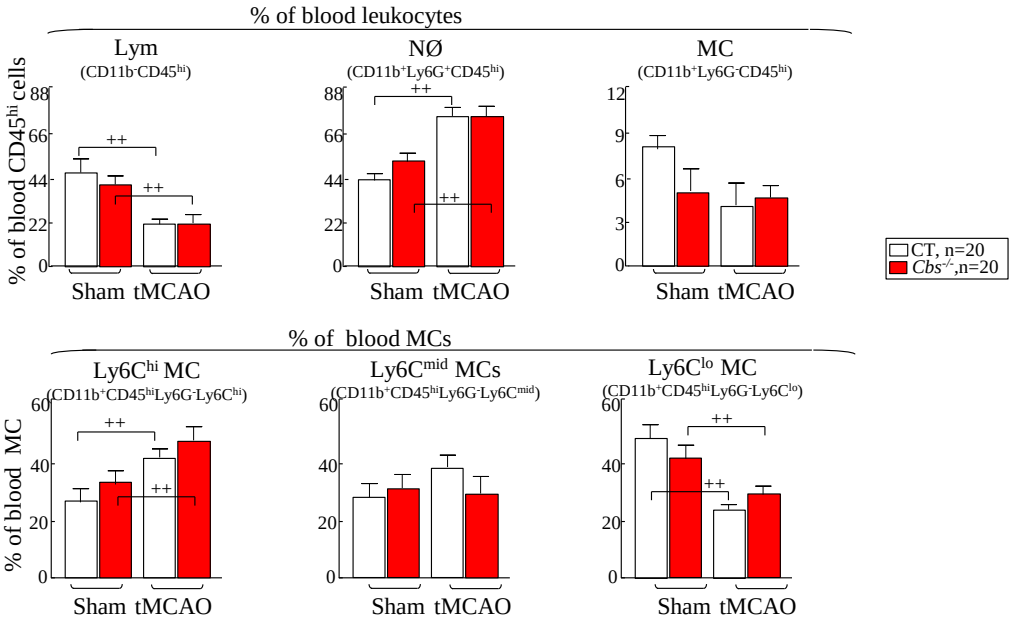

Figure 11. HHcy did not significantly alter the blood immune cell number or composition at 24h post-tMCAO. **A**) Representative dot plots and gating strategies for analyzing blood immune cells of sham- and tMCAO-treated CT, and Tg-hCBS *Cbs*$^{-/-}$ mice. **B**) Quantification of the number of blood leukocyte subsets. **C**) Bars summarizing the composition of blood immune cells. Data were expressed as mean ± SEM; *, P<0.05, **, P<0.01, HHcy/tMCAO vs CT/tMCAO group; ++, P<0.01, sham vs tMCAO; Student's t test. Abbreviations: CT, Control; FACS, Fluorescence-activated cell sorting; Gr, Granulocyte; HHcy, Hyperhomocysteinemia; Lym, Lymphocyte; MG, Microglia; MC, Monocyte; NØ, Neutrophil; tMCAO, Transient middle cerebral artery occlusion.

Clodronate selectively depleted Ly6C^{lo}MC, and increased the proportion of Ly6C^{hi}MC and stroke-induced infarction in CT mice

The detrimental role of NØ in stroke has been well established. However, the role of MC and its subset Ly6C^{hi}MC in stroke continue to be debated. It is necessary to determine whether HHcy-exacerbated, stroke-induced Ly6C^{hi}MC mediates HHcy-exacerbated, stroke-induced brain injury. We firstly hypothesized that the depletion of MC attenuates stroke-induced brain injury. Clodronate liposome was used to deplete MC. Firstly, we tested the effect of different doses of Clodronate liposome (5µl/g, 10µ/g and 15µ/g) on blood MC. The percentage of blood MC subset was determined by FACS analysis. We found that Clodronate liposome indeed significantly decreased the number of MC. However, increasing the doses of Clodronate liposome was accompanied with an increased

percentage of Ly6C^{hi}MC, and a decreased percentage of Ly6C^{lo}MC and Ly6C^{mid}MC (**Figure 12C)**. The percentage of blood Ly6C^{hi} MC was ~30% with PBS liposome, increasing to ~60% and ~90% at two days after receiving10 μ/g and 15μ/g Clodronate liposome respectively. We then subjected the CT mice treated with 15μ/g PBS liposome and CT mice treated with 15μ/g Clodronate liposome treatments for two days prior tMCAO. After 24h, infarct volume was assessed. Infarct volumes were larger in Clodronate liposome-treated mice than in PBS liposome-treated mice (40.2 ± 9.2 mm^3 vs 57.1 ± 8.5 mm^3, p>0.05) (Figure 12D).

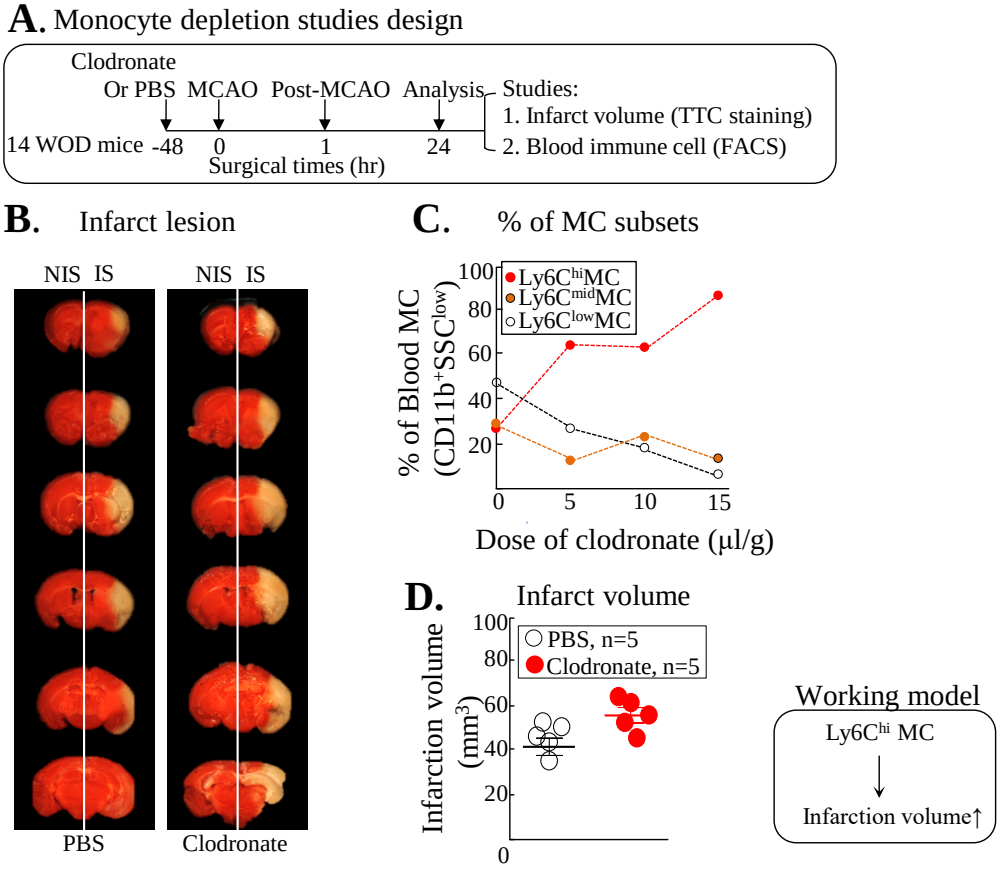

Figure 12. Clodronate selectively depleted Ly6ClowMC and increased the proportion of Ly6Chi MC and stroke-induced infarction in CT mice. **A**) Monocyte depletion study design. **B**) Image of infarct lesion. Representative image of TTC-stained 1mm brain slices from CT mice receiving a PBS or Clodronate injection. **C**) Percentage of MC subsets. Clodronate preferentially depleted the Ly6Clow MC subset. **D**) Infarct volume. Clodronate injection increased stroke-induced infarction in CT mice. Abbreviations: FACS, Fluorescence-activated cell sorting; MCAO, Middle cerebral artery occlusion; MC, Monocyte.

HHcy and stroke elevated inflammatory cytokine levels in the ischemic brain at 24 h post-tMCAO

Cytokines are the products, as well as the contributors of inflammation. We used the cytokines assay to determine whether HHcy-exacerbated brain inflammatory cell infiltration is accompanied with more pro-inflammatory cytokines production. The array also provided an unbiased screening by which to identify potential molecular target-mediated, HHcy-exacerbated, stroke-induced brain injury. Mice were subjected to tMCAO and brain proteins were exacted 24h after for the array, which contained 40 different cytokines. We found that eight cytokines, including anti-inflammatory (TIMP1, IL1RA) and pro-inflammatory ones (MCSF, CCL2, ICAM1, CXCL1, CCL12 and TNFα) were robustly induced or upregulated in the ischemic hemisphere of tMCAO mice, compared to the same side of the hemispheres of sham-operated mice ($P<0.05$) (**Figure 13**). Among

these cytokines, TIMP1, IL1RA, CCL2, ICAM1 and CXCL1 cytokines were higher in tMCAO/Tg-hCBS *Cbs*$^{-/-}$ mice than in tMCAO/CT mice ($P<0.05$). Another two cytokines, CCL3 and CXCL2, were only induced in the ischemic hemisphere of Tg-hCBS *Cbs*$^{-/-}$ mice. IL1α, a pro-inflammatory cytokine, was moderately detected in all mice and not induced by tMCAO, but had a higher level in Tg- tMCAO/hCBS *Cbs*$^{-/-}$ mice than in tMCAO/CT mice. Interestingly, most of these Hcy and stroke-induced cytokines are chemotactic for NØ and MC. For example, CXCL1 and CCL3 were strong NØ attractors. CCL2 mainly attracted Ly6C^{hi} MC. ICAM1 was essential for general leukocyte adhesion and migration. We selected the cytokines as the potential molecules mediating HHcy-exacerbated, stroke-induced brain injury, based on five criteria: induced by HHcy, induced by stroke, fold change >1.5, with moderate or high protein level and pro-inflammatory. Both ICAM1 and

CCL2 met all criteria. However, due to the technical issue in detecting intracellular CCL2, we selected ICAM1 as the studied molecular.

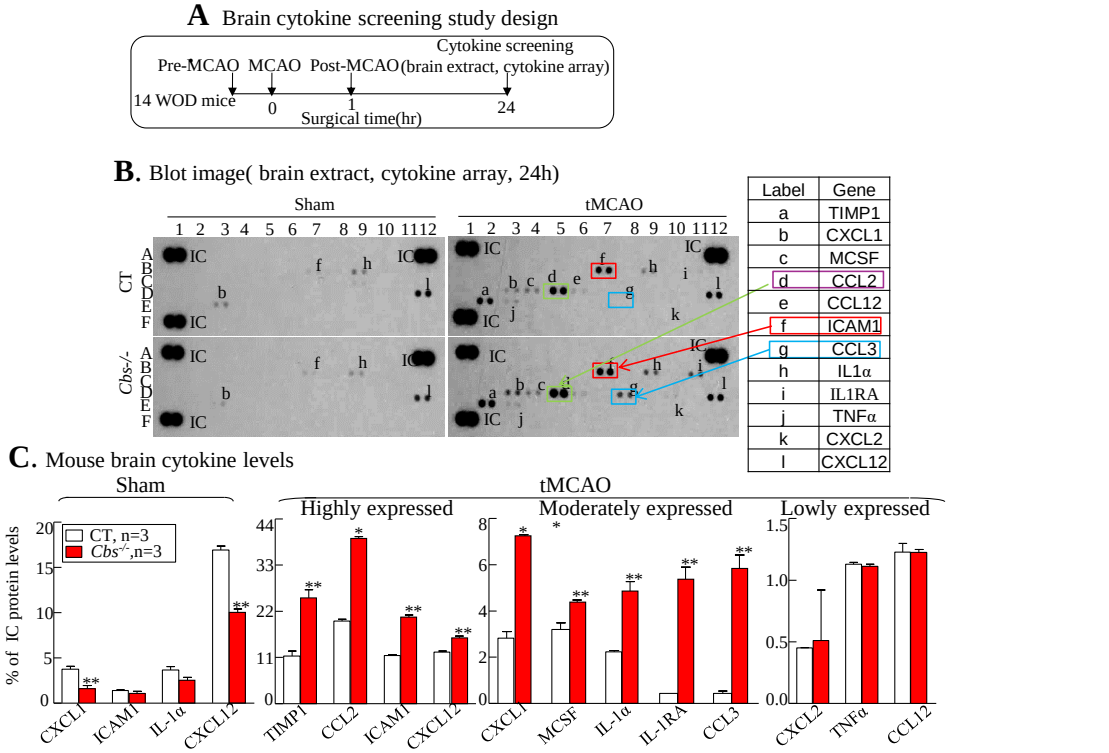

D. HHcy and stroke-elevated cytokines in the brain

Gene symbol (full name)	Functions	Stroke induced (Δ) (tMCAO vs sham) CT	Stroke induced (Δ) (tMCAO vs sham) *Cbs*-/-	HHcy induced (Δ) (*Cbs*-/- vs CT) Sham	HHcy induced (Δ) (*Cbs*-/- vs CT) tmcao	
CCL3 (Chemokine CC motif ligand 3)	↑MC/NØ attraction, ↑acute inflammation	/	/	/	**14.3**	Not induced by stroke
CXCL1 (Chemokine CXC motif ligand 1)	↑NØ attraction, ↑angiogenesis	/	11.7	-2.3	2.6	Dural direction change in HHcy
CCL2 (Chemokine CC motif ligand 2)	↑MC/memory TC/DC attraction ↑AS, ↑neuroinflammation.	43.6	**87.1**	/	2.2	Technique challenge
ICAM1 (Intracellular Adhesion Molecule 1)	↑Leukocyte endothelial transmigration, ↓tight junction	8.19	**18.6**	/	1.8	Molecule studied
CXCL12 (Chemokine CXC motif ligand 12)	↑Lymphocyte attraction, ↓angiogenesis	1.4	1.55	-1.7	1.2	Small change
IL1RA (Interleukin1 receptor antagonist)	↓IL1α/β activity, ↑gastric cancer	/	/	/	11.9	Protective
IL1α (Interleukin1 receptor antagonist)	TNFα synergism, fever, inflammation	/	/	/	2.3	Not induced by stroke
TIMP1 (Tissue inhibitors of metalloproteinases)	↓MMP activity, ↓angiogenesis	25.1	55.7	/	1.7	Protective

Figure 13. HHcy and stroke elevated inflammatory cytokine levels in the ischemic brain at 24h post-tMCAO. A) Brain cytokine screening study design. Representative immunoblot images of cytokines from the IS hemisphere of CT and Tg-hCBS *Cbs*$^{-/-}$ mice, captured following a 10min exposure to x-ray film. Detected cytokines were highlighted

with labels. **B**) Blot image. **C**) Mouse brain cytokine levels. Quantitative analysis of detected cytokines level. Data were expressed in arbitrary units relative to appropriate positive control. **D**) HHcy and stroke-elevated cytokines in the brain. **E**) Table summarized cytokines that were significantly altered by stroke, and their cellular and biological function. Data were expressed as mean ± SEM; **, P<0.05, Tg-hCBS *Cbs*$^{-/-}$/tMCAO vs CT/tMCAO; Student's t test. Abbreviations: CT, Control; HHcy, Hyperhomocysteinemia; tMCAO, Transient middle cerebral artery occlusion; △, fold change.

MC adhesion and transendothelial migration were enhanced to Hcy-treated HBMEC

Our brain immune cell characterization demonstrated that HHcy exacerbated the brain's acute inflammatory response by promoting NØ and inflammatory MC infiltration at 24h after tMCAO. Leukocytes recruitment into the brain relied on their interaction with brain EC. We utilized MC-EC adhesion assay to confirm whether Hcy treatment also enhanced MC adhesion to BMEC in vitro. We treated MC and BMEC individually to determine which cell type responds to Hcy. HMBEC monolayer, THP-1 cells or freshly isolated HPBMC were treated with 50μM DL-Hcy for 24h. THP-1 cells or freshly isolated HPBMC were allowed to adhere to the HMBEC monolayer for 1h. We found that there was an increase in the number of primary THP-1 cells or human HPBMC that adhered to the Hcy-treated HBMEC (**Figures 14B&C)**. However, treating THP-1 with Hcy did not increase its adhesion to HMBEC monolayer, suggesting that Hcy-induced HMBEC EC activation was responsible for Hcy-enhanced THP-1/HBMEC adhesion (**Figure 14D)**. We also

conducted the MC trans-endothelial migration assay by using a Boyden chamber. CCL2 was added to promote the chemotaxis of MC and to mimic the conditions of abundant CCL2 expressed within the IS hemisphere. We found that the number of transmigrated THP-1 was dose dependent and that Hcy treatment could further promoted the THP-1 in the presence of a high dose of CCL2 (100ng/ml) (**Figures 14F&G**).

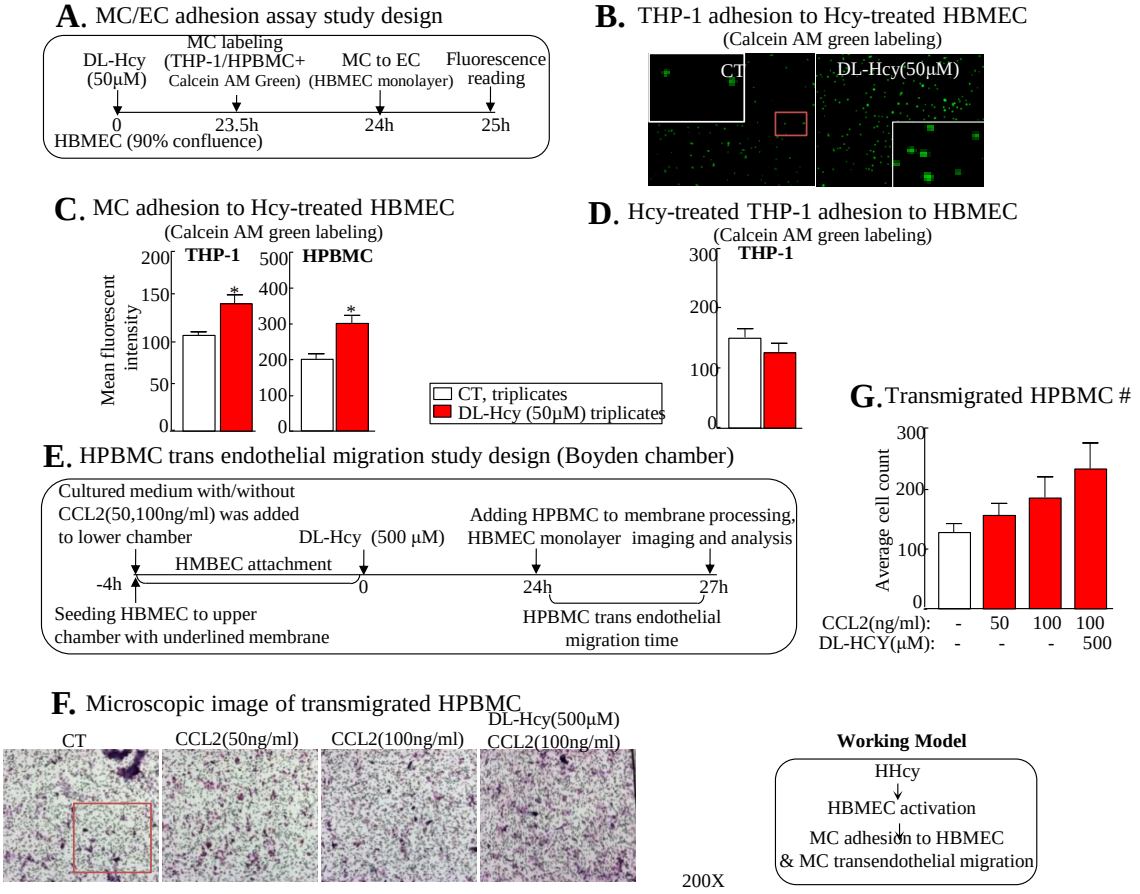

Figure 14. Monocyte-EC adhesion assay with THP-1 cells and primary human monocytes in HBMEC. **A**) MC/EC adhesion assay study design. **B**) THP-1 adhesion to Hcy-treated HBMEC. Representative fluorescence microscopic image of labeled THP-1 cells adhered HBMEC. **C**) MC adhesion to Hcy-treated HBMEC. The percentage of cell

adhesion was determined by a fluorescent plate reader. **D**) Hcy-treated THP-1 adhesion to HBMEC. **E**) HPMC transendothelial migration study design (Boyden chamber). **F**) Microscopic image of transmigrated HPMC. **G**) Transmigrated HPMC #. Purple-stained cells were counted per field. Mean value from three fields was used for quantification and comparison. Hcy increased HPML transendothelial migration. Data were shown as mean ± SEM; *p<0.05, Hcy vs CT; Student's t test. Abbreviations: CCL2, Chemokine CC motif ligand 2; CT, Control; H, H; Hcy, Homocysteine; HPBMC, Human peripheral blood monocyte; HBMEC, Human brain microvascular endothelial cells; MC, Monocyte; #, Cell number.

Role of ICAM1 in HHcy-exacerbated, stroke-induced brain damage

HHcy upregulated ICAM1 in mouse brain EC from the IS hemisphere of Tg-hCBS Cbs$^{-/-}$ mice at 24h post-MCAO

Our brain cytokine array data showed that ICAM1 was upregulated by stroke and HHcy. ICAM1 is an EC-specific adhesion molecule that mediates leukocyte adhesion and transmigration. Moreover, in vitro MC-EC adhesion assay has demonstrated that EC is the cell responsible for mediating Hcy-enhanced MC-EC interaction. Therefore, we hypothesized that HHcy-induced upregulation of ICAM1 of BMEC contributes to HHcy-exacerbated, stroke-induced NØ and inflammatory MC infiltration. Firstly, we needed to confirm the upregulation of ICAM1 in mouse BMEC after stroke. CT and Tg-hCBS *Cbs*$^{-/-}$ mice were subjected to tMCAO, and 24h after, brain microvasculature from the IS and NIS

hemispheres were isolated, and BMEC single cells' suspension was attained, as described in the methods. The BMEC surface level of ICAM1 was examined by FACS. CD31 was used as EC marker and CD45 was used to exclude the granulocyte that also expressed CD31. We found that at 24h after tMCAO, the surface expression level of ICAM1 was significantly higher in mouse BMEC from the IS hemisphere than from the NIS hemisphere. HHcy further enhanced the ICAM1 expression of mouse BMEC from the IS hemisphere, but not from the NIS hemisphere in Tg-hCBS *Cbs*$^{-/-}$mice (**Figure 15)**.

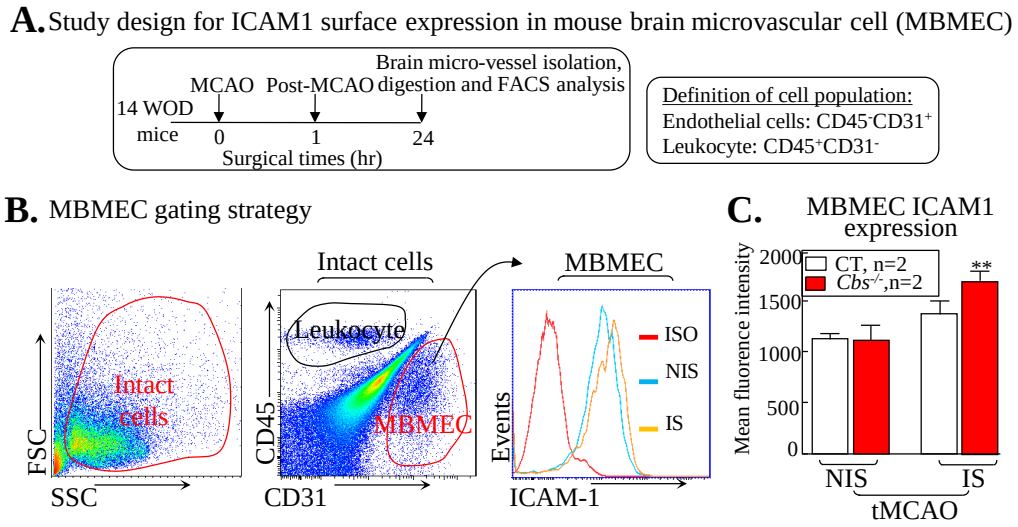

Figure 15. HHcy increased ICAM1 expression in MBMEC of the ischemic hemisphere at 24h post-tMCAO. **A**) Study design for ICAM1 surface expression in mouse brain microvascular cell (MBMEC). **B**) MBMEC gating strategy. Representative dot plots and gating strategies for analyzing MBMEC of the IS and NIS hemisphere from CT and Tg-hCBS *Cbs*$^{-/-}$ mice. **C**) MBMEC ICAM1 expression. Quantification was based on the mean fluorescence intensity of ICAM. Data were shown as mean ± SEM; **,

P<0.05, Tg-hCBS *Cbs*$^{-/-}$/tMCAO vs CT/tMCAO; Student's t test. Abbreviation: IS, Ischemic hemisphere; MBMEC, mouse brain microvascular cell; NIS, Non-ischemic hemisphere; tMCAO, Transient middle cerebral artery occlusion.

Hcy regulated ICAM1 in cultured HBMEC under both normoxia and hypoxia conditions

In order to attain more clinical relevance, we used an in-vitro ischemia-reperfusion model to test the effect of Hcy on primary HBMEC activation. We exposed cultured HBMEC to the conditions of oxygen glucose deprivation (OGD) and found that, compared to normoxia conditions, hypoxia alone significantly upregulates ICAM1 at 1, 4 and 24h, but not SELE or SELP. Under both hypoxia and normoxia conditions, 50μM DL-Hcy upregulated SELE, SELP and ICAM1 after 1 and 4h of treatment. Hcy also upregulated SELE, SELP and ICAM1 of HBMEC subjected to 4h of hypoxia, followed by another 20h of normoxia. Hypoxia and Hcy-induced upregulation SELE and SELP reached their maximum levels at

the early1h point, whereas the expression level of ICAM1 increased with the duration of hypoxia or Hcy treatment (**Figure 16**).

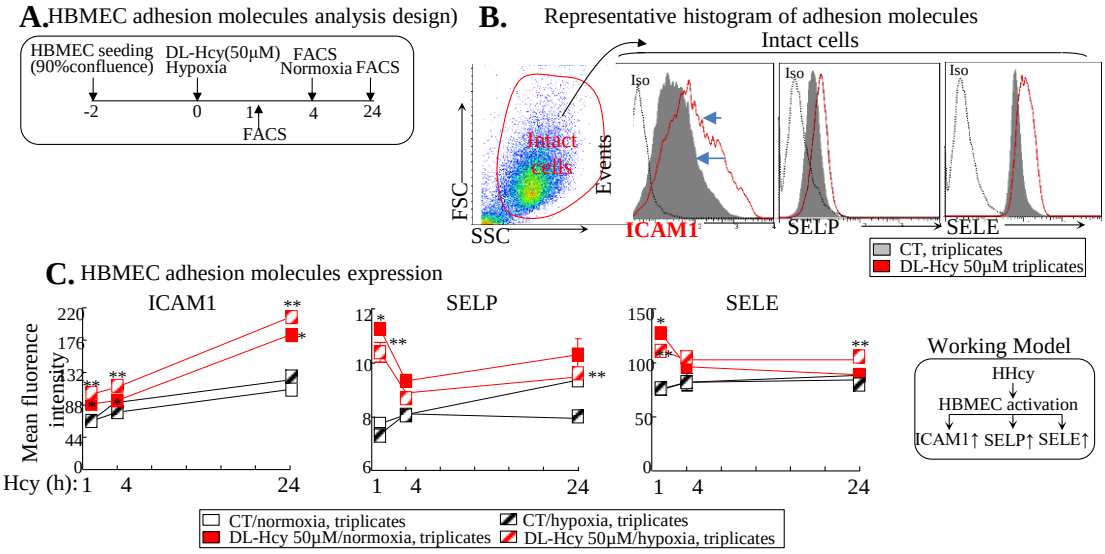

Figure 16. Hcy promoted the upregulation of adhesion molecules in cultured HBMEC. A) HBMEC adhesion molecules analysis design. **B**) Representative dot plots/histograms and gating strategies for measuring the surface expression of HBMEC adhesion molecules. Mean fluorescence intensity was used for quantification and comparison. **C**) HBMEC adhesion molecules expression. Data were shown as mean ± SEM; *, P<0.05, Hcy vs CT; **, P<0.05, Hcy/hypoxia vs CT/hypoxia; Student's t test. Abbreviation: CT, Control; Hcy, Homocysteine; ISO, Isotype; SELE, E-selectin; SELP, P-selectin.

Hcy increased primary HBMEC pro-inflammatory cytokine secretion

Increased pro-inflammatory cytokine secretion is another marker of EC activation. We therefore conducted the HBMEC cytokine array in order to determine whether Hcy increases pro-inflammatory cytokines generation. We treated the primary HBMEC with 50μM DL-Hcy, and subsequently both the cell lysis and cultured medium were collected for array analysis, and the data was summarized in **Figure 17**. We found that 25 cytokines were altered in supernatant, while only eight cytokines were changed in cell lysis, with a common six cytokines changed in both cell supernatant and cell lysis. Interestingly, most of the upregulated cytokines in cell lysis or supernatant (>1.5 fold, $P<0.05$) by 50μM DL-Hcy were pro-inflammatory and shown to be detrimental to stroke, including IL22, IL6, IL8, LCN2, IFNG, CSF2, OPN, CCL3, CCL2 and ICAM1. Relatively few cytokines were downregulated and related to angiogenesis (CXCL1 and Ang), extracellular matrix homeostasis (ACAN) and neuroprotective growth factor (BNDF). It is noteworthy that IL-6, CCL2 and ICAM1 were also repeatedly found upregulated by Hcy in other peripheral

EC or plasma. ICAM1, CCL2 and CCL3 have also been identified in the ischemic hemisphere of tMCAO mice and can be significantly upregulated in Tg-hCBS *Cbs*$^{-/-}$ mice.

A. Hcy altered cytokines in **supernatant** (HBMEC, Hcy 50μM, 24h))

	Gene symbol	Gene full name	Functions	Fold change (Hcy vs CT)
Selected For Conformation	IL22	Interleukin 22	↑BBB permeability	22.4
	IL6	Interleukin 6	↑Stroke risk	8.2
	LCN2	Lipocalin 2	↑Brain inflammation	5.3
	IGFBP2	Insulin like growth factor binding protein 2	Unknown	3.5
	CSF2	Colony stimulating factor 2	↑Stroke recovery	3.1
	IFNG	Interferon gamma	Unclear	3.1
	OPN	Osteopontin	Neuroprotective	3.0
	CD147	Basingin	MMP inducer, ↑stroke-induced brain injury	1.9
	IL8	Interleukin 8	↓Stroke-induced neurological deficit & inflammation	1.6
	Ang 2	Angiopoietin 2	Facilitates angiogenesis,inducing BBB dysruption	1.4
	FGF2	Basic fibroblast growth factor	Neuroprotective	1.3
	VEGF	Vascular endothelial growth factor	↑Stroke-induced brain injury	1.2
	MIF	Microphage migration inhibitory factor	↑Stroke-induced brain injury & neurological deficit	1.2
	PTX 3	Petraxin-3	Stroke biomarker	1.1
	CD105	Endoglin	↓Brain EC apoptosis, ↑stroke recovery	-1.2
	Ang	Angiogen	Inversely correlated with stroke outcome	-1.8
	PLAUR	Plasminogen activator	Dissolving blood clot, ↑stroke hemorrhage	-1.9
	CXCL1	Chemokine CXC motif ligand 1	↑Angiogenesis, ↑leukocyte recruitment	-4
Common induced cytokines in both cell lysis and supernatant	ICAM1	Intracellular Adhesion Molecule1	↑Leukocyte endothelial transmigration, ↓tight junction	2.3
	MIC1	Macrophage inhibitory cytokine 1	Unclear	3.5
	DKK1	Dickkopf WNT signaling pathway inhibitor 1	↓Wnt signaling	2.1
	CCL2	Chemokine CC motif ligand 2	↑MC/memory T C/DC attraction ↑AS, ↑neuroinflammation.	1.1
	FGF19	Fibroblast growth factor 19	↓Hepatic fatty acid synthesis	-1.1
	IL1RL1	Interleukin 1 receptor-like	↓Stroke-induced brain injury	-1.4

B. Hcy altered cytokines in cell **lysis** (HBMEC, Hcy 50μM, 24h))

	BDNF	Brain-derived neurotrophic factor	↑Neuroplasticity	-1.3
	ACAN	Aggrecan1	Extracellular matrix	-5.0
Common induced cytokines in both cell lysis and supernatant	ICAM1	Intracellular Adhesion Molecule1	↑Leukocyte endothelial transmigration, ↓tight junction	2.3
	MIC1	Macrophage inhibitory cytokine 1	Unclear	3.5
	DKK1	Dickkopf WNT signaling pathway inhibitor 1	↓Wnt signaling	2.1
	CCL2	Chemokine CC motif ligand 2	↑MC/memory T C/DC attraction ↑AS, ↑neuroinflammation.	1.1
	FGF19	Fibroblast growth factor 19	↓Hepatic fatty acid synthesis	-1.1
	IL1RL1	Interleukin 1 receptor-like	↓Stroke-induced brain injury	-1.4

Figure 17. Hcy promoted inflammatory cytokines secretion in HBMEC. Cells were treated with DL-Hcy (50μM) for 24h. Both cells and cultured supernatant were collected for cytokines screening. Both the CT and Hcy groups consist of three pooled samples of

cell lysis or corresponding cultured supernatant. **A**) Selected cytokines significantly altered by Hcy in EC culture supernatant. **B**) Selected cytokines significantly altered by Hcy in EC cell lysis.

ICAM1 blocking antibody attenuated HHcy-exacerbated, stroke-induced brain injury

In order to confirm the role of ICAM1 as a mediator in HHcy-exacerbated, stroke-induced brain injury, we injected the CT or Tg-hCBS *Cbs*$^{-/-}$ mice with ICAM1 blocking and subjected the mice to MCAO in order to observe whether ICAMI blockade can reverse the brain injury induced by stroke and exacerbated by HHcy. CT or Tg-hCBS *Cbs*$^{-/-}$ mice injected with the same dose of IgG isotype antibody were used as control. We found that one dose of ICAM1-blocking antibody (2mg/kg) administered directly after reperfusion effectively reduced infarct volume by ~60% in both CT and Tg-hCBS *Cbs*$^{-/-}$ mice at 24h post-tMCAO, compared to the respective genotype mice injected with only IgG isotype. However, Tg-hCBS *Cbs*$^{-/-}$ mice continued to show a trend of higher infarct lesion compared to CT mice, even after blocking down the ICAM1, thereby indicating that other

mechanisms independent of ICAM1 may be involved in HHcy-exacerbated and stroke-induced brain injury (**Figure 18)**.

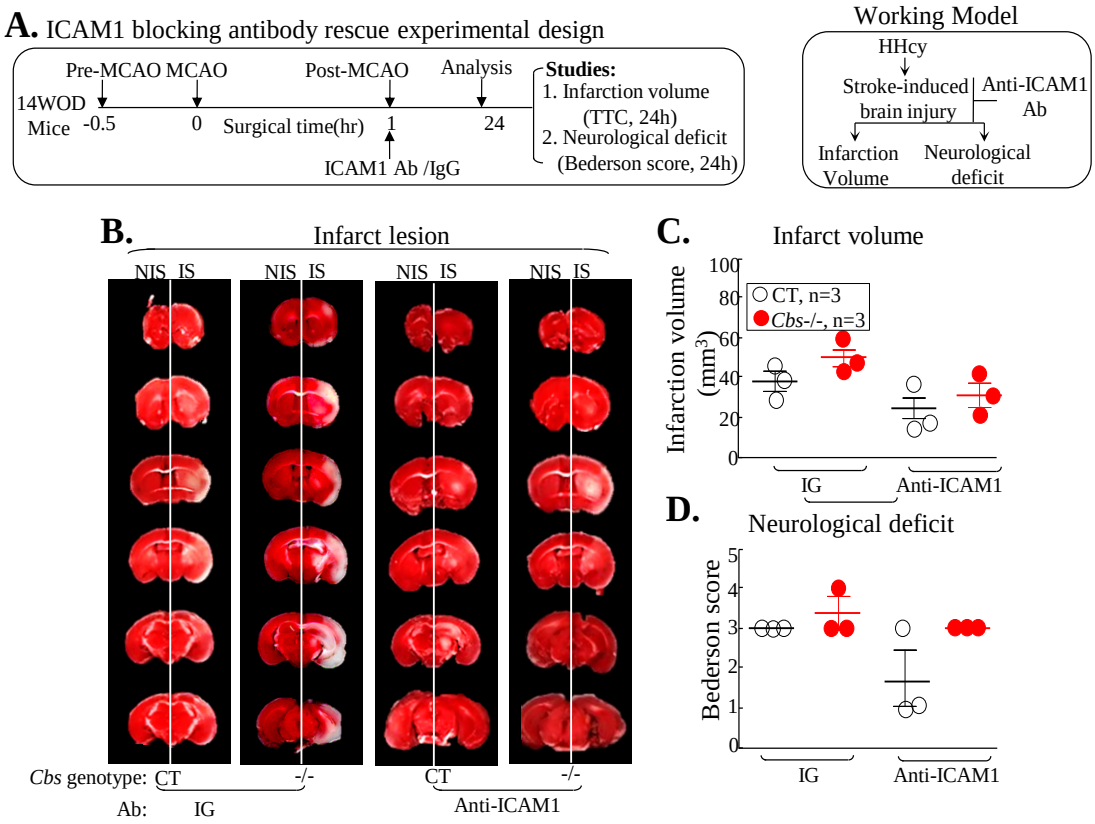

Figure 18. ICAM1 antibody attenuated HHcy-exacerbated and stroke-induced infarction. **A**) ICAM1-blocking antibody rescue study design. **B**) Infarction lesion. Representative image of TTC-stained 1mm brain slices from CT and HHcy mice with IgG antibody or ICAM1-blocking antibody injection. **C**) Infarction volume. Quantitative analysis of infarct volume as shown in scatter dot plot. One scatter plot represents one mouse. **D**. Neurological deficit. The neurological deficit score was graded with Bederson-score scale, where 4 represents the most severe neurological deficit. Data were shown as mean ± SEM. Abbreviations: Ab, antibody; CT, Control; HHcy, Hyperhomocysteinemia;

IS, Ischemic hemisphere; NIS, Non-ischemic hemisphere; tMCAO, Transient middle cerebral artery occlusion; TTC, 2, 3, 5-Triphenyltetrazolium chloride.

CHAPTER 4

DISCUSSION

Significance and working model

The association of HHcy with CVD was recognized decades ago. However, whether Hcy is a biomarker or the cause of CVD continues to be debated. With more and more Hcy-lowering clinical trials being conducted, the generated evidences currently strongly support the hypothesis that Hcy is an independent and reversible risk factor for CVD, at least for stroke, whereas the underlying mechanism underlying Hcy-induced risk of stroke remains unclear. Accumulated evidences from experimental studies suggested EC dysfunction, oxidative stress, inflammation, excitotoxicity and DNA hypomethylation as the major mechanisms. Unfortunately, most of the studies were conducted on the peripheral vasculature. Limited studies were performed on the cerebral vasculature, which is equipped with distinct properties and has a different response to stimuli. Therefore, identified mechanisms may not be applicable in explaining the effect of Hcy on the risk of stroke. Our study focusses on the BMEC and for the first time uses primary HBMEC, thereby providing a more direct and clinically relevant model by which to elucidate the effect of Hcy on stroke pathogenesis. Moreover, our study will investigate the effect of HHcy on stroke prognosis by using a sophisticated tMCAO model and the novel HHcy mouse model Tg hCBS *Cbs*$^{-/-}$ mice. The findings will help us to better understanding the stroke pathology and lead to the discovery of novel therapy for stroke. Finally, it may also provide a clue

through which to find an answer to why stroke is more sensitive to Hcy-lowering CVD than other CVD, as indicated in findings of Hcy-lowering trials.

Our study has made the following findings: 1) HHcy exacerbated stroke-induced brain injury, including increased infarct volume, more severe neurological deficit and higher mortality; 2) HHcy aggravated stroke-induced neuroinflammation by promoting the infiltration of NØ and Ly6C^{hi} MC; 4) HHcy did not alternate blood immune cell count and composition after stroke; 5) ICAM1 was potential molecule mediating Hcy-exacerbated brain injury and infiltration of NØ and Ly6C^{hi} MC.

HHcy worsened stroke outcome

Despite the fact that increasingly more clinical studies have recently suggested that HHcy predicts poor stroke prognosis, including increased mortality, worse neurological deterioration and delayed recovery, controversial results exist and evidence from experimental study is rare. In 2005, it was reported that FA diet deficiency-induced HHcy (with an ~6 fold increase of plasma Hcy level), increased with an ~2 fold change of infarction volume and neurological deficit in a 30min tMCAO model performed on 129/Sv mice (Endres et al., 2005). Two subsequent studies using the FA diet deficiency-induced HHcy rodent model also demonstrated the beneficial effect of FA on stroke outcome, including promoting transplanted neural-progenitor proliferation, learning and memory function after tMCAO (Huang, Liu, Wang, & Ren, 2007; H. Liu et al., 2013). However, the FA diet deficiency-induced HHcy model cannot differentiate between the lack of folate

and increased homocysteine levels as potential causes of worse stroke severity. Our study adopts the novel genetic HHcy model Tg-hCBS *Cbs*$^{-/-}$ mice to test whether HHcy is the causative mediator of increased stroke vulnerability.

Pure CBS deficiency causes homocystinuria in humans, but results in a high rate of neonatal lethality in mice. Therefore, Dr. Kurger generated the Tg-hCBS *Cbs*$^{-/-}$ mice, in which a Zn^{2+} inducible human CBS transgene was introduced to circumvent the neonatal lethality of the *Cbs* gene deficiency (Tg-hCBS *Cbs*$^{-/-}$ mice). Considering that stroke may influence Hcy metabolism, tail blood was withdrawn one week before surgery to confirm the development of HHcy in Tg-hCBS *Cbs*$^{-/-}$ mice. In our study, the level of plasma of CT mice (Tg-hCBS *Cbs*$^{+/+}$ & Tg-hCBS *Cbs*$^{+/-}$) was ~5 μmol/L and increased to ~150μmol/L at 14 weeks prior to surgery. Therefore, our results represent the effect of 'severe HHcy' on stroke prognosis.

Our study uses the most frequently used 'tMCAO' as the ischemic stroke model. The basis of the procedure is to block the blood flow to the MCA with an intraluminal suture inserted through the internal carotid artery of the neck. Retracting the suture allows the cerebral reperfusion. The model targets the MCA, which is the most commonly affected in stroke patients. Infarct severity in this model can be controlled according the time of occlusion. Generally, 15min of MCA can cause a detectable lesion and >=30min leads to a substantial and relatively stable infarct lesion (Pedrono et al., 2010). We adopt an occlusion time of 60min, which will allow a more reproducible infarct in both the striatum and cortical

regions. Infarct lesion induced in the tMCAO model will also develop a penumbra, as occurs in human stroke. In order to conquer the insufficient occlusion of MCA and to prevent the high rate (18%) of subarachnoid hemorrhage (SAH) that is often observed in this model, and using the home-made poly lysine-coated suture, we used the silicon-coated filament (cat:) made by the company Doccol, which has been shown to drastically decrease the within-group variation of stroke models, as well as the rate of SAH. Another major pitfall of this model is the obstruction of the hypothalamic artery (HA), which is associated with pathologic hyperthermia, which confounds the results of the investigation. Therefore, we monitored and maintained the mice body temperature at ~37°C during and after surgery. Mice with abnormal body temperatures will be excluded from study. During the surgical procedure, we carefully avoid the stimulation of valgus nerve and reduce the invention of vessel to a minimum. The success of the procedure is determined by the positive infarct lesion, which is examined with TTC staining, neurological deficit and reduced cerebral blood flow (CBF), monitored by a Doppler flow meter (>80% of the baseline level). Unfortunately, we were unable to monitor the CBF for all performed mice. However, before the study, we used at least 20 mice for training purposes and the success rate of surgery that was determined by infarct lesion is >99%.

When animals underwent MCA occlusion/reperfusion, Tg-hCBS *Cbs*$^{-/-}$ had larger brain-infarct volumes than CT mice. Moreover, this was accompanied by worse neurological scores and a trend of increased mortality, thereby suggesting that the increases in brain

damage corresponded to functional outcome. In addition to a not significantly reduced bodyweight, Tg-hCBS *Cbs*$^{-/-}$ mice did not differ from CT mice in their systemic physiological parameters, such as glucose level, cerebral vasculature, extent of blood-flow reduction and re-flow during tMCAO, thereby indicating that the increased fragility of HHcy mice to I/R is unlikely explained by effects of *Cbs* deficiency along these parameters. Our findings suggest that HHcy exacerbated stroke-induced brain injury, which is consistent with Endres' findings from the FA diet deficiency-induced HHcy mice model. However, we did not observe the dramatic increase of infarct lesion and neurological deficit as Endres did (>2 fold change), even though our Tg-hCBS *Cbs*$^{-/-}$ mice have much higher plasma levels than FA deficiency-induced HHcy mice. Several factors may account for this phenomenon. Firstly, our tMCAO model adopts a longer occlusion time (60min) that already resulted in infarct of a substantial proportion of the hemisphere and the observation of moderate-severe neurological deficit in CT mice. Secondly, we measured the infarct lesion at 24h after tMCAO, instead of 72h, as in Endres' study. During the period between 24h and 72h, the repairing process takes place and the infarct lesion develops. HHcy may have major effects on the processes that occur during this period. Finally, FA deficiency-exacerbated, stroke-induced brain injury may partly independent of elevated Hcy level (Endres et al., 2005). We also use mice with C57Bl/6 genetic background instead of Sv/129. However, a published paper showed that the C57Bl/6 and Sv/129 genetic background was not the major confounding factor of infarct size and cerebral perfusion in the tMCAO model(Pham et al., 2010).

There are several limitations in this aim. Firstly, our Tg-hCBS *Cbs*$^{-/-}$ mice develop severe HHcy that rarely occurs in most stroke patients. However, compared to humans, who have far longer life spans and longer periods of exposure to HHcy, mice only suffered 10 weeks of HHcy prior to stroke. In epidemiologic study, the HHcy-induced risk of stroke is concentration dependent. In Hcy-lowering clinical trials, patients with greater basal Hcy levels have higher response to therapy. In this case, a higher Hcy level may facilitate discovering certain critical molecular mechanisms that are shared between mild and severe HHcy. Meanwhile, our future study will use mild to moderate HHcy mice model, include FA-deficient diet and HM diet-induced HHcy mode to support our findings.

Secondly, the effect of Tg-hCBS *Cbs*$^{-/-}$ on stroke outcome may be due to the defect of other CBS functions that are independent of HHcy. As shown in the Hcy metabolism cycle, CBS can convert cysteine to H_2S. In the brain, the detected physiological level of H_2S is about 50-160μM /L. Some studies also suggest that, unlike peripheral tissue, using CSE severed as the major enzyme generating H_2S brain mainly relies on CBS to modulate levels of cysteine-derived H_2S. In the cardiovascular system, H_2S has been shown to mediate vasodilation. The role of H_2S in CNS has also been widely studied in recent years. Several studies have investigated the effect of H_2S on stroke prognosis in a rodent experimental stroke model. However, the results were greatly discrepant. Research by Qu demonstrated that H_2S was the mediator of stroke-induced brain injury (Qu, Chen, Halliwell, Moore, & Wong, 2006). They found that tMCAO could cause an increased level of H_2S in the

lesioned cortex of rats. The inhibition of H_2S synthesis by intraperitoneal administration of 2 CBS inhibitors (AOAA and HA) or 2 CSE inhibitors (-CNA and PAG) significantly reduced tMCAO-induced infarct lesion in a dose-dependent manner, whereas the administration of sodium hydrosulfide (NaHS), a H_2S donor, increased infarct volume. A recently published research supports this finding by using a novel CBS inhibitor, called 6s, that mimics the cystathionine structure and specifically blocks H_2S generation from CBS. They found that the intracerebroventricular administration of this novel inhibitor dramatically reduced infarct volume in the rat tMCAO (30&60min) model(McCune et al., 2016). Additionally, SH-SY5Y (a neuroblastoma cell line) overexpressing CBS reduced viability by ~50% when subjected to oxygen glucose deprivation (OGD) for 24h, but CBS inhibitor 6s blocks this effect(Chan et al., 2015). However, opposite results have been generated in several other studies. For example, findings from Wei showed that rats underwent tMCAO (2h) and subsequently received 40 ppm or 80 ppm H2S inhalation for 3h after reperfusion reduced neurological deficits, infarct size and brain edema (Wei et al., 2015). Jiang found that slow-releasing H_2S organic donor 2-dithiole-3-thione (ADT), as well as a low dose of inorganic donor NaHS, not only reduce infarct volume and neurological deficit, but also BBB integrity (Jiang et al., 2015). Wang also found that ADT and NaHS attenuated tPA-induced cerebral hemorrhage following MCAO (Y. Wang et al., 2014). The reason for the great discrepancy among these studies is unclear, but they may attribute to the use of different types or doses of H_2S donor that lead to different H_2S concentrations. It has been firmly demonstrated that H_2S is a dual sword. Low doses of

H_2S have an anti-inflammatory effect, while high doses of H_2S are pro-inflammatory and have excitotoxicity. Another explanation is that the effect of H_2S may be cell-type dependent. The negative aspect of H_2S on stroke outcome is observed by applying a novel CBS inhibitor intracerebroventricularly. Reduced neuron apoptosis accounts for the positive aspect of H_2S inhibition. On the other hand, the observed benefits of H_2S on stroke in other studies appear to mainly attribute its protective effect on BBB. More importantly, the above findings from CBS inhibition cannot be considered to be purely the effect of H_2S. Evidently, the inhibition of CBS may also affect Hcy metabolism, thereby resulting in the alteration of Hcy level and cysteine, as well as the antioxidant glutathione. Similarly, our results from Tg-hCBS *Cbs*$^{-/-}$ mice cannot fully be explained by the elevated Hcy level. In the future, another mice mode of HHcy, namely high methionine diet-induced HHcy, will also be used in our study. Hcy-lowering experiment, made by applying zinc water to induce human CBS expression or by feeding mice with folic acid and B vitamins, will be conducted in order to confirm the causal role of HHcy on stroke outcome.

Thirdly, our stroke model, tMCAO, induced a reperfusion which is not involved in some ischemic-stroke patients. Discovered mechanisms and therapy that is derived based on the tMCAO model may not be suitable for all types of ischemic stroke. For example, ICAM1-reduced brain injury is strictly restricted to the tMCAO model(Kanemoto, Nakase, Akita, & Sakaki, 2002). This is one explanation for the failure of clinical trials using ICAM1-blocking antibodies.

Experimental studies have demonstrated a distinct pathology process in ischemic stroke with and without reperfusion, by comparing the tMCAO with the pMCAO model. In the tMCAO model, primary core damage may recover and a secondary delayed injury evolves after a free interval of up to 12h (Hossmann, 2012). This is a long therapeutic window that is not observed in human stroke. In contrast, the permanent MCAO is characterized by primary core damage that expands in peripheral brain regions and achieves its maximum at approximately 3h after MCAO. Thus, due to the two different kinds of pathophysiology, unequal results may be expected from the permanent and transient MCAO model, which has been suggested to contribute to the failure of neuroprotective agents in clinical trials.

Finally, we observed the stroke severity within a relatively short window. Infarct lesion can continue to expand after 24h of tMCAO. Moreover, repairing processes, such as resolution of inflammation, angiogenesis, neurogenesis and neural plasticity take place especially after three days. These events contribute to infarct development and particularly neurological-function recovery. Strong evidence has demonstrated that HHcy inhibits angiogenesis (Q. Zhang et al., 2012), neurogenesis (Rabaneda et al., 2016) and neural plasticity (Kidd, 2009). Therefore, it is very likely that HHcy also impaired these events, thereby preventing stroke recovery. The strongest evidence supporting this possibility is that a post-hoc analysis of HOPE2 study, one of the major Hcy-lowering clinical trials on stroke risk and prognosis, found Hcy-lowering to confer a tendency towards faster recovery from stroke(Saposnik, Ray, Sheridan, McQueen, & Lonn, 2009). In the future, we will

contribute to investigate the effect of Hcy on stroke-induced infarct lesion, at post-MCAO 3 days, 7 days and 21 days. More sophisticated behavior tests such as Y maze and water mazing will be used in evaluating learning memory, and Rotard rod test for motor function will be conducted to evaluate the effect of Hcy on neurological-function recovery.

Exacerbated post-stroke brain inflammation played a role in HHcy-accelerated, stroke-induced brain injury

Inflammation contributes to the secondary brain injury after stroke. Previous studies demonstrated that HHcy-enhanced inflammation contributes to atherosclerosis(Hofmann et al., 2001), angiotensin II-induced abdominal aortic aneurysm(Z. Liu et al., 2012), Colitis(S. Zhu et al., 2015) and insulin resistance(Pang et al., 2016). Therefore, we investigated whether inflammation plays a role in HHcy-exacerbated brain injury after tMCAO. We tested the effect of HHcy on stroke-triggered brain inflammation by characterizing the immune cell population and by measuring the cytokines production. FACS analysis of isolated brain immune cells from the ischemic hemisphere, non-ischemic hemisphere and the brain of sham-operated mice revealed that, after 24h of tMCAO, HHcy significantly increased the number of infiltrated NØ and inflammation MC in the IS hemisphere, but not in the NIS hemisphere of Tg-hCBS *Cbs*$^{-/-}$ mice. We further analyzed the MC subset according to the Ly6C marker and found that HHcy increased the inflammatory MC (Ly6C^{hi} & Ly6C^{mid}) population without affecting the number of ly6C^{low} MC. We also observed a trend towards, but not significant increase of infiltrated Lym in

Tg-hCBS *Cbs*$^{-/-}$ mice, to a lesser extent than NØ and inflammatory cells. The reason for why HHcy selectively promotes NØ and inflammatory MC over Lym is unclear. One possible explanation is that during 1-24h after tMCAO, the major chemokines generated in the brain were more NØ and inflammatory MC-specific in Tg-hCBS *Cbs*$^{-/-}$ mice. In order to test the hypothesis, we conducted a mouse cytokine/chemokine array containing 40 different cytokines by using protein extracted from the brain of CT and Tg-hCBS *Cbs*$^{-/-}$ mice at 24h after tMCAO or sham operation. We found that, compared to sham mice, tMCAO significantly increased the production of pro-inflammatory cytokines, including M-CSF, CCL2, ICAM1, CXCL1, CCL12 and TNFα, and anti-inflammatory cytokines, including TIMP1 and IL-1RA. ICAM1 is involved in recruiting all types of leukocytes. Interestingly, CXCL1, especially attracting NØ by interacting with CXCR2, and CCL2 especially attracting inflammatory MC by interacting with CCR2 were abundantly expressed and upregulated. These data indicate that NØ and pro-inflammatory MC are the predominant circulation-derived immune cells at 24h after tMCAO, as demonstrated in our FACS analysis of brain immune cells in CT mice, as well as by previously published studies. M-CSF is the major stimulator for MC/macrophage/microglia activation, proliferation and differentiation. Its upregulation explained the significant increase in the number of MG in the ischemic hemisphere after tMCAO. TIMP1 and IL-1RA are anti-inflammatory cytokines, the upregulation of which indicated a compensatory response for the brain to limit the over-reacting inflammation. More severe brain injury is associated with a higher expression of TIMP1 and IL-RA. We also observed the regulation of TNFα,

as frequently demonstrated in other stroke studies. However, its protein level is very low and we did not detect the upregulation of IL1β or IL6 as did other studies. This may be due to the relatively low sensitivity of array compared to standard western blot. In order to elucidate the specific effect of HHcy on brain inflammation, we compared the brain cytokine production in Tg-hCBS *Cbs*$^{-/-}$ mice to CT mice after tMCAO as well as after sham surgery. We found that the brain has few detected inflammatory cytokines in sham/CT and sham/Tg-hCBS *Cbs*$^{-/-}$ mice, thereby supporting the notion that, under normal conditions, the brain is resistant to inflammation. Under the conditions of tMCAO-induced stroke, Tg-hCBS *Cbs*$^{-/-}$ mice have higher levels of TIMP1, IL-1RA, ICAM1, CCL2, CCL3 and CXCL1, and to a less extent CXCL12, compared to CT mice. Increased levels of TIMP1 and IL1RA indirectly reflect a more severe brain injury in Tg-hCBS *Cbs*$^{-/-}$ mice. The higher ICAM1 expression explained that total leukocyte infiltration increased in Tg-hCBS *Cbs*$^{-/-}$ mice. The most dramatic upregulation of CCL2, CCL3 and CXCL1 explained why HHcy preferentially promoted NØ and inflammatory MC infiltration in Tg-hCBS *Cbs*$^{-/-}$ mice after tMCAO. It is necessary to mentioned that this study cannot rule out the possibility that the increased percentage of inflammatory MC in the ischemic brain of Tg-hCBS *Cbs*$^{-/-}$ mice is due to the effect of HHcy on inflammatory MC differentiation. Our lab previously clearly demonstrated severe HHcy-promoted inflammatory MC differentiation and M1 polarization in peripheral tissue. Therefore, the effect of HHcy on inflammatory MC differentiation after its infiltration into the brain, as well as its polarization will be examined in future study. We did not observe a further increase of MCSF in Tg-hCBS *Cbs*$^{-/-}$ mice

after tMCAO. This is also in line with our data of brain immune cell characterization, showing no further increased number of MG in the ischemic hemisphere of Tg-hCBS *Cbs*$^{-/-}$ mice.

Our immune cell analysis and cytokine array strongly support that HHcy is associated with exacerbated brain inflammatory response 24h after tMCAO. We then addressed the question of whether aggravated brain inflammation occurs through HHcy affecting circulation-inflammatory response. Indeed, stroke also triggers an acute immune response in the blood, which also contributes to secondary brain injury. Exacerbated systemic inflammatory response by applying systemic LPS or IL1 cytokine increases infarct size, neurological deficit and mortality after stroke. Therefore, we characterize the blood immune cells' population by using FACS analysis. We found tMCAO to significantly reduce the number of all leukocyte populations at 24h after tMCAO. This phenomenon was termed 'stroke-induced immune suppression' and has been observed in severe tMCAO mice as well as in severe stroke patients. The immune suppression causes infection in a later stage but is regarded to be a compensatory response by which to reduce the inflammatory injury in the acute phase of stroke. Compared to CT/tMCAO mice, Tg-hCBS *Cbs*$^{-/-}$ mice showed an increasing trend, but not a significant increase of all leukocyte populations in blood. We also conducted a correlation analysis between the number of blood leukocyte populations and the number of brain infiltration leukocyte populations, and did not observe a significant and positive correlation, thereby indicating that HHcy-

exacerbated brain inflammation after stroke is more likely to occur due to its direct impact on the brain. After tMCAO surgery, we found that there was a significantly higher percentage of inflammatory MC, compared to sham surgery, thereby indicating that tMCAO induces inflammatory MC differentiation. However, HHcy did not further promote inflammatory MC differentiation in Tg-hCBS *Cbs*$^{-/-}$ mice. It is possible that there is no cumulative effect on inflammatory MC differentiation between HHcy and tMCAO. Another explanation is that more inflammatory MC from the peripheral reservoir infiltrated into the ischemic hemisphere after tMCAO in Tg-hCBS *Cbs*$^{-/-}$ mice. The major limitation in this study is the lack of measurement of plasma cytokines. Increased inflammatory cytokines such as IL6 and CCL2 have been reported in diet-induced and genetically-induced HHcy mice. Even if HHcy indeed does not alter the immune-cell profile, after stroke it may exacerbate systemic inflammation by the increased release of inflammatory cytokines from blood cells.

ICAM1 is one of the major molecules mediating HHcy-exuberated inflammation

Inflammation initiation and progression involve a complex set of interactions between brain endothelial cells and leukocytes, including rolling adhesion, tight adhesion and transmigration. ICAM1 is the major mediator in all inflammatory disease, including stroke. In our brain cytokine array, ICAM1 is also one of the major cytokines that are upregulated in the IS hemispheres of Tg-hCBS *Cbs*$^{-/-}$ mice. Despite the fact that it was not the molecule with the highest fold change, it was consistently found to be elevated in Hcy-treated

peripheral EC and in our lab it was demonstrated to be the major molecule-mediating HHcy-accelerated thrombosis, which may explain the increased risk of stroke in HHcy patients. Experimental studies had suggest that the extent of the upregulation level of ICAM1 mediated by inflammatory cytokines was different between brain EC and peripheral EC(Molema, 2010). These unique characteristics may contribute to the different response to HHcy or HHcy-lowering therapy between stroke and other peripheral CVD. Indeed, our lab has demonstrated a lower surfaces ICAM1 expression in HBMEC, compared to HAEC and ICAM1 upregulation occurs to a lesser extent in HBMEC than in HAEC when exposed to the same dose of DL-Hcy treatment, but has a higher sensitivity to FA treatment(unpublished data). After selecting our potential molecule, we confirmed its upregulation in the ischemic hemisphere of Tg-hCBS *Cbs*$^{-/-}$ mice. Because ICAM1 is EC specific and found to be mainly located in the cerebral vessel of the ischemic hemisphere by immunochemistry, we isolated the microvessel from both the NIS and the IS hemisphere of CT and Tg-hCBS *Cbs*$^{-/-}$ mice, digesting it with collagenases, and stained with CD31 and CD45 FACS antibody to define EC ($CD31^{+}CD45^{+}$), and ICAM1 FACS antibody to examine its expression level. As we expected, tMCAO significantly upregulated ICAM1 in BMEC of the IS hemisphere and HHcy promoted a further upregulation in Tg-hCBS *Cbs*$^{-/-}$ mice. In order to facilitate testing the molecular mechanism and be more clinically relevant, we cultured the primary HBMEC, treating it with DL-Hcy and measuring the three major adhesion molecules involving leukocyte adhesion and transendothelial migration, including SELE, SELP and ICAM1. We found that Hcy

treatment increased all these three adhesion molecules at 1h under both normal and OGD conditions. The upregulation of ICAM1 induced by Hcy treatment continued with time and reached its maximum at 24h. The upregulation of SELE and SELP induced by Hcy treatment reached its maximum extent at 1h and decreased after that. In order to confirm the role of Hcy-unregulated ICAM1 in leukocyte adhesion and trans-endothelial migration, we conducted the leukocyte adhesion assay and the trans-endothelial migration assay. We found that THP-1 and the primary isolated human blood leukocyte adherent to monolayer of HBMEC were enhanced after Hcy-treating HBMEC for 24h. Interestingly, Hcy-treating THP-1 cells did not enhance their adhesion to non-treated HBMEC, thereby indicating that EC is the major cellular target mediating Hcy/HHcy-enhanced leukocyte adhesion/migration.

Potential cytokines mediating HHcy-exacerbated brain injury in stroke

Induced leukocyte attracting chemokines/cytokines by Hcy may also play a role in HHcy-enhanced leukocyte recruitment. The data of the cytokine array of mouse-brain tissue had demonstrated a dramatic increase of leukocyte chemiotactic cytokines in Tg-hCBS Cbs-/- mice, including CCL2, CCL3, CXCL1 and CXCL12. We further investigated whether BMEC will also be the contributor of these chemokines induced in Tg-hCBS *Cbs*$^{-/-}$ mice. We conducted the cytokine array using the primary HBMEC treated with/without DL-Hcy (50uM, 24h) treatment. In the array, we found that ICAM1 and CCL2 were significantly increased in Hcy-treated HBMEC supernatant, thereby suggesting that BMEC was one of

the major cellular sources for increased ICAM1 and CCL2 observed in the brain of Tg-hCBS *Cbs*$^{-/-}$ mice after 24h post-MCAO. On the contrary, there is no change of CCL3 and CXCL12, and a significant decrease of CXCL1, thereby suggesting that the elevation of these three chemokines in the ischemic hemisphere of Tg-hCBS *Cbs*$^{-/-}$ mice are from other cells, rather than from BMEC. In addition to ICAM1 and CCL2, we also identified several cytokines that can be altered by Hcy. We classified these altered cytokines by their biological function and found that most of the upregulated cytokines are proinflammatory, such as IL22, IL6, IL8, LCN2, IFNG, CSF2, OPN, MIC1, MCP1 and ICAM, and that most of the downregulated ones are critical for angiogenesis, such as CXCL1, ANG, ACAN and BNDF. These data are in line with previous findings indicating that Hcy has a pro-inflammatory effect on EC and inhibiting effect on angiogenesis. We further narrow down these Hcy-altered cytokines by their fold change (>1.5 fold), as well as by their role in leukocyte recruitment and stroke. In addition to ICAM1, another three cytokines, including LCN2, CD147, IL-8 and IL-22 were selected and considered to be critical EC-derived cytokines mediating HHcy-exacerbated, stroke-induced brain injury. IL22 has the highest fold change (22 fold) , and has been demonstrated to be a mediator of BBB disruption. However, its exact role in stroke remains undefined and there is lack of experimental study in animal stroke models. LCN2 and IL8 are promising targets as they have been demonstrated to be upregulated in the ischemic brain tissue, as well as promote brain inflammation and neuron cell death after stroke in the mice tMCAO model (G. Wang et al., 2015). LCN2 was mainly located in Neu. Its role in EC and Hcy-medicated CVD is

unknown. In contrast, IL8 is relatively EC specific and has been reported to be upregulated by Hcy in cultured HAEC(Poddar et al., 2001). In the human renal proximal tubule, IL8 was shown to amplify CD40/CD154-mediated ICAM1 production(Li & Nord, 2009). In the future, it would be interesting to examine whether IL8 serves as an upstream mediator of Hcy-induced ICAM1 upregulation in BMEC and subsequent exacerbated brain inflammation and injury after stroke. Another promising molecular target mediating Hcy-exacerbated, stroke-induced brain injury is CD147: a transmembrane glycoprotein that is expressed on all leukocytes, platelets and ECs. Its upregulation has been observed in many inflammatory diseases, such as lung inflammation, rheumatoid arthritis, multiple sclerosis, myocardial infarction and ischemic stroke (X. Zhu, Song, Zhang, Nanda, & Li, 2014). It is a potent inducer of extracellular matrix metalloproteinase and currently considered to be a novel modulator of inflammatory response. Interestingly, its expression can be modulated by DNA methylation and the hypomethylation of its promoter increases its expression. As discussed below, Hcy is a strong DNA hypomethylation inducer and it-induced promoter hypomethylation is responsible for the upregulation of ICAM1. In our preliminary data, we have confirmed that it will be significantly upregulated in the HBMEC surface by DL-Hcy treatment. In addition, from our lab's unpublished DNA deep-sequencing analysis of Hcy-treated HAECs, the demethylation effect of Hcy in CD147 promoter was observed. In future studies, we will test whether HHcy increases CD147 expression in isolated BMEC from the ischemic hemisphere of Tg-hCBS *Cbs*$^{-/-}$ mice at 24h post-tMCAO. If yes, it is possible that CD147 may serve as a novel mediator of Hcy-exacerbated inflammation and

brain injury after tMCAO. We will also test the relationship between ICAM1, CD147, LCN2 and IL8, and hope to identify the most upstream molecule.

ICAM1 blocking partially reversed HHcy-aggravated stroke severity

After we confirmed the causative role of ICAM1 in Hcy-promoted leukocyte adhesion in vitro, we tested the hypothesis that HHcy-induced ICAM1 upregulation promotes leukocyte recruitment in the tMCAO mice model. In order to test the hypothesis, we injected the CT and Tg-hCBS *Cbs*$^{-/-}$ mice with IgG control or mice-specific ICAM1-blocking antibody (YN1/1.7.4). This clone YN1/1.7.4 antibody has been shown to effectively inhibit endotoxin-induced leukocyte recruitment in the lungs(Kumasaka et al., 1996). The antibody was injected directly after induced reperfusion in a dose of 2mg/kg. In line with previous studies, ICAM1-blocking significantly reduced stroke-induced brain injury in both CT and Tg-hCBS *Cbs*$^{-/-}$ mice, as demonstrated by the lower infarct volume and neurological deficit than mice injected with IgG control. However, we continued to observe a larger infarct volume in Tg-hCBS *Cbs*$^{-/-}$ mice than in CT mice after treatment with ICAM1- blocking antibody, thereby suggesting that other molecule mechanisms are involved in HHcy-accelerated and stroke-induced brain injury. In the future, we will increase the number of mice in the rescue experiment by using the ICAM1-blocking antibody. In addition, we have already generated the Tg-hCBS *Cbs*$^{-/-}$ ICAM1$^{-/-}$ double-knockout mice by crossing Tg-hCBS *Cbs*$^{-/-}$ mice with ICAM1$^{-/-}$ mice. Similar experiments will be conducted with these mice.

Other potential cellular and molecular mechanisms involved in HHcy-exacerbated, stroke-induced brain injury

The above data demonstrated that ICAM1-mediated NØ and inflammatory MC infiltration contribute to stroke-induced and HHcy-exacerbated brain injury. However, Tg-hCBS *Cbs*$^{-/-}$ mice receiving ICAM1-blocking antibody continue to show a trend of greater brain injury and neurological deficit than CT mice, thereby indicating that other cellular and molecular mechanisms may also play a role in HHcy-exacerbated brain injury. On the cellular level, in addition to BMEC, cells such as neurons and other infiltrated immune cell subsets may also play a role in the effect of HHcy on stroke severity.

Neuron apoptosis is the direct and most important cellular index of brain injury. It has been demonstrated that Hcy promotes neuron apoptosis by activating NMDAR in the presence of high levels of glycine, which have been observed in cases of head trauma or stroke. However, most studies are conducted in vitro where neurons are exposed to a dose of exogenous Hcy by the circulating Hcy level. It is unclear what the Hcy level in the brain under HHcy conditions is. Our lab's unpublished data showed that the Hcy level is around in CT mice and is around in Tg-hCBS *Cbs*$^{-/-}$ mice. These data suggest that, even in the severe HHcy, the brain Hcy level is only mildly increased. One reason for the far lower Hcy level in the brain compared to other tissue may be that the integrity of BBB prevents high levels of plasma Hcy from entering the brain. However, in the condition of stroke, BBB will be disrupted and thereby facilitate the influx of plasma Hcy into the brain. This

hypothesis was supported by our preliminary data, showing that, in CT mice, stroke can significantly increase Hcy in ischemic brain tissue at 6h after tMCAO, but not in the non-ischemic hemisphere or the brain of sham mice. Unfortunately, whether the Hcy is further increased in Tg-hCBS *Cbs*$^{-/-}$ mice is unknown. If it is, we will examine the effect of a relevant dose of Hcy/HHcy on neuron apoptosis in the OGD condition, in an in-vitro model of ischemic/reperfusion injury and in the ischemic brain of CT and Tg-hCBS *Cbs*$^{-/-}$ mice. NMDAR inhibitor will be used to rescue Hcy/HHcy-exacerbated neuron apoptosis, as well as the infarct volume and neurological deficit.

Regarding other immune cell type subsets and their functional study, our study only characterized the number and percentage of leukocyte population and the effect of HHcy on cytokines production in each population is not yet studied. For example, we did not observe more infiltrated lym cells and MG in Tg-hCBS *Cbs*$^{-/-}$ mice than in CT mice at 24h post-tMCAO. However, we cannot rule out the possibility that HHcy may enhance their neurotoxic cytokines release. Moreover, as increasingly more subsets with different functions were identified in immune cells, it will be interesting to define a more specific immune cell population that is responsible for the effect of HHcy on stroke.

DNA hypomethylation is a proposed major molecular mechanism in HHcy-mediated CVD pathogenesis. Our lab's former Ph.D. student, Shu, also showed that HHcy-induced DNA hypomethylation in ICAM1 promoter contributes to the Hcy-induced upregulation of ICAM1 in HAECs and exacerbated thrombosis. Interestingly, we also found that ICAM1

was also upregulated by Hcy in HBMEC cells. We proposed that DNA hypomethylation was a shared molecular mechanism for the upregulation of ICAM1 in both HAECs and BMEC. In addition to BMEC, we also detected an increase of SAH: a potent inhibitor of DNA methylation in the whole brain tissue of Tg-hCBS *Cbs*$^{-/-}$ mice. Interestingly, SAH was also found to be increased in the ischemic hemisphere compared to the non-ischemic hemisphere in CT/MCAO mice. Increased SAH likely induced the brain's global DNA hypomethylation and played a role in ischemic stroke. Indeed, two mice experimental studies suggest that DNA methylation is involved in ischemic stroke. On the contrary, they found that tMCAO induces the neuronal 'hypermethylation', which was harmful in ischemic stroke. However, 'DNA hypermethylation was negative' is not equivalent to 'DNA hypomethylation was good'. In their studies, they also found that neuronal is negative only in the case of mild brain injury. Neurons without any DNMT1 are not actually protective from ischemic stroke. Moreover, these studies were limited to neurons and only one DNMT isoform, namely DNMT1. We currently continue to lack direct evidence showing that HHcy induced brain DNA hypomethylation after tMCAO. However, if it does, DNA hypomethylation in cells other than neurons, especially in BMEC, is a potential molecular mechanism underlying HHcy-exacerbated, stroke-induced brain injury.

Summary

Our study demonstrated that HHcy exacerbated stroke-induced brain injury, as demonstrated by the increased infarct volume and neurological deficit in Tg-hCBS *Cbs*$^{-/-}$ mice: a novel HHcy mice model. We are the first to demonstrate that HHcy aggravated NØ and inflammatory MC in the ischemic hemisphere of Tg-hCBS *Cbs*$^{-/-}$ mice and that the upregulation of ICAM1 is one of the cellular mechanisms that are involved in HHcy-exacerbated stroke-induced brain injury. This exacerbated neuroinflammation after stroke is at least partly due to HHcy-induced ICAM1 upregulation in BMEC. Inhibiting ICAM1 by injecting a specific ICAM1-blocking antibody reduced both stroke-induced and HHcy-exacerbated brain injury. However, our data did not rule out other cellular mechanisms that may also be critical in HHcy-exacerbated brain injury and the exact molecular mechanisms will be examined in the future.

REFERENCE

Audebert, H. J., Rott, M. M., Eck, T., & Haberl, R. L. (2004). Systemic inflammatory response depends on initial stroke severity but is attenuated by successful thrombolysis. *Stroke, 35*(9), 2128-2133. doi: 10.1161/01.STR.0000137607.61697.77

Baccarelli, A., Wright, R., Bollati, V., Litonjua, A., Zanobetti, A., Tarantini, L., . . . Schwartz, J. (2010). Ischemic heart disease and stroke in relation to blood DNA methylation. [Research Support, N.I.H., Extramural

Research Support, Non-U.S. Gov't

Research Support, U.S. Gov't, Non-P.H.S.]. *Epidemiology, 21*(6), 819-828. doi: 10.1097/EDE.0b013e3181f20457

Barber, P. A., Hoyte, L., Colbourne, F., & Buchan, A. M. (2004). Temperature-regulated model of focal ischemia in the mouse: a study with histopathological and behavioral outcomes. *Stroke, 35*(7), 1720-1725. doi: 10.1161/01.STR.0000129653.22241.d7

Beard, R. S., Jr., Reynolds, J. J., & Bearden, S. E. (2011). Hyperhomocysteinemia increases permeability of the blood-brain barrier by NMDA receptor-dependent regulation of adherens and tight junctions. [Research Support, N.I.H., Extramural

Research Support, Non-U.S. Gov't]. *Blood, 118*(7), 2007-2014. doi: 10.1182/blood-2011-02-338269

Bostom, A. G., Jacques, P. F., Nadeau, M. R., Williams, R. R., Ellison, R. C., & Selhub, J. (1995). Post-methionine load hyperhomocysteinemia in persons with normal fasting total plasma homocysteine: initial results from the NHLBI Family Heart Study. [Multicenter Study

Research Support, U.S. Gov't, Non-P.H.S.

Research Support, U.S. Gov't, P.H.S.]. *Atherosclerosis, 116*(1), 147-151.

Buck, B. H., Liebeskind, D. S., Saver, J. L., Bang, O. Y., Yun, S. W., Starkman, S., . . . Ovbiagele, B. (2008). Early neutrophilia is associated with volume of ischemic tissue in acute stroke. [Research Support, N.I.H., Extramural

Research Support, Non-U.S. Gov't]. *Stroke, 39*(2), 355-360. doi: 10.1161/STROKEAHA.107.490128

Capasso, R., Sambri, I., Cimmino, A., Salemme, S., Lombardi, C., Acanfora, F., . . . Ingrosso, D. (2012). Homocysteinylated albumin promotes increased monocyte-endothelial cell adhesion and up-regulation of MCP1, Hsp60 and ADAM17. [Research Support, Non-U.S. Gov't]. *PLoS One, 7*(2), e31388. doi: 10.1371/journal.pone.0031388

Carluccio, M. A., Ancora, M. A., Massaro, M., Carluccio, M., Scoditti, E., Distante, A., . . . De Caterina, R. (2007). Homocysteine induces VCAM-1 gene expression through NF-kappaB and NAD(P)H oxidase activation: protective role of Mediterranean diet polyphenolic antioxidants. *Am J Physiol Heart Circ Physiol, 293*(4), H2344-2354. doi: 10.1152/ajpheart.00432.2007

Carmichael, S. T. (2005). Rodent models of focal stroke: size, mechanism, and purpose. [Research Support, N.I.H., Extramural

Research Support, Non-U.S. Gov't

Review]. *NeuroRx, 2*(3), 396-409. doi: 10.1602/neurorx.2.3.396

Castro, R., Rivera, I., Struys, E. A., Jansen, E. E., Ravasco, P., Camilo, M. E., . . . Tavares de Almeida, I. (2003). Increased homocysteine and S-adenosylhomocysteine concentrations and DNA hypomethylation in vascular disease. [Research Support, Non-U.S. Gov't]. *Clin Chem, 49*(8), 1292-1296.

Chambers, J. C., Obeid, O. A., & Kooner, J. S. (1999). Physiological increments in plasma homocysteine induce vascular endothelial dysfunction in normal human subjects. [Clinical Trial]. *Arterioscler Thromb Vasc Biol, 19*(12), 2922-2927.

Chan, S. J., Chai, C., Lim, T. W., Yamamoto, M., Lo, E. H., Lai, M. K., & Wong, P. T. (2015). Cystathionine beta-synthase inhibition is a potential therapeutic approach to

treatment of ischemic injury. [Research Support, Non-U.S. Gov't]. *ASN Neuro, 7*(2). doi: 10.1177/1759091415578711

Chen, H., Fitzgerald, R., Brown, A. T., Qureshi, I., Breckenridge, J., Kazi, R., . . . Moursi, M. M. (2005). Identification of a homocysteine receptor in the peripheral endothelium and its role in proliferation. [Comparative Study

Research Support, U.S. Gov't, Non-P.H.S.]. *J Vasc Surg, 41*(5), 853-860. doi: 10.1016/j.jvs.2005.02.021

Cheng, Z., Jiang, X., Kruger, W. D., Pratico, D., Gupta, S., Mallilankaraman, K., . . . Wang, H. (2011). Hyperhomocysteinemia impairs endothelium-derived hyperpolarizing factor-mediated vasorelaxation in transgenic cystathionine beta synthase-deficient mice. [Research Support, N.I.H., Extramural]. *Blood, 118*(7), 1998-2006. doi: 10.1182/blood-2011-01-333310

Cheng, Z., Jiang, X., Pansuria, M., Fang, P., Mai, J., Mallilankaraman, K., . . . Wang, H. (2015). Hyperhomocysteinemia and hyperglycemia induce and potentiate endothelial dysfunction via mu-calpain activation. [Research Support, N.I.H., Extramural

Research Support, Non-U.S. Gov't]. *Diabetes, 64*(3), 947-959. doi: 10.2337/db14-0784

Cheng, Z., Yang, X., & Wang, H. (2009). Hyperhomocysteinemia and Endothelial Dysfunction. *Curr Hypertens Rev, 5*(2), 158-165. doi: 10.2174/157340209788166940

Chu, H. X., Broughton, B. R., Kim, H. A., Lee, S., Drummond, G. R., & Sobey, C. G. (2015). Evidence That Ly6C(hi) Monocytes are Protective in Acute Ischemic Stroke by Promoting M2 Macrophage Polarization. [Research Support, Non-U.S. Gov't]. *Stroke, 46*(7), 1929-1937. doi: 10.1161/STROKEAHA.115.009426

Chu, H. X., Kim, H. A., Lee, S., Moore, J. P., Chan, C. T., Vinh, A., . . . Sobey, C. G. (2014). Immune cell infiltration in malignant middle cerebral artery infarction: comparison with transient cerebral ischemia. [Comparative Study]. *J Cereb Blood Flow Metab, 34*(3), 450-459. doi: 10.1038/jcbfm.2013.217

Clarkson, B. D., Ling, C., Shi, Y., Harris, M. G., Rayasam, A., Sun, D., . . . Fabry, Z. (2014). T cell-derived interleukin (IL)-21 promotes brain injury following stroke in mice. [Research Support, N.I.H., Extramural

Research Support, Non-U.S. Gov't]. *J Exp Med, 211*(4), 595-604. doi: 10.1084/jem.20131377

Dai, J., Wang, X., Feng, J., Kong, W., Xu, Q., & Shen, X. (2008). Regulatory role of thioredoxin in homocysteine-induced monocyte chemoattractant protein-1 secretion in monocytes/macrophages. [Research Support, Non-U.S. Gov't]. *FEBS Lett, 582*(28), 3893-3898. doi: 10.1016/j.febslet.2008.10.030

Dalal, S., Parkin, S. M., Homer-Vanniasinkam, S., & Nicolaou, A. (2003). Effect of homocysteine on cytokine production by human endothelial cells and monocytes. *Ann Clin Biochem, 40*(Pt 5), 534-541. doi: 10.1258/000456303322326452

Dayal, S., Arning, E., Bottiglieri, T., Boger, R. H., Sigmund, C. D., Faraci, F. M., & Lentz, S. R. (2004). Cerebral vascular dysfunction mediated by superoxide in hyperhomocysteinemic mice. [Research Support, Non-U.S. Gov't

Research Support, U.S. Gov't, Non-P.H.S.

Research Support, U.S. Gov't, P.H.S.]. *Stroke, 35*(8), 1957-1962. doi: 10.1161/01.STR.0000131749.81508.18

Dimitrijevic, O. B., Stamatovic, S. M., Keep, R. F., & Andjelkovic, A. V. (2007). Absence of the chemokine receptor CCR2 protects against cerebral ischemia/reperfusion injury in mice. [Research Support, N.I.H., Extramural]. *Stroke, 38*(4), 1345-1353. doi: 10.1161/01.STR.0000259709.16654.8f

Dong, F., Zhang, X., Li, S. Y., Zhang, Z., Ren, Q., Culver, B., & Ren, J. (2005). Possible involvement of NADPH oxidase and JNK in homocysteine-induced oxidative stress and apoptosis in human umbilical vein endothelial cells. [Comparative Study

Research Support, N.I.H., Extramural

Research Support, Non-U.S. Gov't

Research Support, U.S. Gov't, P.H.S.]. *Cardiovasc Toxicol, 5*(1), 9-20.

Durga, J., van Tits, L. J., Schouten, E. G., Kok, F. J., & Verhoef, P. (2005). Effect of lowering of homocysteine levels on inflammatory markers: a randomized controlled trial. [Clinical Trial

Randomized Controlled Trial

Research Support, Non-U.S. Gov't]. *Arch Intern Med, 165*(12), 1388-1394. doi: 10.1001/archinte.165.12.1388

Endres, M., Ahmadi, M., Kruman, I., Biniszkiewicz, D., Meisel, A., & Gertz, K. (2005). Folate deficiency increases postischemic brain injury. [Research Support, Non-U.S. Gov't]. *Stroke, 36*(2), 321-325. doi: 10.1161/01.STR.0000153008.60517.ab

Endres, M., Fan, G., Meisel, A., Dirnagl, U., & Jaenisch, R. (2001). Effects of cerebral ischemia in mice lacking DNA methyltransferase 1 in post-mitotic neurons. [Research Support, Non-U.S. Gov't

Research Support, U.S. Gov't, P.H.S.]. *Neuroreport, 12*(17), 3763-3766.

Endres, M., Meisel, A., Biniszkiewicz, D., Namura, S., Prass, K., Ruscher, K., . . . Dirnagl, U. (2000). DNA methyltransferase contributes to delayed ischemic brain injury. [Research Support, Non-U.S. Gov't

Research Support, U.S. Gov't, P.H.S.]. *J Neurosci, 20*(9), 3175-3181.

Erba, E. M., Fadel, J. G., & Famula, T. R. (1991). The use of integer programming in dairy sire selection. [Comparative Study]. *J Dairy Sci, 74*(10), 3552-3560. doi: 10.3168/jds.S0022-0302(91)78547-0

Fang, P., Zhang, D., Cheng, Z., Yan, C., Jiang, X., Kruger, W. D., . . . Wang, H. (2014). Hyperhomocysteinemia potentiates hyperglycemia-induced inflammatory monocyte differentiation and atherosclerosis. [Research Support, N.I.H., Extramural]. *Diabetes, 63*(12), 4275-4290. doi: 10.2337/db14-0809

Furlan, J. C., Vergouwen, M. D., Fang, J., & Silver, F. L. (2014). White blood cell count is an independent predictor of outcomes after acute ischaemic stroke. [Research Support, Non-U.S. Gov't]. *Eur J Neurol, 21*(2), 215-222. doi: 10.1111/ene.12233

Gronberg, N. V., Johansen, F. F., Kristiansen, U., & Hasseldam, H. (2013). Leukocyte infiltration in experimental stroke. [Research Support, Non-U.S. Gov't

Review]. *J Neuroinflammation, 10*, 115. doi: 10.1186/1742-2094-10-115

Guo, Z., Yu, S., Xiao, L., Chen, X., Ye, R., Zheng, P., . . . Liu, X. (2016). Dynamic change of neutrophil to lymphocyte ratio and hemorrhagic transformation after thrombolysis in stroke. *J Neuroinflammation, 13*(1), 199. doi: 10.1186/s12974-016-0680-x

Hammond, M. D., Taylor, R. A., Mullen, M. T., Ai, Y., Aguila, H. L., Mack, M., . . . Sansing, L. H. (2014). CCR2+ Ly6C(hi) inflammatory monocyte recruitment exacerbates acute disability following intracerebral hemorrhage. [Research Support, N.I.H., Extramural

Research Support, Non-U.S. Gov't]. *J Neurosci, 34*(11), 3901-3909. doi: 10.1523/JNEUROSCI.4070-13.2014

Hofmann, M. A., Lalla, E., Lu, Y., Gleason, M. R., Wolf, B. M., Tanji, N., . . . Schmidt, A. M. (2001). Hyperhomocysteinemia enhances vascular inflammation and accelerates atherosclerosis in a murine model. [Research Support, Non-U.S. Gov't

Research Support, U.S. Gov't, P.H.S.]. *J Clin Invest, 107*(6), 675-683. doi: 10.1172/JCI10588

Horstmann, L., Kuehn, S., Pedreiturria, X., Haak, K., Pfarrer, C., Dick, H. B., . . . Joachim, S. C. (2016). Microglia response in retina and optic nerve in chronic experimental autoimmune encephalomyelitis. *J Neuroimmunol, 298*, 32-41. doi: 10.1016/j.jneuroim.2016.06.008

Hossmann, K. A. (2012). The two pathophysiologies of focal brain ischemia: implications for translational stroke research. *J Cereb Blood Flow Metab, 32*(7), 1310-1316. doi: 10.1038/jcbfm.2011.186

Hu, X., Li, P., Guo, Y., Wang, H., Leak, R. K., Chen, S., . . . Chen, J. (2012). Microglia/macrophage polarization dynamics reveal novel mechanism of injury expansion after focal cerebral ischemia. [Research Support, N.I.H., Extramural

Research Support, Non-U.S. Gov't]. *Stroke, 43*(11), 3063-3070. doi: 10.1161/STROKEAHA.112.659656

Huang, G. W., Liu, H., Wang, Y. M., & Ren, D. L. (2007). [Effects of folic acid, vitamin B(6) and vitamin B(12) on learning and memory function in cerebral ischemia rats]. [Research Support, Non-U.S. Gov't]. *Zhonghua Yu Fang Yi Xue Za Zhi, 41*(3), 212-214.

Hughes, P. M., Allegrini, P. R., Rudin, M., Perry, V. H., Mir, A. K., & Wiessner, C. (2002). Monocyte chemoattractant protein-1 deficiency is protective in a murine stroke model. *J Cereb Blood Flow Metab, 22*(3), 308-317. doi: 10.1097/00004647-200203000-00008

Isotalo, P. A., Wells, G. A., & Donnelly, J. G. (2000). Neonatal and fetal methylenetetrahydrofolate reductase genetic polymorphisms: an examination of C677T and A1298C mutations. [Research Support, Non-U.S. Gov't]. *Am J Hum Genet, 67*(4), 986-990. doi: 10.1086/303082

Jack, C., Ruffini, F., Bar-Or, A., & Antel, J. P. (2005). Microglia and multiple sclerosis. [Research Support, Non-U.S. Gov't

Review]. *J Neurosci Res, 81*(3), 363-373. doi: 10.1002/jnr.20482

Jacobsen, D. W., Catanescu, O., Dibello, P. M., & Barbato, J. C. (2005). Molecular targeting by homocysteine: a mechanism for vascular pathogenesis. [Review]. *Clin Chem Lab Med, 43*(10), 1076-1083. doi: 10.1515/CCLM.2005.188

Jamaluddin, M. D., Chen, I., Yang, F., Jiang, X., Jan, M., Liu, X., . . . Wang, H. (2007). Homocysteine inhibits endothelial cell growth via DNA hypomethylation of the cyclin A gene. [Research Support, N.I.H., Extramural]. *Blood, 110*(10), 3648-3655. doi: 10.1182/blood-2007-06-096701

Jiang, Z., Li, C., Manuel, M. L., Yuan, S., Kevil, C. G., McCarter, K. D., . . . Sun, H. (2015). Role of hydrogen sulfide in early blood-brain barrier disruption following transient focal cerebral ischemia. [Research Support, N.I.H., Extramural

Research Support, Non-U.S. Gov't]. *PLoS One, 10*(2), e0117982. doi: 10.1371/journal.pone.0117982

Jickling, G. C., Liu, D., Ander, B. P., Stamova, B., Zhan, X., & Sharp, F. R. (2015). Targeting neutrophils in ischemic stroke: translational insights from experimental studies. [Research Support, N.I.H., Extramural

Research Support, Non-U.S. Gov't

Review]. *J Cereb Blood Flow Metab, 35*(6), 888-901. doi: 10.1038/jcbfm.2015.45

Justicia, C., Martin, A., Rojas, S., Gironella, M., Cervera, A., Panes, J., . . . Planas, A. M. (2006). Anti-VCAM-1 antibodies did not protect against ischemic damage either in rats or in mice. [Comparative Study

Research Support, Non-U.S. Gov't]. *J Cereb Blood Flow Metab, 26*(3), 421-432. doi: 10.1038/sj.jcbfm.9600198

Kaito, M., Araya, S., Gondo, Y., Fujita, M., Minato, N., Nakanishi, M., & Matsui, M. (2013). Relevance of distinct monocyte subsets to clinical course of ischemic stroke patients. [Comparative Study

Research Support, Non-U.S. Gov't]. *PLoS One, 8*(8), e69409. doi: 10.1371/journal.pone.0069409

Kalani, A., Kamat, P. K., & Tyagi, N. (2015). Diabetic Stroke Severity: Epigenetic Remodeling and Neuronal, Glial, and Vascular Dysfunction. [Research Support, N.I.H., Extramural]. *Diabetes, 64*(12), 4260-4271. doi: 10.2337/db15-0422

Kamat, P. K., Kalani, A., Tyagi, S. C., & Tyagi, N. (2015). Hydrogen Sulfide Epigenetically Attenuates Homocysteine-Induced Mitochondrial Toxicity Mediated Through NMDA Receptor in Mouse Brain Endothelial (bEnd3) Cells. [Research Support, N.I.H., Extramural]. *J Cell Physiol, 230*(2), 378-394. doi: 10.1002/jcp.24722

Kanemoto, Y., Nakase, H., Akita, N., & Sakaki, T. (2002). Effects of anti-intercellular adhesion molecule-1 antibody on reperfusion injury induced by late reperfusion in the rat middle cerebral artery occlusion model. *Neurosurgery, 51*(4), 1034-1041; discussion 1041-1032.

Kennedy, S. M. (1992). Acquired airway hyperresponsiveness from nonimmunogenic irritant exposure. [Review]. *Occup Med, 7*(2), 287-300.

Kerr, S. J. (1972). Competing methyltransferase systems. *J Biol Chem, 247*(13), 4248-4252.

Kidd, P. M. (2009). Integrated brain restoration after ischemic stroke--medical management, risk factors, nutrients, and other interventions for managing inflammation and enhancing brain plasticity. [Review]. *Altern Med Rev, 14*(1), 14-35.

Kim, E., Yang, J., Beltran, C. D., & Cho, S. (2014). Role of spleen-derived monocytes/macrophages in acute ischemic brain injury. [Research Support, N.I.H., Extramural

Research Support, Non-U.S. Gov't]. *J Cereb Blood Flow Metab, 34*(8), 1411-1419. doi: 10.1038/jcbfm.2014.101

Kitagawa, K., Matsumoto, M., Yang, G., Mabuchi, T., Yagita, Y., Hori, M., & Yanagihara, T. (1998). Cerebral ischemia after bilateral carotid artery occlusion and intraluminal suture occlusion in mice: evaluation of the patency of the posterior communicating artery. [Research Support, Non-U.S. Gov't]. *J Cereb Blood Flow Metab, 18*(5), 570-579. doi: 10.1097/00004647-199805000-00012

Kleinschnitz, C., Schwab, N., Kraft, P., Hagedorn, I., Dreykluft, A., Schwarz, T., . . . Stoll, G. (2010). Early detrimental T-cell effects in experimental cerebral ischemia are neither related to adaptive immunity nor thrombus formation. [Research Support, Non-U.S. Gov't]. *Blood, 115*(18), 3835-3842. doi: 10.1182/blood-2009-10-249078

Krizbai, I. A., Deli, M. A., Pestenacz, A., Siklos, L., Szabo, C. A., Andras, I., & Joo, F. (1998). Expression of glutamate receptors on cultured cerebral endothelial cells. [Research

Support, Non-U.S. Gov't]. *J Neurosci Res, 54*(6), 814-819. doi: 10.1002/(SICI)1097-4547(19981215)54:6<814::AID-JNR9>3.0.CO;2-3

Kumasaka, T., Quinlan, W. M., Doyle, N. A., Condon, T. P., Sligh, J., Takei, F., . . . Doerschuk, C. M. (1996). Role of the intercellular adhesion molecule-1(ICAM-1) in endotoxin-induced pneumonia evaluated using ICAM-1 antisense oligonucleotides, anti-ICAM-1 monoclonal antibodies, and ICAM-1 mutant mice. [Research Support, Non-U.S. Gov't]. *J Clin Invest, 97*(10), 2362-2369. doi: 10.1172/JCI118679

Lee, S., Hong, Y., Park, S., Lee, S. R., & Chang, K. T. (2014). Comparison of surgical methods of transient middle cerebral artery occlusion between rats and mice. [Comparative Study

Research Support, Non-U.S. Gov't]. *J Vet Med Sci, 76*(12), 1555-1561. doi: 10.1292/jvms.14-0258

Li, H., & Nord, E. P. (2009). IL-8 amplifies CD40/CD154-mediated ICAM-1 production via the CXCR-1 receptor and p38-MAPK pathway in human renal proximal tubule cells. [Research Support, Non-U.S. Gov't]. *Am J Physiol Renal Physiol, 296*(2), F438-445. doi: 10.1152/ajprenal.90214.2008

Lipton, S. A., Kim, W. K., Choi, Y. B., Kumar, S., D'Emilia, D. M., Rayudu, P. V., . . . Stamler, J. S. (1997). Neurotoxicity associated with dual actions of homocysteine at the N-methyl-D-aspartate receptor. [Research Support, Non-U.S. Gov't

Research Support, U.S. Gov't, P.H.S.]. *Proc Natl Acad Sci U S A, 94*(11), 5923-5928.

Liu, H., Cao, J., Zhang, H., Qin, S., Yu, M., Zhang, X., . . . Huang, G. (2013). Folic acid stimulates proliferation of transplanted neural stem cells after focal cerebral ischemia in rats. [Research Support, Non-U.S. Gov't]. *J Nutr Biochem, 24*(11), 1817-1822. doi: 10.1016/j.jnutbio.2013.04.002

Liu, Z., Luo, H., Zhang, L., Huang, Y., Liu, B., Ma, K., . . . Wang, X. (2012). Hyperhomocysteinemia exaggerates adventitial inflammation and angiotensin II-induced abdominal aortic aneurysm in mice. [Meta-Analysis

Research Support, Non-U.S. Gov't]. *Circ Res, 111*(10), 1261-1273. doi: 10.1161/CIRCRESAHA.112.270520

Lowering blood homocysteine with folic acid based supplements: meta-analysis of randomised trials. Homocysteine Lowering Trialists' Collaboration. (1998). [Meta-Analysis

Research Support, Non-U.S. Gov't]. *BMJ, 316*(7135), 894-898.

McColl, B. W., Rothwell, N. J., & Allan, S. M. (2007). Systemic inflammatory stimulus potentiates the acute phase and CXC chemokine responses to experimental stroke and exacerbates brain damage via interleukin-1- and neutrophil-dependent mechanisms. [Research Support, Non-U.S. Gov't]. *J Neurosci, 27*(16), 4403-4412. doi: 10.1523/JNEUROSCI.5376-06.2007

McCully, K. S. (2009). Chemical pathology of homocysteine. IV. Excitotoxicity, oxidative stress, endothelial dysfunction, and inflammation. [Review]. *Ann Clin Lab Sci, 39*(3), 219-232.

McCune, C. D., Chan, S. J., Beio, M. L., Shen, W., Chung, W. J., Szczesniak, L. M., . . . Berkowitz, D. B. (2016). "Zipped Synthesis" by Cross-Metathesis Provides a Cystathionine beta-Synthase Inhibitor that Attenuates Cellular H2S Levels and Reduces Neuronal Infarction in a Rat Ischemic Stroke Model. *ACS Cent Sci, 2*(4), 242-252. doi: 10.1021/acscentsci.6b00019

McRae, M. P. (2013). Betaine supplementation decreases plasma homocysteine in healthy adult participants: a meta-analysis. *J Chiropr Med, 12*(1), 20-25. doi: 10.1016/j.jcm.2012.11.001

Mhairi Macrae, I. (1992). New models of focal cerebral ischaemia. [Review]. *Br J Clin Pharmacol, 34*(4), 302-308.

Miro-Mur, F., Perez-de-Puig, I., Ferrer-Ferrer, M., Urra, X., Justicia, C., Chamorro, A., & Planas, A. M. (2016). Immature monocytes recruited to the ischemic mouse brain differentiate into macrophages with features of alternative activation. [Research Support, Non-U.S. Gov't]. *Brain Behav Immun, 53*, 18-33. doi: 10.1016/j.bbi.2015.08.010

Molema, G. (2010). Heterogeneity in endothelial responsiveness to cytokines, molecular causes, and pharmacological consequences. [Review]. *Semin Thromb Hemost, 36*(3), 246-264. doi: 10.1055/s-0030-1253448

Mozaffarian, D., Benjamin, E. J., Go, A. S., Arnett, D. K., Blaha, M. J., Cushman, M., . . . Turner, M. B. (2015). Heart disease and stroke statistics--2015 update: a report from the American Heart Association. *Circulation, 131*(4), e29-322. doi: 10.1161/CIR.0000000000000152

Mudd, S. H., Finkelstein, J. D., Refsum, H., Ueland, P. M., Malinow, M. R., Lentz, S. R., . . . Rosenberg, I. H. (2000). Homocysteine and its disulfide derivatives: a suggested consensus terminology. [Review]. *Arterioscler Thromb Vasc Biol, 20*(7), 1704-1706.

Nappo, F., De Rosa, N., Marfella, R., De Lucia, D., Ingrosso, D., Perna, A. F., . . . Giugliano, D. (1999). Impairment of endothelial functions by acute hyperhomocysteinemia and reversal by antioxidant vitamins. [Clinical Trial

Randomized Controlled Trial]. *JAMA, 281*(22), 2113-2118.

Offner, H., Subramanian, S., Parker, S. M., Wang, C., Afentoulis, M. E., Lewis, A., . . . Hurn, P. D. (2006). Splenic atrophy in experimental stroke is accompanied by increased regulatory T cells and circulating macrophages. [Research Support, N.I.H., Extramural

Research Support, U.S. Gov't, Non-P.H.S.]. *J Immunol, 176*(11), 6523-6531.

Ong, P. K. (1976). Fractures of the neck of the femur. *Nurs J Singapore, 16*(1), 16-19.

Pang, Y., Li, Y., Lv, Y., Sun, L., Zhang, S., Wang, Y., . . . Jiang, C. (2016). Intermedin Restores Hyperhomocysteinemia-induced Macrophage Polarization and Improves Insulin Resistance in Mice. [Research Support, Non-U.S. Gov't]. *J Biol Chem, 291*(23), 12336-12345. doi: 10.1074/jbc.M115.702654

Park, S. Y., Marasini, S., Kim, G. H., Ku, T., Choi, C., Park, M. Y., . . . Kim, S. S. (2014). A method for generating a mouse model of stroke: evaluation of parameters for blood flow, behavior, and survival [corrected]. *Exp Neurobiol, 23*(1), 104-114. doi: 10.5607/en.2014.23.1.104

Patel, A. R., Ritzel, R., McCullough, L. D., & Liu, F. (2013). Microglia and ischemic stroke: a double-edged sword. *Int J Physiol Pathophysiol Pharmacol, 5*(2), 73-90.

Pedrono, E., Durukan, A., Strbian, D., Marinkovic, I., Shekhar, S., Pitkonen, M., . . . Tatlisumak, T. (2010). An optimized mouse model for transient ischemic attack. [Research Support, Non-U.S. Gov't]. *J Neuropathol Exp Neurol, 69*(2), 188-195. doi: 10.1097/NEN.0b013e3181cd331c

Pennypacker, K. R., & Offner, H. (2015). The role of the spleen in ischemic stroke. [Research Support, N.I.H., Extramural

Review]. *J Cereb Blood Flow Metab, 35*(2), 186-187. doi: 10.1038/jcbfm.2014.212

Pham, M., Helluy, X., Braeuninger, S., Jakob, P., Stoll, G., Kleinschnitz, C., & Bendszus, M. (2010). Outcome of experimental stroke in C57Bl/6 and Sv/129 mice assessed by multimodal ultra-high field MRI. *Exp Transl Stroke Med, 2*, 6. doi: 10.1186/2040-7378-2-6

Plaza-Zabala, A., Sierra-Torre, V., & Sierra, A. (2017). Autophagy and Microglia: Novel Partners in Neurodegeneration and Aging. [Review]. *Int J Mol Sci, 18*(3). doi: 10.3390/ijms18030598

Poddar, R., Sivasubramanian, N., DiBello, P. M., Robinson, K., & Jacobsen, D. W. (2001). Homocysteine induces expression and secretion of monocyte chemoattractant protein-1 and interleukin-8 in human aortic endothelial cells: implications for vascular disease. [Research Support, U.S. Gov't, P.H.S.]. *Circulation, 103*(22), 2717-2723.

Postea, O., Koenen, R. R., Hristov, M., Weber, C., & Ludwig, A. (2008). Homocysteine up-regulates vascular transmembrane chemokine CXCL16 and induces CXCR6+ lymphocyte recruitment in vitro and in vivo. [Research Support, Non-U.S. Gov't]. *J Cell Mol Med, 12*(5A), 1700-1709. doi: 10.1111/j.1582-4934.2008.00223.x

Qu, K., Chen, C. P., Halliwell, B., Moore, P. K., & Wong, P. T. (2006). Hydrogen sulfide is a mediator of cerebral ischemic damage. [Research Support, Non-U.S. Gov't]. *Stroke, 37*(3), 889-893. doi: 10.1161/01.STR.0000204184.34946.41

Qun, S., Tang, Y., Sun, J., Liu, Z., Wu, J., Zhang, J., . . . Ge, W. (2017). Neutrophil-To-Lymphocyte Ratio Predicts 3-Month Outcome of Acute Ischemic Stroke. *Neurotox Res*. doi: 10.1007/s12640-017-9707-z

Rabaneda, L. G., Geribaldi-Doldan, N., Murillo-Carretero, M., Carrasco, M., Martinez-Salas, J. M., Verastegui, C., & Castro, C. (2016). Altered regulation of the Spry2/Dyrk1A/PP2A triad by homocysteine impairs neural progenitor cell proliferation. *Biochim Biophys Acta, 1863*(12), 3015-3026. doi: 10.1016/j.bbamcr.2016.09.018

Saposnik, G., Ray, J. G., Sheridan, P., McQueen, M., & Lonn, E. (2009). Homocysteine-lowering therapy and stroke risk, severity, and disability: additional findings from the HOPE 2 trial. [Randomized Controlled Trial]. *Stroke, 40*(4), 1365-1372. doi: 10.1161/STROKEAHA.108.529503

Scherbakov, N., Dirnagl, U., & Doehner, W. (2011). Body weight after stroke: lessons from the obesity paradox. [Research Support, Non-U.S. Gov't]. *Stroke, 42*(12), 3646-3650. doi: 10.1161/STROKEAHA.111.619163

Sergeant, P., & Meyns, B. (1997). La critique est aisee mais l'art est difficile. [Criticism is easy but the method is hard; comment]. [Comment]. *Lancet, 350*(9085), 1114-1115.

Siesjo, B. K., Bengtsson, F., Grampp, W., & Theander, S. (1989). Calcium, excitotoxins, and neuronal death in the brain. [Research Support, Non-U.S. Gov't

Research Support, U.S. Gov't, P.H.S.

Review]. *Ann N Y Acad Sci, 568*, 234-251.

Sipkens, J. A., Hahn, N., van den Brand, C. S., Meischl, C., Cillessen, S. A., Smith, D. E., . . . Niessen, H. W. (2013). Homocysteine-induced apoptosis in endothelial cells coincides with nuclear NOX2 and peri-nuclear NOX4 activity. *Cell Biochem Biophys, 67*(2), 341-352. doi: 10.1007/s12013-011-9297-y

Soriano-Tarraga, C., Jimenez-Conde, J., Giralt-Steinhauer, E., Mola, M., Ois, A., Rodriguez-Campello, A., . . . Roquer, J. (2014). Global DNA methylation of ischemic

stroke subtypes. [Research Support, Non-U.S. Gov't]. *PLoS One*, *9*(4), e96543. doi: 10.1371/journal.pone.0096543

Stam, F., Smulders, Y. M., van Guldener, C., Jakobs, C., Stehouwer, C. D., & de Meer, K. (2005). Folic acid treatment increases homocysteine remethylation and methionine transmethylation in healthy subjects. [Research Support, Non-U.S. Gov't]. *Clin Sci (Lond), 108*(5), 449-456. doi: 10.1042/CS20040295

Stubbe, T., Ebner, F., Richter, D., Engel, O., Klehmet, J., Royl, G., . . . Brandt, C. (2013). Regulatory T cells accumulate and proliferate in the ischemic hemisphere for up to 30 days after MCAO. [Research Support, Non-U.S. Gov't]. *J Cereb Blood Flow Metab, 33*(1), 37-47. doi: 10.1038/jcbfm.2012.128

Su, S. J., Huang, L. W., Pai, L. S., Liu, H. W., & Chang, K. L. (2005). Homocysteine at pathophysiologic concentrations activates human monocyte and induces cytokine expression and inhibits macrophage migration inhibitory factor expression. [Research Support, Non-U.S. Gov't]. *Nutrition, 21*(10), 994-1002. doi: 10.1016/j.nut.2005.01.011

Sun, W., Wang, G., Zhang, Z. M., Zeng, X. K., & Wang, X. (2005). Chemokine RANTES is upregulated in monocytes from patients with hyperhomocysteinemia. [Research Support, Non-U.S. Gov't]. *Acta Pharmacol Sin, 26*(11), 1317-1321. doi: 10.1111/j.1745-7254.2005.00178.x

Tang, Y., & Le, W. (2016). Differential Roles of M1 and M2 Microglia in Neurodegenerative Diseases. [Research Support, Non-U.S. Gov't

Review]. *Mol Neurobiol, 53*(2), 1181-1194. doi: 10.1007/s12035-014-9070-5

Tokgoz, S., Kayrak, M., Akpinar, Z., Seyithanoglu, A., Guney, F., & Yuruten, B. (2013). Neutrophil lymphocyte ratio as a predictor of stroke. *J Stroke Cerebrovasc Dis, 22*(7), 1169-1174. doi: 10.1016/j.jstrokecerebrovasdis.2013.01.011

Tokgoz, S., Keskin, S., Kayrak, M., Seyithanoglu, A., & Ogmegul, A. (2014). Is neutrophil/lymphocyte ratio predict to short-term mortality in acute cerebral infarct independently from infarct volume? *J Stroke Cerebrovasc Dis, 23*(8), 2163-2168. doi: 10.1016/j.jstrokecerebrovasdis.2014.04.007

Tyagi, N., Gillespie, W., Vacek, J. C., Sen, U., Tyagi, S. C., & Lominadze, D. (2009). Activation of GABA-A receptor ameliorates homocysteine-induced MMP-9 activation by ERK pathway. [Research Support, N.I.H., Extramural]. *J Cell Physiol, 220*(1), 257-266. doi: 10.1002/jcp.21757

Vallet, P., Charnay, Y., Steger, K., Ogier-Denis, E., Kovari, E., Herrmann, F., . . . Szanto, I. (2005). Neuronal expression of the NADPH oxidase NOX4, and its regulation in mouse experimental brain ischemia. [Comparative Study]. *Neuroscience, 132*(2), 233-238. doi: 10.1016/j.neuroscience.2004.12.038

Vogt, G., Laage, R., Shuaib, A., & Schneider, A. (2012). Initial lesion volume is an independent predictor of clinical stroke outcome at day 90: an analysis of the Virtual International Stroke Trials Archive (VISTA) database. *Stroke, 43*(5), 1266-1272. doi: 10.1161/STROKEAHA.111.646570

Walsh, K. B., Sekar, P., Langefeld, C. D., Moomaw, C. J., Elkind, M. S., Boehme, A. K., . . . Adeoye, O. (2015). Monocyte Count and 30-Day Case Fatality in Intracerebral Hemorrhage. [Multicenter Study

Research Support, N.I.H., Extramural]. *Stroke, 46*(8), 2302-2304. doi: 10.1161/STROKEAHA.115.009880

Wang, G., Siow, Y. L., & O, K. (2001). Homocysteine induces monocyte chemoattractant protein-1 expression by activating NF-kappaB in THP-1 macrophages. [Research Support, Non-U.S. Gov't]. *Am J Physiol Heart Circ Physiol, 280*(6), H2840-2847.

Wang, G., Weng, Y. C., Han, X., Whaley, J. D., McCrae, K. R., & Chou, W. H. (2015). Lipocalin-2 released in response to cerebral ischaemia mediates reperfusion injury in mice. [Research Support, N.I.H., Extramural

Research Support, Non-U.S. Gov't]. *J Cell Mol Med, 19*(7), 1637-1645. doi: 10.1111/jcmm.12538

Wang, H., Yoshizumi, M., Lai, K., Tsai, J. C., Perrella, M. A., Haber, E., & Lee, M. E. (1997). Inhibition of growth and p21ras methylation in vascular endothelial cells by homocysteine but not cysteine. [Comparative Study

Research Support, Non-U.S. Gov't

Research Support, U.S. Gov't, P.H.S.]. *J Biol Chem, 272*(40), 25380-25385.

Wang, L., Chen, X., Tang, B., Hua, X., Klein-Szanto, A., & Kruger, W. D. (2005). Expression of mutant human cystathionine beta-synthase rescues neonatal lethality but not homocystinuria in a mouse model. [Research Support, N.I.H., Extramural

Research Support, Non-U.S. Gov't

Research Support, U.S. Gov't, P.H.S.]. *Hum Mol Genet, 14*(15), 2201-2208. doi: 10.1093/hmg/ddi224

Wang, Y., Jia, J., Ao, G., Hu, L., Liu, H., Xiao, Y., . . . Cheng, J. (2014). Hydrogen sulfide protects blood-brain barrier integrity following cerebral ischemia. [Research Support, Non-U.S. Gov't]. *J Neurochem, 129*(5), 827-838. doi: 10.1111/jnc.12695

Watson, D. J., Parker, A. J., & Slack, R. W. (1988). Manipulating broken noses. [Clinical Trial

Letter

Randomized Controlled Trial]. *Lancet, 1*(8584), 533.

Wei, X., Zhang, B., Cheng, L., Chi, M., Deng, L., Pan, H., . . . Wang, G. (2015). Hydrogen sulfide induces neuroprotection against experimental stroke in rats by down-regulation of AQP4 via activating PKC. [Research Support, Non-U.S. Gov't]. *Brain Res, 1622*, 292-299. doi: 10.1016/j.brainres.2015.07.001

Westberry, J. M., Prewitt, A. K., & Wilson, M. E. (2008). Epigenetic regulation of the estrogen receptor alpha promoter in the cerebral cortex following ischemia in male and female rats. [Research Support, N.I.H., Extramural]. *Neuroscience, 152*(4), 982-989. doi: 10.1016/j.neuroscience.2008.01.048

Wu, X. Q., Ding, J., Ge, A. Y., Liu, F. F., Wang, X., & Fan, W. (2013). Acute phase homocysteine related to severity and outcome of atherothrombotic stroke. [Research

Support, Non-U.S. Gov't]. *Eur J Intern Med, 24*(4), 362-367. doi: 10.1016/j.ejim.2013.01.015

Xi, H., Zhang, Y., Xu, Y., Yang, W. Y., Jiang, X., Sha, X., . . . Wang, H. (2016). Caspase-1 Inflammasome Activation Mediates Homocysteine-Induced Pyrop-Apoptosis in Endothelial Cells. *Circ Res, 118*(10), 1525-1539. doi: 10.1161/CIRCRESAHA.116.308501

Xue, J., Huang, W., Chen, X., Li, Q., Cai, Z., Yu, T., & Shao, B. (2016). Neutrophil-to-Lymphocyte Ratio Is a Prognostic Marker in Acute Ischemic Stroke. *J Stroke Cerebrovasc Dis*. doi: 10.1016/j.jstrokecerebrovasdis.2016.11.010

Yang, J., Fang, P., Yu, D., Zhang, L., Zhang, D., Jiang, X., . . . Wang, H. (2016). Chronic Kidney Disease Induces Inflammatory CD40+ Monocyte Differentiation via Homocysteine Elevation and DNA Hypomethylation. *Circ Res, 119*(11), 1226-1241. doi: 10.1161/CIRCRESAHA.116.308750

Yang, J., Zhang, L., Yu, C., Yang, X. F., & Wang, H. (2014). Monocyte and macrophage differentiation: circulation inflammatory monocyte as biomarker for inflammatory diseases. *Biomark Res, 2*(1), 1. doi: 10.1186/2050-7771-2-1

Yilmaz, G., & Granger, D. N. (2008). Cell adhesion molecules and ischemic stroke. [Review]. *Neurol Res, 30*(8), 783-793. doi: 10.1179/174313208X341085

Zeng, X., Dai, J., Remick, D. G., & Wang, X. (2003). Homocysteine mediated expression and secretion of monocyte chemoattractant protein-1 and interleukin-8 in human monocytes. [Research Support, Non-U.S. Gov't

Research Support, U.S. Gov't, P.H.S.]. *Circ Res, 93*(4), 311-320. doi: 10.1161/01.RES.0000087642.01082.E4

Zhang, D., Fang, P., Jiang, X., Nelson, J., Moore, J. K., Kruger, W. D., . . . Wang, H. (2012). Severe hyperhomocysteinemia promotes bone marrow-derived and resident inflammatory monocyte differentiation and atherosclerosis in LDLr/CBS-deficient mice. [Research Support, N.I.H., Extramural]. *Circ Res, 111*(1), 37-49. doi: 10.1161/CIRCRESAHA.112.269472

Zhang, F., Guo, R. M., Yang, M., Wen, X. H., & Shen, J. (2012). A stable focal cerebral ischemia injury model in adult mice: assessment using 7T MR imaging. [Research Support, Non-U.S. Gov't]. *AJNR Am J Neuroradiol, 33*(5), 935-939. doi: 10.3174/ajnr.A2887

Zhang, Q., Li, Q., Chen, Y., Huang, X., Yang, I. H., Cao, L., . . . Tan, H. M. (2012). Homocysteine-impaired angiogenesis is associated with VEGF/VEGFR inhibition. [Research Support, Non-U.S. Gov't]. *Front Biosci (Elite Ed), 4*, 2525-2535.

Zhang, Q. G., Laird, M. D., Han, D., Nguyen, K., Scott, E., Dong, Y., . . . Brann, D. W. (2012). Critical role of NADPH oxidase in neuronal oxidative damage and microglia activation following traumatic brain injury. *PLoS One, 7*(4), e34504. doi: 10.1371/journal.pone.0034504

Zhu, S., Li, J., Bing, Y., Yan, W., Zhu, Y., Xia, B., & Chen, M. (2015). Diet-Induced Hyperhomocysteinaemia Increases Intestinal Inflammation in an Animal Model of Colitis. [Evaluation Studies

Research Support, Non-U.S. Gov't]. *J Crohns Colitis, 9*(9), 708-719. doi: 10.1093/ecco-jcc/jjv094

Zhu, X., Song, Z., Zhang, S., Nanda, A., & Li, G. (2014). CD147: a novel modulator of inflammatory and immune disorders. [Research Support, N.I.H., Extramural

Review]. *Curr Med Chem, 21*(19), 2138-2145.

Zou, C. G., Zhao, Y. S., Gao, S. Y., Li, S. D., Cao, X. Z., Zhang, M., & Zhang, K. Q. (2010). Homocysteine promotes proliferation and activation of microglia. [Research Support, Non-U.S. Gov't]. *Neurobiol Aging, 31*(12), 2069-2079. doi: 10.1016/j.neurobiolaging.2008.11.007